NASA CONTRACTOR REPORT

NASA CR-167

GAUGE CALIBRATION STUDY IN EXTREME HIGH VACUUM

by F. Feakes, F. L. Torney, Jr., and F. J. Brock

Prepared under Contract No. NASw-625 *by*
NATIONAL RESEARCH CORPORATION
Cambridge, Mass.
for

NATIONAL AERONAUTICS AND SPACE ADMINISTRATION • WASHINGTON, D. C. • FEBRUARY 1965

GAUGE CALIBRATION STUDY IN EXTREME HIGH VACUUM

By F. Feakes, F. L. Torney, Jr., and F. J. Brock

Prepared under Contract No. NASw-625 by
NATIONAL RESEARCH CORPORATION
Cambridge, Mass.

for

NATIONAL AERONAUTICS AND SPACE ADMINISTRATION

For sale by the Office of Technical Services, Department of Commerce,
Washington, D.C. 20230 -- Price $4.00

TABLE OF CONTENTS

LIST OF FIGURES

LIST OF FIGURES (continued)

LIST OF TABLES

SUMMARY

The measurement of total gas density and pressure at the levels expected on the surface of the moon and in interplanetary space (probably about 10^{-15} torr) is beyond present technological capabilities. This deficiency causes even greater concern when it is realized that there is little doubt that gas densities as low as those in outer space can be produced routinely in the laboratory today. Pressures in the ranges above 10^{-11} torr may be measured with considerable certainty. However, below 10^{-11} torr the reliability of measurement quickly becomes marginal as the pressure decreases.

The main objective of the present program was to examine the operating characteristics and low pressure limits of those sensors which were most likely to be useful at pressures below 10^{-11} torr. The gauges chosen for detailed study were a normal magnetron gauge, an inverted magnetron, a nude modulated ion gauge, and a suppressor grid gauge. The results obtained are summarized below under Gauge Calibration. Two other sub-programs also received considerable theoretical and experimental attention. They are discussed under the sections entitled "Directional Sensitivity" and "Dynamic Response". The principal conclusions developed in this program are stated at the end of this Summary.

GAUGE CALIBRATION

In order to study gauge performance at low pressures it was not only necessary to carry out the work in an apparatus which was capable of achieving pressures well below 10^{-11} torr, but it was also necessary to be able to produce definite, known pressures in the desired range with certainty. Both these requirements were met by using a special pressure ratio technique which involved bleeding helium gas from a

known pressure source through a known conductance, into NRC's Extreme High Vacuum (XHV)* system. In this way, each gauge was studied independently and calibrated without reference to another gauge operating at the same pressure level. This method is considered to represent a considerable advance in the state-of-the-art of calibration of gauges in the UHV and XHV ranges. The method has been applied with success down to pressures of 3×10^{-13} torr. There is every indication that it is applicable to even lower pressures. Useful data on general operating characteristics were also obtained by direct comparison of gauges at the higher pressure levels, above 10^{-11} torr. In this latter method, the gauge under study was generally cross-calibrated against a modulated Nottingham gauge. The main results of the gauge calibration studies are summarized below in separate discussions of each gauge type.

Normal Magnetron Gauge

The gauge used in this work was an NRC Model 552 gauge. When operated with an anode voltage of +4500 volts and using a magnet with a field strength of 1000 gauss, the gauge was found to give an output current which was linear with pressures over the range 1×10^{-6} to 2×10^{-10} torr. The sensitivity was approximately 4.5 amps/torr. Below 2×10^{-10} torr confirmation evidence was obtained that the gauge was non-linear with the gauge current (i_+) (amp) being related to the pressure (P) (torr) by the relationship

$$i_+ = kP^n$$

Both k and n were found to be functions of the operating characteristics of the gauge. The value of k was determined primarily by the anode voltage. The sensitivity increased with increased anode voltage but gauge instabilities were also increased. The effect of increased noise was more significant at lower pressures. The exponent

* A Trade Mark of National Research Corporation

n was a strong function of the magnetic field strength. Above 2×10^{-10} torr, $n = 1.0$. However, below 2×10^{-10} torr the value of n decreased from 1.89 at 890 gauss to 1.34 at 1050 gauss. Over this range of magnetic field strength, the slope decreased linearly with increases in the magnetic field strength. However, a magnetic field strength as high as 1560 failed to reduce the value of n below 1.3. Redhead[1], has recently shown that a distinct change in the nature of the magnetron oscillations takes place at a magnetic field strength of 1200 gauss. Consequently, the data at 1560 gauss are not really comparable to those below 1200 gauss. The normal magnetron was calibrated down to 3×10^{-13} torr. At this pressure the output current was 7×10^{-14} amps.

Inverted Magnetron Gauge

Previous experimental data by Hobson and Redhead[2] had shown that the inverted magnetron had a substantially lower sensitivity than the normal magnetron at pressures above 2×10^{-10} torr. In addition, the inverted magnetrons studied by Hobson and Redhead were non-linear with the exponent n (cf Normal Magnetron Gauge) varying from 1.1 to 1.4. These results suggested the possibility of an inverted magnetron with a low exponent (say 1.1) having a sensitivity which became equal to and then greater than the sensitivity of the normal magnetron as the pressure decreased.

Some five inverted magnetron designs were studied during the present program. The lowest exponent found was 1.25. This was obtained with an inverted magnetron gauge specially designed and built so as to reduce the possibility of leakage currents giving erroneous results at very low pressures. The gauge was operated at 6000 volts and gave an exponent of 1.25 with a magnetic field strength of 2100 gauss. The gauge was calibrated down to a pressure of 3×10^{-13} torr. At this pressure the output current of the gauge was 3.7×10^{-14} amps. Consequently, even at this pressure the

sensitivity of the inverted magnetron was lower than the normal magnetron.

By extrapolation it appeared that the inverted magnetron with an exponent of 1.25 would not have a greater sensitivity than the normal magnetron (exponent 1.45) until the pressure had decreased below approximately 2×10^{-14} torr. At this pressure both the normal and inverted magnetrons would have output currents of approximately 1×10^{-15} amps. At very low pressures, the signal to noise ratio of the inverted magnetron was approximately the same as the normal magnetron.

Nude Modulated Ion Gauge

A modulating electrode was mounted inside the grid of a nude Nottingham ion gauge. The gauge collector current was then modulated by switching the potential of the modulating electrode between ground and grid potentials according to the method of Redhead[3]. When the gauge was operated with a 3.0 Ma emission, the sensitivity was 0.1 amp/torr (N_2). Using the modulation technique the residual current (i_r) (X-ray current) was measured to be 1.3×10^{-12} amps (1.3×10^{-11} torr) at 3.0 Ma emission. The value of i_r was directly proportional to the emission current.

By means of the modulation technique it was possible to obtain consistent results down to ion currents equal to about one-half the residual current, that is, 6×10^{-13} amps or 6×10^{-12} torr. Below this value noise problems become significant. It is quite likely that the gauge structure used was not vibration free and consequently microphonics probably became a major source of noise. However, the main practical problem in using a hot filament gauge at pressures below 10^{-11} torr is that associated with cleaning the gauge and making certain that it remains clean. One of the principal advantages of the modulation technique is that it may be used to monitor the cleanliness of the gauge by monitoring the total residual ion current. If the measured

total residual current rises above the known X-ray-induced residual current, the additional component of the residual current must be assigned to gauge contamination.

Suppressor Grid Gauge (Modulated)

The suppressor grid gauge was calibrated over the range 10^{-5} to 10^{-13} torr (N_2). The complete suppression of the soft X-ray-induced secondary electron emission from the ion collector required the application of -665 volts to the suppressor grid. The required suppressor grid voltage was found to be a strong function of geometry of the gauge elements. While the suppressor grid efficiently suppressed the ordinary ion gauge residual current consisting of secondary electron emission from the ion collector induced by soft X-ray photons directly incident upon the collector, the very existence of the suppressor grid introduced a new residual current consisting of secondary electron emission from the suppressor grid to the collector induced by soft X-ray photons reflected from the ion collector to the suppressor grid. This reflected X-ray-induced secondary electron emission current is very much smaller than the direct X-ray-induced secondary electron emission current and is negative in sign. This negative residual current causes the total measured collector current to pass through zero at a pressure of 2.7×10^{-12} torr and becomes negative below this pressure (for an emission current of 1.0 Ma). The negative residual current of the suppressor grid gauge was -5.4×10^{-14} amps.

The final version of the suppressor grid gauge used in this program was equipped with a modulation electrode. The modulation technique was used to separate the negative residual current from the true ion current. It was found that the modulation technique substantially lowered the limit of detectability for pressure measurement of the suppressor grid gauge. In fact, pressures of the order of 10^{-12} torr were measured using the modulation technique, but without

the use of the modulation technique the suppressor grid gauge could be used to measure pressures only as low as approximately 10^{-11} torr.

The modulated suppressor grid gauge is considered the most reliable of the hot cathode ion gauges studied. It also has a limit of detectability for pressure that is lower than any of the other hot cathode ion gauges. However, its operating characteristics were found to be quite sensitive to small changes in the geometrical location of the gauge elements. This condition is untenable in practice since small changes in the relative location of the gauge elements are to be expected as a result of the high temperature required in degassing the gauge. Another inherent difficulty with the suppressor grid gauge is that at low pressures the signal to noise ratio is low since the gauge sensitivity is relatively low, the measured gauge constant being only 20 $torr^{-1}$. This gauge constant may be increased somewhat for the modulated suppressor grid gauge by redefining the normal mode of operation such that the modulator is normally at ground potential rather than grid potential as is the custom.

DIRECTIONAL SENSITIVITY

For this work a nude modulated gauge was mounted in the XHV system on a support which could be rotated through an angle of 90 degrees. A beam of argon atoms was admitted to the experimental chamber through a capillary aimed directly at the gauge. The argon was pumped with a high capture probability by the inner surface of the experimental chamber which was maintained at less than 10°K. The beam intensity as measured by the ion gauge closely approximated that predicted by beam theory. Beam intensities corresponding to approximately 3×10^{-9} torr were measured when the pressure at the inlet to the capillary was 7.5×10^{-4} torr. Signal to background ratios in excess of 10^3 were measured. When the gauge was placed so that the beam impinged normally

on the axis of the cylindrical grid cage, the output of the gauge was at a minimum. As the angle between the beam and the axis of the grid cage was decreased, the signal increased. With the beam axis parallel to the grid cage axis, the signal was approximately 25 per cent greater than at right angles to it. The increased signal was apparently caused by back-scattering of argon from the glass press used as a support structure for the gauge elements. This glass passthrough assembly was not cryogenically cooled and rotated into the argon beam as the angle between the gauge and beam decreased. Assuming cosine law distribution of back-scattering from the gauge support, an increase of 21 per cent in ion current was predicted. Consequently, independent of back-scattering, the nude ion gauge sensitivity did not appear to be directionally dependent.

DYNAMIC RESPONSE

The dynamic response characteristics of an ion gauge were studied by using a flash filament technique to generate a short, steep rise gas pulse and measuring the time history of the ion gauge output current (collector current). Argon was adsorbed on a 77°K filament which was flashed to about 190°K by a 7 microsecond heating current pulse. From the time history of the ion gauge collector current and the calculated time of flight of the argon gas pulse from the flash desorption filament to the ion gauge grid cage, the response time of the ion gauge was determined to be of the order of several microseconds. That is, the time interval between the arrival of the gas pulse at the surface of the ion gauge grid cage and the appearance of an ion current at the collector was about 2.6 microseconds. This gauge time constant agrees well with the value calculated from theory for the gauge and gas used in this experiment. The above result implies that the Nottingham ion gauge used in this experiment would have a flat dynamic response to about 385 Kc/s.

The intrinsic dynamic response properties of an ion gauge depend on the gas, the geometry of the gauge and the operating voltages applied to the gauge electrodes. However, in most practical applications the fastest pressure variation that can be measured with an ion gauge will also depend on the location of the gas source, the temperature of the gas, the shape and size of the vacuum enclosure. It should be clear that the ion gauge cannot measure a change in pressure until that change reaches the gauge proper. However, since the gas molecules have a wide velocity distribution, the actual density variation with time at various points in the system will differ if the pressure variations are very fast (say of the order of tens of microseconds).

CONCLUSIONS

1. An advanced method of calibrating gauges in the UHV and XHV ranges was developed and tested with success down to 3×10^{-13} torr. There is every indication that the method is applicable to even lower pressures.

2. New gauge designs which gave superior performance were tested for the inverted magnetron gauge and a modulated suppressor grid gauge.

3. The lowest limits of gauge calibration were not limited by the pressures attainable in the calibration system. The gauge performance was generally limited by low signal to noise ratios at the lowest limits. The lowest limits established for each of the gauges were:—

Normal Magnetron Gauge	3×10^{-13} torr N_2
Inverted Magnetron Gauge	3×10^{-13} torr N_2
Nude Modulated Ion Gauge	6×10^{-12} torr N_2
Modulated Suppressor Grid Gauge	1.3×10^{-12} torr N_2

4. The normal magnetron gauge had the highest sensitivity of all gauges examined at all pressures tested.

However, both types of magnetron gauges were non-linear in the pressure range of interest in this program. The inverted magnetron required higher magnetic fields and higher anode voltages for optimum performance than did the normal magnetron.

5. For both hot filament gauges - the nude modulated ion gauge and the suppressor grid gauge - extreme care was required to obtain adequate degassing by electron bombardment. In addition, the experimental and mathematical procedures required to measure true pressure were complex and sophisticated and yet not completely without ambiguity.

6. Major advances would result if the normal magnetron could be made linear below 2×10^{-10} torr. There does not appear to be any theoretical reason why this should not be feasible.

7. Further developments are required to advance the techniques of measuring exceedingly small currents. Major difficulties are presently caused by dielectric polarization, instabilities and noise in power supplies, capacitance effects between gauge elements, microphonics, and leakage currents caused by non-perfect insulation materials.

8. The studies involving argon beam techniques showed that a nude Nottingham gauge gave output signals which were independent of the incidence angle of flux on the gauge if back-scatter from gauge support elements were neglected. In most practical applications, back-scatter with cosine law distribution will be a factor in determining the gauge reading.

9. The response time for a nude ion gauge was found to be approximately 2.6 microseconds - a time which is comparable to the time required for an ion to travel from the point of ionization within the grid structure to the collector. In most practical cases, the response time will be determined by the rate of travel of the gas to the gauge.

1.0 INTRODUCTION

With the extension of the Space Program to more distant missions such as the moon, many of the requirements for measuring the properties of space are beyond the limits of the state-of-the-art for present day sensors. The measurement of gas density and/or pressure is in this category. If missions to deep space, such as Mars are considered, the problems are further magnified. Moreover, it is now apparent that current vacuum technology is capable of routinely producing pressures comparable to that in outer space. However, measurement of such pressures and gas densities is severely limited. Pressures in the range 10^{-10} and 10^{-11} torr may be measured with some certainty but skill and care are required. Below 10^{-11} torr the problems become acute and reliability of measurement quickly becomes marginal as the pressure decreases. And yet, it is an undoubted fact that pressures lower than 10^{-13} torr can be produced routinely. But at the present time, they cannot be measured with any degree of confidence.

The basic approach in this program was to select a number of gauges which appeared to have good prospects of being useful gauges at extremely low pressures and then to test these gauges in the XHV range to determine their low pressure limitations and general operating characteristics. The results should then lead to the logical choice of gauge or gauge principle which should receive research and developmental effort in order to produce a sensor with sufficient accuracy and sensitivity to measure pressures below the present limits of measurement. In order to meet these requirements, not only was it necessary to produce extremely low pressures, but a method of producing a known pressure with a considerable degree of certainty was required. The NRC Extreme High Vacuum system was used to produce the low

background pressures and a pressure-ratio technique using helium gas was the basis of the method of producing known pressures for calibration purposes.

In addition to the investigation of very low pressure performance of certain promising gauges, two other response problems of considerable significance were investigated. The first concerned possible variations in the output signal from an ion gauge according to the angle at which a beam of gas entered the grid structure of the gauge. The question arose as to whether the angle at which a nude ion gauge was placed in a gas beam would have any effect on the gauge output. Also would the amount of gas back-scattered from the base and supporting structure of a gas significantly increase the signal? For this part of the program an argon beam with an intensity equivalent to approximately 10^{-9} torr was introduced into the experimental chamber of the XHV system. With the experimental chamber at 10°K, the angle between the gauge and the beam was changed from zero to $\pi/2$ by rotating the gauge. During the rotation the gauge output was recorded.

The second problem was to determine the rate at which an ion gauge would respond to rapid changes in gas density. A rate of rise in gas density of approximately one decade per millisecond was required in order to carry out experimental measurements of actual gauge rise times. A technique involving the flash desorption of argon from a tungsten filament was used in this part of the program.

Both of these problems are involved in the proper interpretation of pressure and density measurements on board satellites. They are also involved in interpreting measurements in vacuum systems in which there is a steady or time varying gas flow.

The results of part of the work in this program have been published[4]. The work has also resulted in a patent application covering the modulated suppressor grid gauge.

2.0 OBJECTIVES

Initially, the primary objectives of the present program were as follows:

1. Cross-calibration of gauges suitable for extreme high vacuum application against the NRC-552 cold cathode ion gauge to the lowest pressure limits.
2. Investigation of the lowest possible limits of pressures and stability of several selected types of gauges.
3. Determination of the directional and dynamic response characteristics of several pressure gauges.
4. Investigation of the positional dependence where directional response was found to be a strong function of angle of incidence.

During the course of the research work, theoretical, experimental and technical considerations necessitated repeated re-evaluation and redefinition of the details and course of the experimental work. For instance, early in the program, it became apparent that several of the gauges initially chosen for study were not potentially sound gauges for the measurement of extremely low pressures. Accordingly, the Scope of Work was revised to include a number of gauges which had more substantial prospects of being useful gauges. The following gauges were to be included in the study:—

a. Normal Magnetron Gauge
b. Nude Ion Gauge
c. Inverted Magnetron
d. Suppressor Grid Gauge
e. G.E. Lafferty Gauge

The Lafferty gauge unfortunately was not available for testing.

In the course of the program, experimental results showed that calibration at low pressures by the pressure-ratio technique was superior to the cross-calibration against the NRC 552 cold-cathode (normal magnetron) gauge. In general, it was possible by the pressure-ratio procedure to obtain essentially independent calibrations of each gauge at extremely low pressures. In addition, it also became apparent that several of the gauges designed for operation at higher pressures - say above 10^{-10} torr - required extensive modifications and rebuilding in order to ensure any usefulness of the gauge for the measurement of extremely low pressures. As a result, the work statement was further amended and supplemented to include the following:

1. Determine the nitrogen sensitivity of the normal magnetron in the XHV range using the capillary pressure ratio technique.

2. Determine the helium sensitivity of the modified inverted magnetron gauge in the XHV range using the capillary ratio technique.

3. Determine the helium sensitivity of the modified suppressor grid gauge in the XHV range using the capillary ratio technique.

4. Conduct a modulated argon beam experiment on either the modified suppressor grid gauge or on the modulated Nottingham ion gauge to determine the gauge sensitivity dependence on the flux incidence angle.

5. Conduct a chopped atomic beam experiment to determine the dynamic response of either the modified suppressor grid gauge or the modulated Nottingham ion gauge.

During a preliminary theoretical analysis of the response time characteristics of an ion gauge it was shown that high rates of change of gas density could be applied to a gauge by using flash desorption of gas (argon) previously adsorbed on a tungsten filament. This procedure was used to measure the dynamic response characteristics in lieu of the chopped atomic beam.

Otherwise, the work adhered to the main objectives of the program as set out above. Each of the above objectives was achieved.

3.0 GAUGE CALIBRATION

In examining the response characteristics of the various gauges tested in the present program, two methods were used. In the first method the gauge under examination was compared directly with a gauge of known characteristics — generally a modulated Nottingham gauge. A UHV system was used for this procedure which is referred to as cross-calibration throughout this report. Gauge calibration down to approximately 1×10^{-11} torr (N_2) was feasible with this method. The second method involved the use of the Extreme High Vacuum system and a pressure ratio technique was used for gauge calibration. Although the method can be used to calibrate gauges over a wide pressure range it was generally convenient to use a range of approximately 10^{-10} to 10^{-13} torr (N_2) for the gauges examined.

The two methods therefore overlapped by about one decade. They are described in more detail below.

All pressures noted in this report are equivalent nitrogen pressures unless otherwise specified.

3.1 PROCEDURES

3.1.1 Cross-Calibration

3.1.1.1 Description of System

The cross-calibration of gauges was carried out in the small glass UHV system shown in Figure 1. The gauges under test were tubulated onto the system with one-inch diameter Pyrex in such a way as to minimize pumping speed errors and reduce ion interaction between gauges. Prior to a calibration the system was baked at 400°C for at least 24 hours.

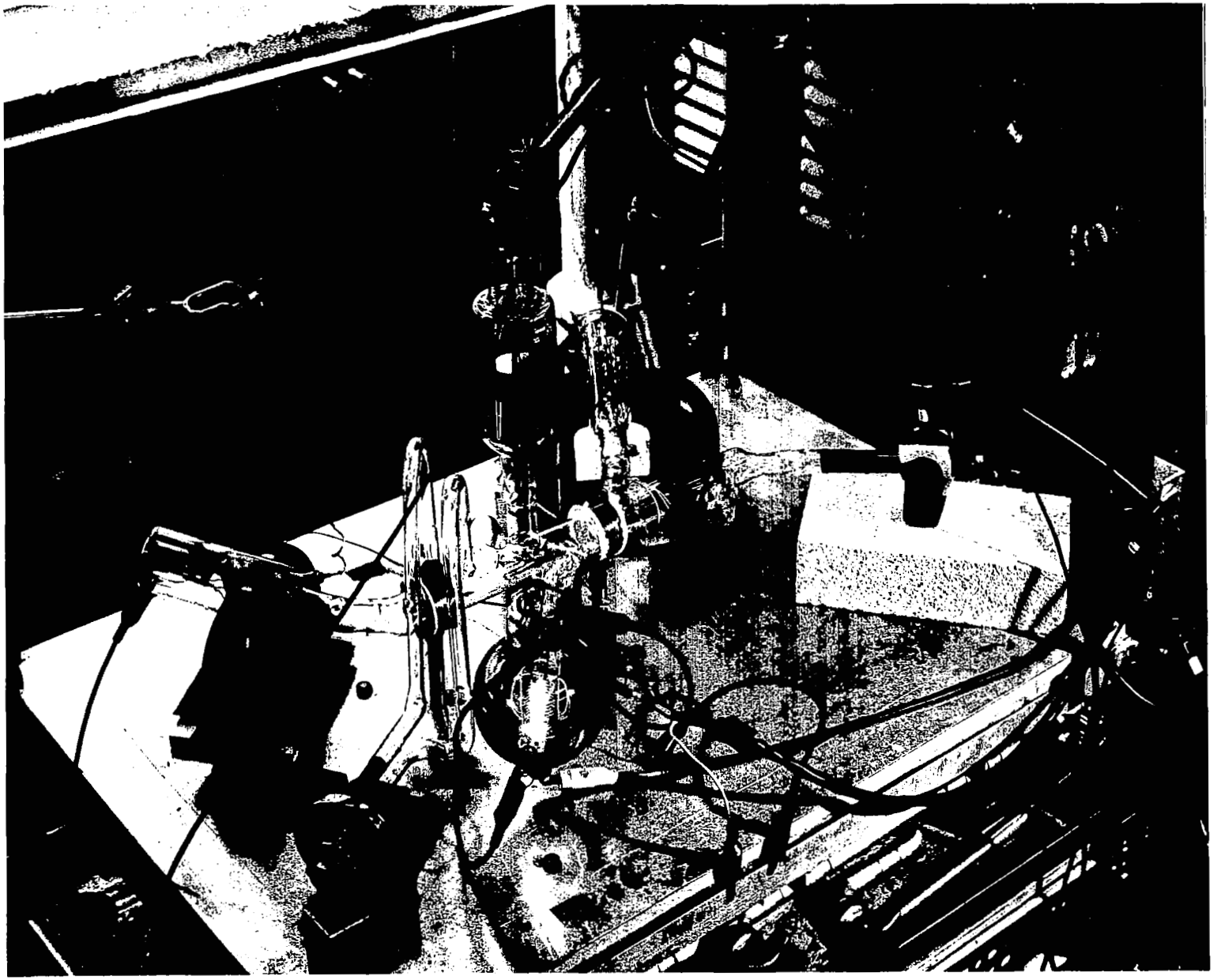

Fig. 1: GLASS UHV SYSTEM SHOWING TEST GAUGES

3.1.1.2 Method of Cross Calibration

After a sufficiently low background pressure had been reached (approximately 1 x 10^{-11} torr) and the hot filament gauges degassed by electron bombardment, the calibration gas was admitted through controlled leak valves. The pressure was then stabilized by balancing the gas inlet rate against the gauge pumping speeds for each pressure.

For the major part of the work a modulated Nottingham gauge was used as the comparison standard. This gauge was previously calibrated on the NRC calibration facility[5]. In this way, the gauge under study could be referenced to a McLeod gauge through the modulated Nottingham gauge. During any experiment the modulator was used continually to monitor residual current of the reference gauge. From these data, the true ion current in the gauge was calculated and plotted independent of residuals.

3.1.2 Pressure Ratio Technique

3.1.2.1 Description of the XHV System

The Extreme High Vacuum System (XHV), is shown schematically in Figure 2. The experimental chamber is 24 inches long and 18 inches in diameter. It is constructed of copper and can be baked to several hundred degress Centigrade by radiant heaters, and then cooled to 10°K by a closed loop helium refrigerator. Outgassing from the walls of this chamber is then held to an extremely low value. Furthermore, all gases except hydrogen, neon and helium are pumped at high speed by the walls at cryogenic temperatures.

The working chamber is surrounded by an intermediate shell which is also bakeable and may be cooled to 77°K to minimize outgassing. This in turn is surrounded by an outer shell which restrains the atmospheric pressure and also confines a guard volume between it and the intermediate

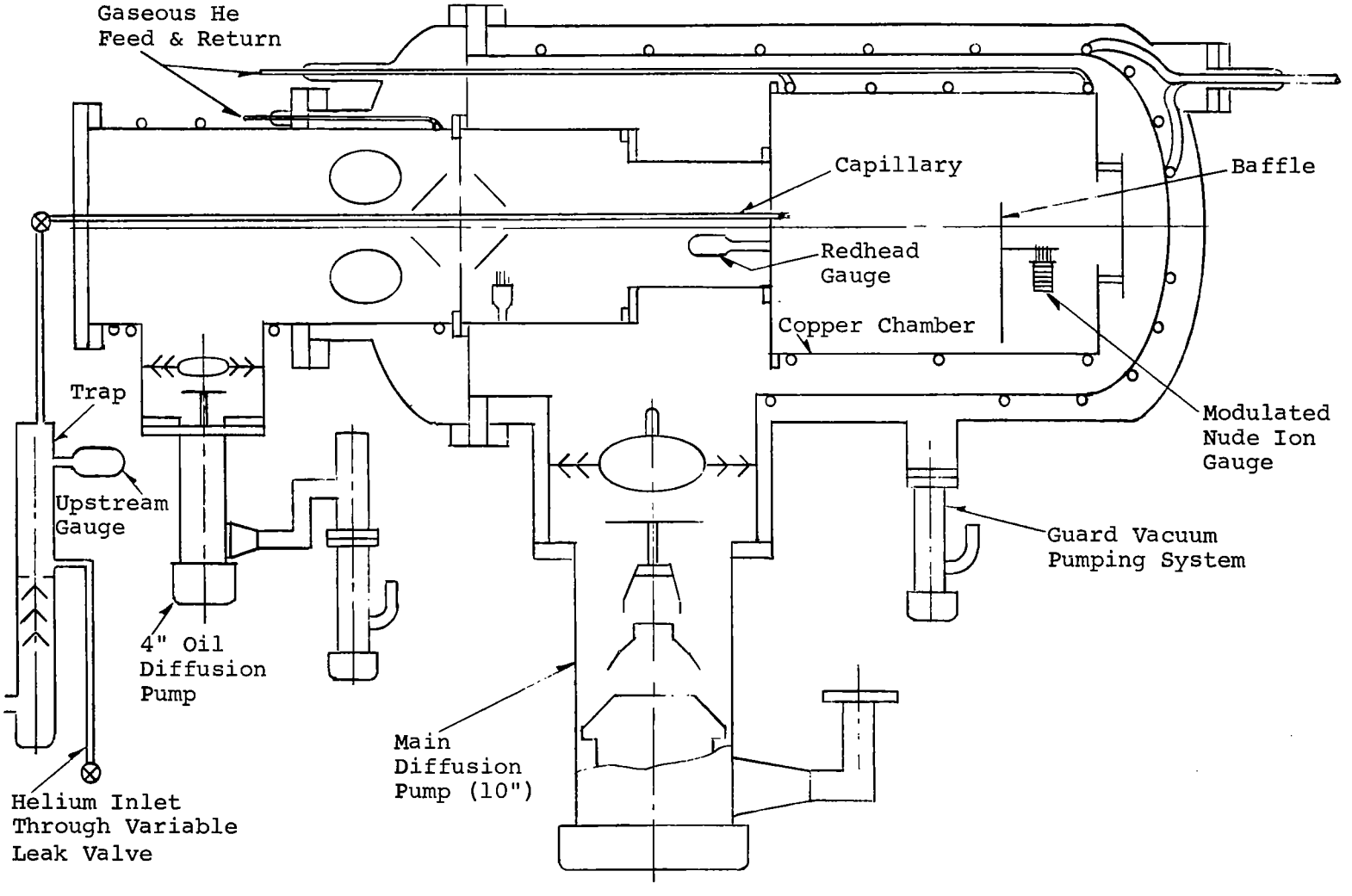

FIGURE 2 EXTREME HIGH VACUUM SYSTEM

shell. The purpose of the guard volume is to reduce the consequence of leaks and to provide thermal insulation for the cold intermediate shell. The flanged joints in the outer and intermediate shells are of cooled double O-ring design. The two main pumping systems each employ oil diffusion pumps with cold caps and liquid-nitrogen-cooled baffles. Each is backed by a second diffusion pump and by a mechanical pump.

The two outermost shells form an integral unit which can easily be rolled back on tracks to provide access to the experimental chamber. The experimental chamber is supported on a tubular cantilever structure which maintains a low conductive heat leakage. This structure also forms a separately pumped tunnel section for the entry of electrical leads. Gauges and other experimental devices are mounted in this section and tubulated through the closed end of the experimental chamber or are mounted inside the experimental chamber on the end closure with the leads carried out through the tunnel section.

A pressure of 1×10^{-10} torr within the intermediate shell (and therefore within the experimental chamber) is obtained when pumped by the diffusion pumps. Baking the experimental chamber and then cooling it to 10°K or below reduces the pressure to a value beyond the present limit of measurement.

3.1.2.2 Method of Gauge Calibration

The method of gauge comparison used in this part of the present study is an extension of the dynamic pressure ratio technique reported by Roehrig and Simons[5] for calibration of gauges above 10^{-9} torr. The essential elements of the system are represented schematically in Figure 3. A combination of oil-diffusion pumping and cryopumping was used to reduce the pressure in the test chamber to pressures estimated to be below 10^{-15} torr.

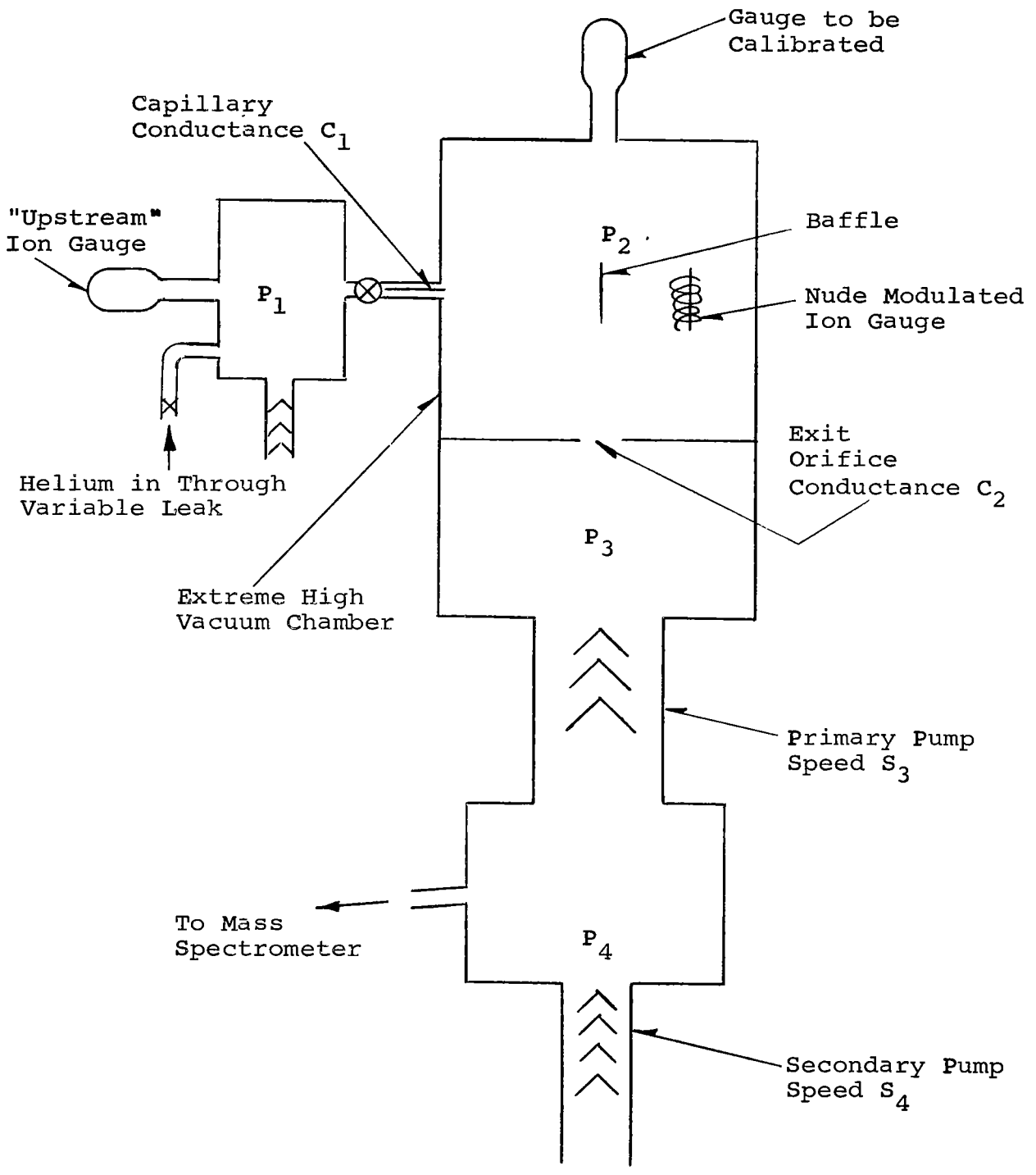

FIGURE 3 SCHEMATIC OF XHV CALIBRATION SYSTEM

Experimental Method -- For a particular experiment, thermal stability of the system was established and the system pressure reduced to a value below the limit of detectability. Highly purified helium was then admitted to a separately pumped system through a variable leak valve. Helium flowed from this system (controlled at pressures in the range 1×10^{-4} torr to 1×10^{-9} torr) to the extreme high vacuum chamber through an accurately dimensioned capillary. The helium pressure at the inlet to the capillary was measured with a tubulated hot filament ion gauge of the Nottingham type. This gauge was calibrated for helium using NRC's ultrahigh vacuum gauge calibration system with the McLeod gauge as the primary standard. The gauges to be tested are located in the tunnel section of the XHV system and are tubulated to the extreme high vacuum chamber. This chamber was operated at temperatures (approximately 10°K), such that cryosorption of helium was negligible. Helium was removed by diffusion pumping. The flow of helium from the test chamber was restricted by an orifice (conductance, C_2). Consequently, for a flow rate, Q, of helium through the capillary, the pressures in the various parts of the system were related as follows:

$$Q = C_1(P_1 - P_2) = C_2(P_2 - P_3) = S_3P_3 = S_4P_4$$

where:

C_1 = Conductance of capillary, l/sec
C_2 = Conductance of exit orifice, l/sec
P_1 = "Upstream" pressure, torr
P_2 = Pressure in test chamber, torr
P_3 = Pressure of inlet to primary diffusion pump, torr
P_4 = Pressure of inlet to secondary diffusion pump, torr
S_3 = Speed of primary diffusion pump, l/sec
S_4 = Speed of secondary diffusion pump, l/sec

The values of C_1, C_2, and S_3 were designed so that

$$P_2 \ll P_1 \text{ also } C_2 \ll S_3 \text{ or } P_3 \ll P_2$$

Consequently,

$$C_1P_1 \approx C_2P_2 \approx S_3P_3$$

Therefore,

$$P_2 \approx C_1P_1/C_2$$

From a knowledge of the ratio C_1/C_2 and measured values of P_1, values of P_2 were calculated. In order to determine whether this procedure was satisfactory, the following tests were made:

1. Measurements of the pressure ratio P_1/P_2 using two Nottingham type ion gauges.

2. Measurements of the ratio of the helium pressure P_1 to a mass spectrometric measurement of helium partial pressure P_4.

Direct Measurement of the Pressure Ratio P_1/P_2 -- For this purpose a nude Nottingham type ion gauge containing a modulating electrod was mounted in the test chamber. After rigorous cleaning of both the "upstream" and nude gauges, the pressure ratio P_1/P_2 was measured. This ratio remained constant (within $\pm 7\%$) for all values of P_2 from 5×10^{-9} torr to 3.0×10^{-11} torr. Pressure ratios P_1/P_2 of the order of 10^4 to 10^5 were used. It should be noted that because the system is not isothermal, the calculation of conductances requires a knowledge of the temperatures involved. In addition, care must be taken to correct for thermal transpiration effects, particularly for gauges tubulated to the test chamber and not isothermal with it. In this regard, it must be remembered that both magnetron and hot filament ion gauges measure molecular number density and calculation of the true pressure requires a temperature correction. In the following discussion when quotation marks are used, for

example, "pressure", it is to be understood that the temperature correction has not been applied to the "pressure" corresponding to the molecular number density.

Mass spectrometric measurement of the helium partial pressure, P_4, in the outlet of the primary pump showed a constant ratio of P_1/P_4. This ratio remained constant for values of P_1 from 1×10^{-9} torr to saturation of the mass spectrometer at 3.6×10^{-6} torr. The mass spectrometer had a sensitivity of 4.3×10^{-9} torr He per scale division. The variable leak used was capable of controlling the helium flow rate to within approximately one scale division. With a pressure ratio across the primary diffusion pump of at least 10^6 the above results infer that helium partial pressures of less than 10^{-14} torr He could be controlled at the inlet to the primary diffusion pump. The results are also consistent with the assumption of a constant pumping speed for the primary pump. The secondary pump was operating in a pressure range at which it is known to have a constant speed. However, as has been shown[5], if $C_2 \ll S_3$ variations in pumping speed will have little effect on the pressure ratio P_1/P_2.

The excellent agreement between the data taken in the XHV system (using the pressure ratio technique) and that obtained from the UHV system (using the leak-up technique) for helium was confirmation that the pressure ratio procedure was valid. Thus the operation of the pressure ratio system indicated that the upstream pressure gauge could be used to compute pressures in the XHV chamber. Since the background on the "upstream" gauge was less than 3×10^{-9} torr, the data suggest that the "pressure" in the XHV chamber with zero helium flow was less than 1×10^{-14} torr.

3.1.2.3 Electronic Measurements

For calibration at pressures below 10^{-11} torr, the measurement of currents of the order of 10^{-12} amps and below becomes necessary. Keithley Model 410 and 610 electrometers as well as a Wayne-Kerr Dynamic Capacitor Electrometer have been used in this work. Keithley 410 and 610 electrometers have full scale sensitivities of 3×10^{-13} amps and 1×10^{-13} amps respectively. Consequently, it is not possible to make accurate current measurements with these instruments below about 2×10^{-14} amps. In many cases the signal to noise ratio approaches unity at those current levels. In addition, it has been noticed that some gauge measurements at low pressures gave apparent negative ion currents. This was traced to polarization of the glass insulation. In order to reduce the effects of dielectric polarization and reduce possible leakage currents in the cathode circuit, a special cathode lead system was constructed. This involved the use of vacuum insulation (10^{-9} torr) where possible. A minimum of quartz was used elsewhere. Double shielding of the system was used. The inner shield was isolated from ground and automatically driven at the approximate potential of the collector lead by a feedback circuit in the electrometer. Also it has been shown that extreme care must be taken to maintain low voltage levels in the collector circuit. Since the collector voltage is dependent on the scale range used on the Keithley 610 it is important that optimum methods of instrument scaling be used. For the Keithley 610 operated in the fast position on the 0.01 volt multiplier scale, dielectric polarization effects were shown to be negligible at these current levels. However, electrical noise problems such as those due to mechanical vibration of conductors and power line noise often prevent the making of accurate current measurements below 10^{-13} amps.

The Wayne-Kerr Dynamic Capacitor Precision Electrometer has a full scale sensitivity of 10^{-15} amps. It increased

the effectiveness of the electronic measurements when it became available during the latter part of the program.

3.2 RESULTS

3.2.1 Normal Magnetron

The gauge used in these studies was an NRC 552 gauge. This form of the normal magnetron is often referred to as a Redhead gauge. The gauge geometry used in the present studies is similar to that described by Redhead[6] and later by F. L. Torney and F. Feakes[7]. It has been established that the normal magnetron gauge has an ion current which is a linear function of pressure down to approximately 2×10^{-10} torr. Using an anode voltage of 5000 volts and a magnetic field of 1000 gauss the current pressure relationship is linear according to the following relationship:

$$i_+ = 4.5P$$

where i_+ = current at cathode (amps)

P = pressure torr (nitrogen)

Below a pressure of 2×10^{-10} torr the relationship is non-linear and represented by:

$$i_+ = kP^n$$

where $k = 3.1 \times 10^5$ amp/(torr)^n

and $n = 1.5$ approximately

Consequently, above a pressure of 2×10^{-10} torr, a log-log plot of cathode current versus pressure yields a straight line with a slope of 1.0. Below 2×10^{-10} torr the plot has a slope of approximately 1.5.

The efforts in this program have been largely devoted to obtaining more information about the response characteristics

of the gauge below 2 x 10^{-10} torr. Considerable activity was applied to the measurement of the effects of anode voltage and magnetic field variations and determining the gauge noise characteristics at low pressure levels.

3.2.1.1 Results of Cross-Calibration Studies of Normal Magnetron

The pertinent results obtained in the cross-calibration and pressure ratio methods are summarized below. The nitrogen response characteristics for the normal magnetron gauge (compared with the modulated Nottingham gauge) for two different magnetic fields (1560 gauss and 900 gauss) are shown in Figure 4. The strength of the magnetic field appears to play a major role in the pressure-current response of the magnetron gauge below 10^{-9} torr. The data indicate that the 1560 gauss field reduced the point at which the ion current characteristic changes from a linear to a power function. When the gauge was operated with a magnet of 1560 gauss it was not possible to obtain useful data at higher pressure levels because of excessive noise. Even at the lower pressure levels the gauge was much noiser than when operated at lower magnetic fields.

The response curve for the normal magnetron gauge for both helium and nitrogen (again compared with the modulated Nottingham gauge) are given in Figure 5. There are apparently three different sections to the response curves for both gases. Furthermore, the slopes of the helium and nitrogen curves do not agree over the low pressure region of these characteristics.

The relationships between cathode current and anode voltage with constant magnetic field and constant pressure are shown in Figure 6. The upper curve (2.5 x 10^{-10} torr) shows that between 4500 and 7000 volts the anode voltage has little influence on the cathode current.

Curves 1 and 2 show that an increase in anode potential

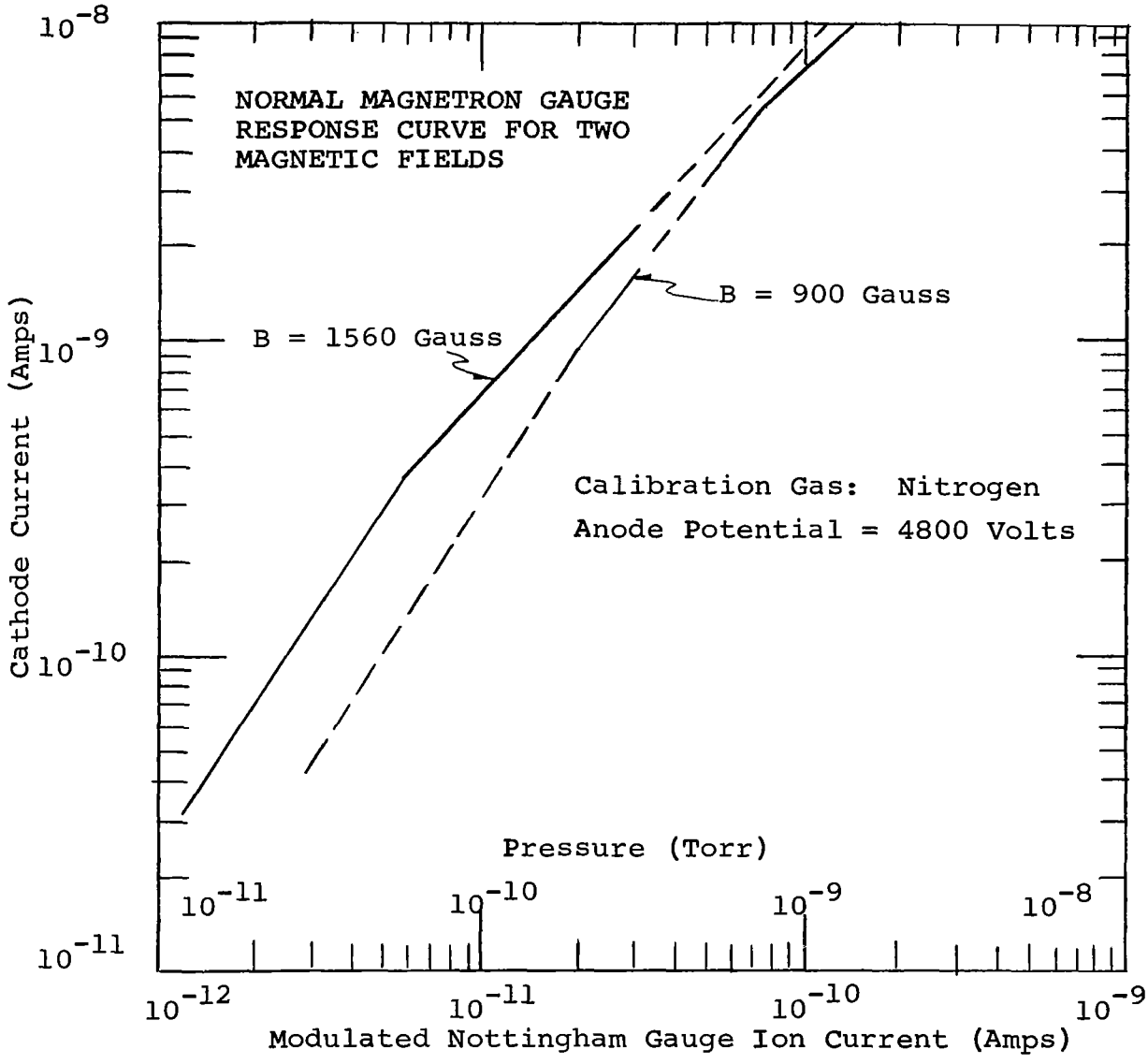
NORMAL MAGNETRON GAUGE
RESPONSE CURVE FOR TWO
MAGNETIC FIELDS
B = 900 Gauss
B = 1560 Gauss
Calibration Gas: Nitrogen
Anode Potential = 4800 Volts
Cathode Current (Amps)
10-8
10-9
10-10
10-11
Pressure (Torr)
10-11
10-10
10-9
10-8
10-12
10-11
10-10
10-9
Modulated Nottingham Gauge Ion Current (Amps)

FIGURE 4

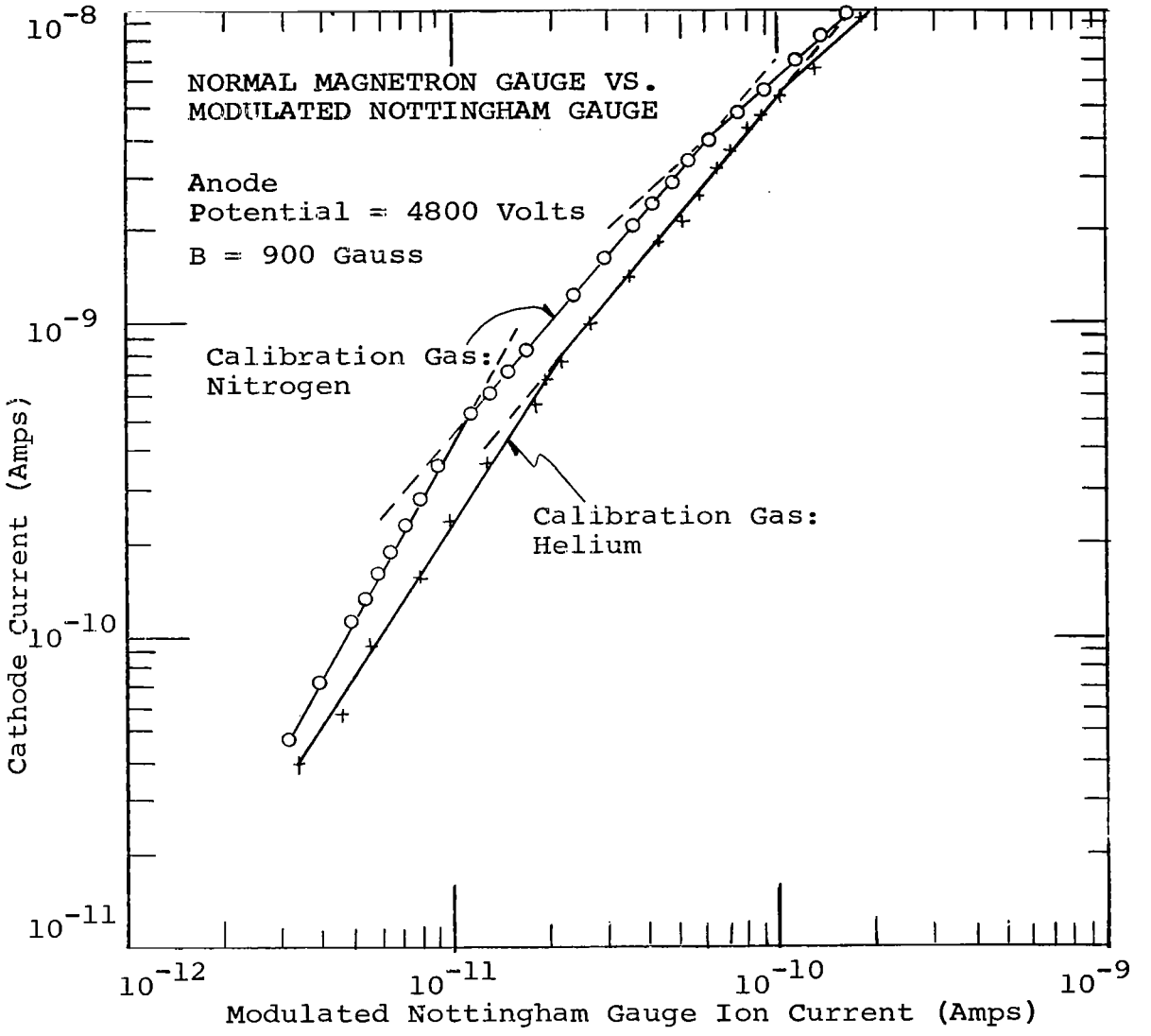
NORMAL MAGNETRON GAUGE VS.
MODULATED NOTTINGHAM GAUGE
Anode
Potential = 4800 Volts
B = 900 Gauss
Calibration Gas:
Nitrogen
Calibration Gas:
Helium
Cathode Current (Amps)
Modulated Nottingham Gauge Ion Current (Amps)
10^-8
10^-9
10^-10
10^-11
10^-12
10^-11
10^-10
10^-9

FIGURE 5

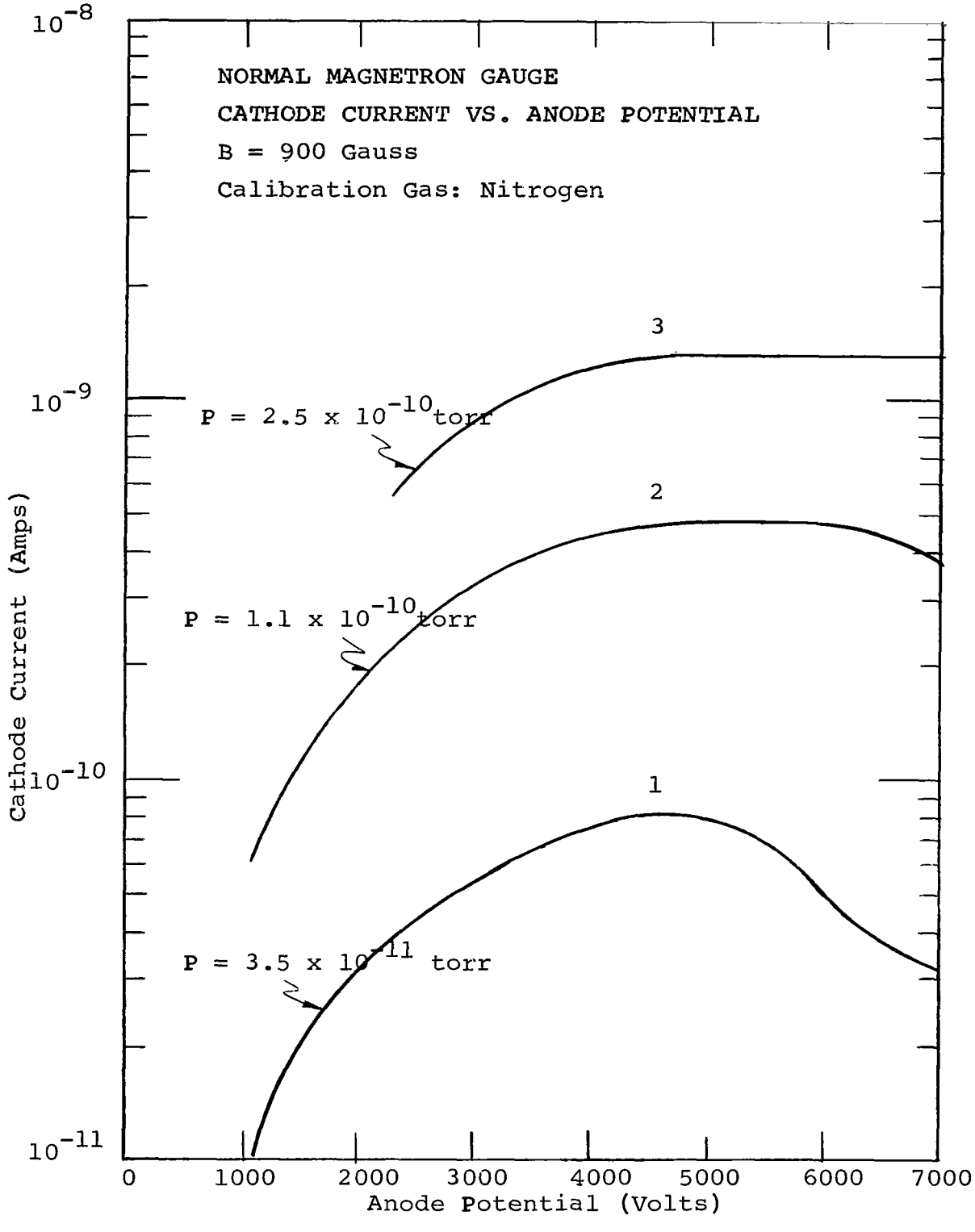
NORMAL MAGNETRON GAUGE
CATHODE CURRENT VS. ANODE POTENTIAL
B = 900 Gauss
Calibration Gas: Nitrogen
3
2
1
P = 2.5 x 10^-10 torr
P = 1.1 x 10^-10 torr
P = 3.5 x 10^-11 torr
Cathode Current (Amps)
10^-8
10^-9
10^-10
10^-11
0
1000
2000
3000
4000
5000
6000
7000
Anode Potential (Volts)

FIGURE 6

reduces the cathode current and that at lower pressures this reduction is more pronounced. Curves 1 and 2 were taken in the pressure region of non-linear response, while Curve 3 was taken just above the transition pressure in the linear response region.

Cathode and auxiliary cathode currents were both measured as a function of pressure. The results are shown in Figure 7. It will be noted that the auxiliary cathode current is a linear function of pressure in the range where the main cathode current departs from linearity. Also the auxiliary cathode current is only about 1.5% of the main cathode current. It is apparent from these data that the auxiliary cathode collects an insignificant fraction of the ions generated in the gauge. Further, there appears to be no connection between the onset of the non-linear response of the main cathode and the response of the auxiliary cathode. From the data of Figures 4, 5, and 6, and from the noise characteristics, it is concluded that the most desirable operating parameters for the normal magnetron are: Magnetic field between 1000 and 1050 gauss, and anode potential between 4500 and 5000 volts. Operation in this region not only gives lower noise, but also results in only one change in the slope of the gauge response curve.

3.2.1.2 Results of Pressure Ratio Studies in XHV

Two separate experiments were completed for an NRC 552 Redhead magnetron gauge tubulated onto the experimental chamber within the XHV system. The gauge was operated at 4500 volts with a magnet of field strength 1020 gauss. The results are presented in Figure 8. The slope of the response curve is 1.44 for magnetron cathode currents of less than 1×10^{-9} amps. For both experiments the results coincided for magnetron cathode currents greater than 4×10^{-13} amps. Lower currents could not be obtained while the nude

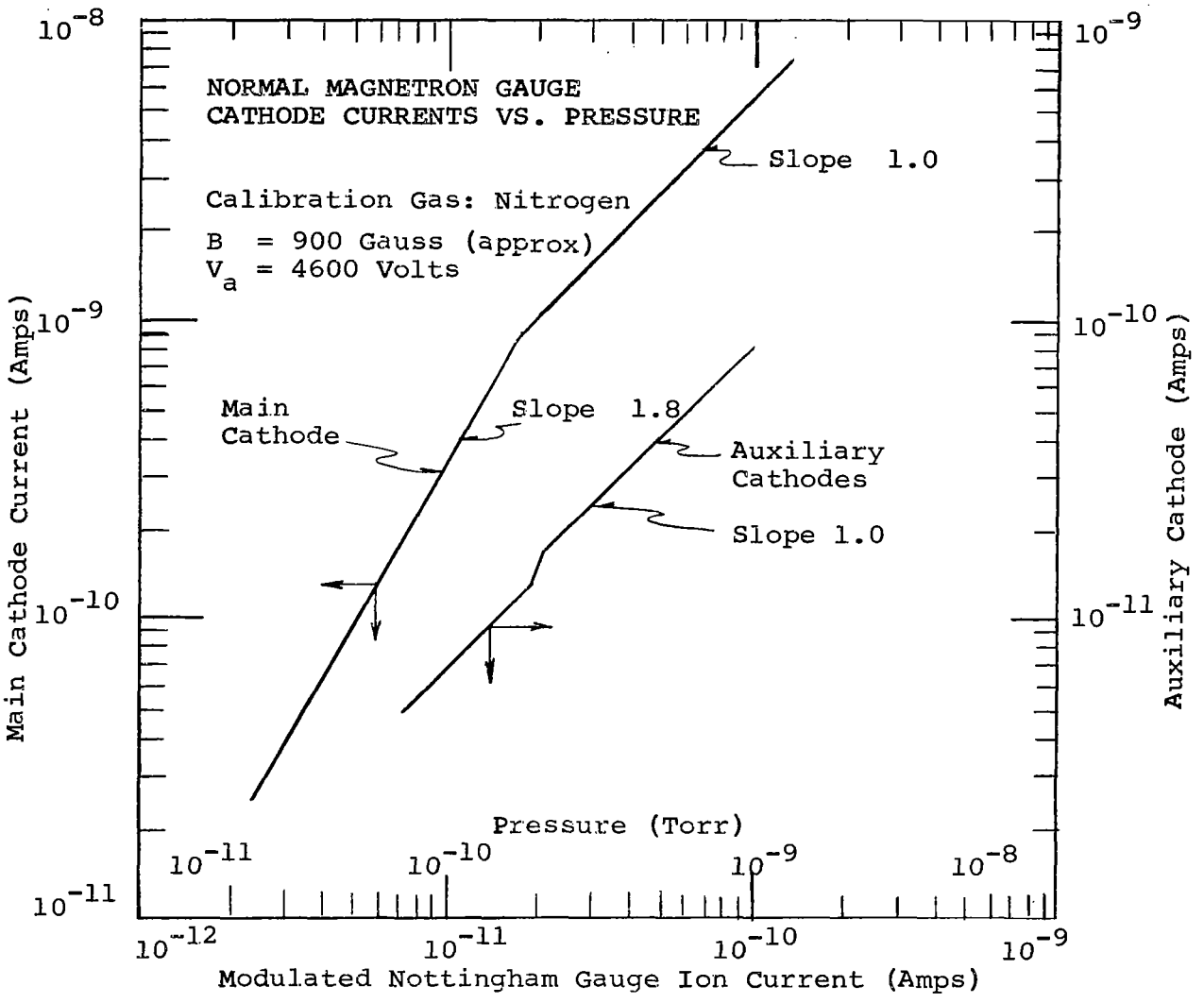
NORMAL MAGNETRON GAUGE
CATHODE CURRENTS VS. PRESSURE
Calibration Gas: Nitrogen
B = 900 Gauss (approx)
V_a = 4600 Volts
Slope 1.0
Main Cathode
Slope 1.8
Auxiliary Cathodes
Slope 1.0
Main Cathode Current (Amps)
Auxiliary Cathode (Amps)
Pressure (Torr)
Modulated Nottingham Gauge Ion Current (Amps)
10^{-8}
10^{-9}
10^{-10}
10^{-11}
10^{-12}

FIGURE 7

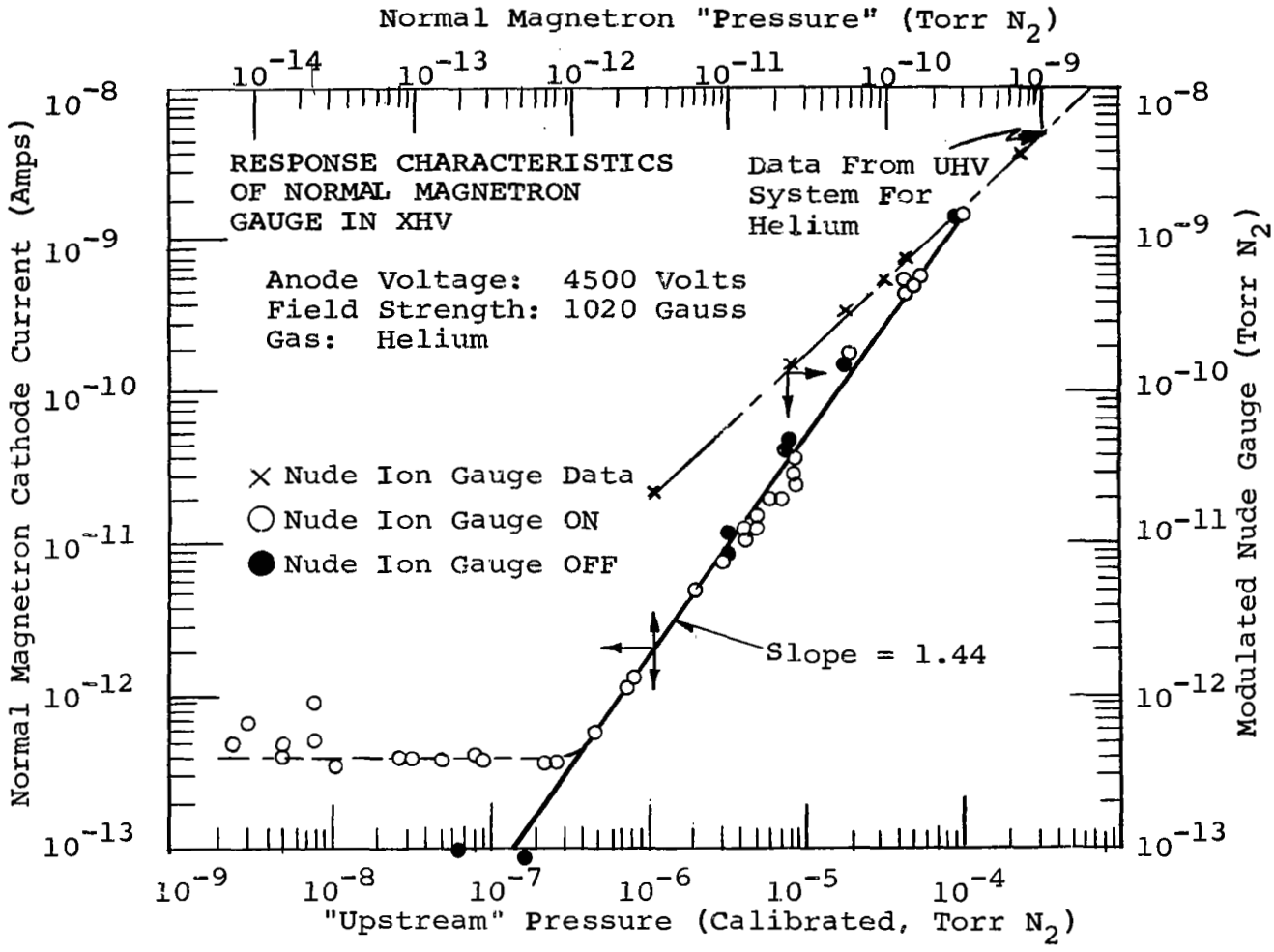
Normal Magnetron "Pressure" (Torr N_2)
10^{-14}
10^{-13}
10^{-12}
10^{-11}
10^{-10}
10^{-9}
RESPONSE CHARACTERISTICS
OF NORMAL MAGNETRON
GAUGE IN XHV
Data From UHV
System For
Helium
Anode Voltage: 4500 Volts
Field Strength: 1020 Gauss
Gas: Helium
× Nude Ion Gauge Data
○ Nude Ion Gauge ON
● Nude Ion Gauge OFF
Slope = 1.44
Normal Magnetron Cathode Current (Amps)
10^{-8}
10^{-9}
10^{-10}
10^{-11}
10^{-12}
10^{-13}
Modulated Nude Gauge (Torr N_2)
10^{-9}
10^{-8}
10^{-7}
10^{-6}
10^{-5}
10^{-4}
"Upstream" Pressure (Calibrated, Torr N_2)

FIGURE 8

ion gauge was operating even though the magnetron and ion gauges were separated by a cold baffle. Cathode currents down to 9×10^{-14} amps were relatively consistent with the higher pressure data when the ion gauge was not operating. These results suggest that even in a system with high pumping speeds it is difficult to eliminate the gas desorption caused by hot filament ion gauges so that very low molecular densities may be obtained. Although the normal magnetron gauge under test was tubulated to the copper chamber it was not isothermal with it. The gauge operated at 175°K while the average copper chamber temperature was controlled at 10°K. Consequently, the number density of helium atoms in the gauge volume was less than that in the experimental chamber. The thermal transpiration correction factor was equal to $(10/175)^{1/2}$. Making this allowance, the atom number density ratio between the "upstream" gauge and the magnetron gauge under test was 3.1×10^{5}. The upper pressure scale in Figure 8 (magnetron "pressure") was located in accordance with this ratio. The data suggest that the calibration procedure is satisfactory to at least 4×10^{-13} torr. Values above 10^{-4} torr for the "upstream" pressure were not useful because the gauge became non-linear in this region.

The extension of the useful range of the normal magnetron gauge below 9×10^{-14} amps or approximately 3×10^{-13} torr is largely a problem of low current measurement techniques. Electrical noise, dielectric absorption and leakage currents are the principal problems.

3.2.2 Inverted Magnetron Studies

The inverted magnetron is a potentially useful total pressure gauge for the XHV range. This gauge has been described by Hobson and Redhead[2]. It has the inverse geometry of the normal magnetron gauge. It requires a higher magnetic field and higher anode voltages to operate satisfactorily.

It is known to have a non-linear, pressure-current response curve. This response curve is, however, a more nearly linear function than that of the normal magnetron in its non-linear range. For this reason, it was anticipated that the inverted magnetron might have a higher sensitivity in the XHV pressure ranges than does the normal magnetron. It was also possible that the inverted magnetron was less noisy than the normal magnetron. This factor is of great importance in measuring the low currents associated with very low pressures.

In the course of this program five different inverted magnetron gauges were studied. They were designated as follows:-

MARK I: This gauge was loaned by the National Research Council of Canada. It was broken in transit and required a welding repair to the gauge structure.

MARK II: This gauge was a rebuilt version of MARK I using a new base, new envelope and new mounting.

MARK III: This gauge was a completely new gauge with new base, new gauge elements, new mounting and new envelope. It had a grounded platinum metal coating on parts of the inside of the glass envelope.

MARK IV: This gauge was MARK III with the platinum coating removed.

MARK V: This gauge was again a completely rebuilt gauge using a new base, new envelope, new mountings and new metal parts. It was fabricated to permit rigorous chemical cleaning of all parts and vacuum firing. In the design, emphasis was given to reducing possible leakage currents from the anode to the cathode.

3.2.2.1 Results of Cross-Calibration Studies of Inverted Magnetron

The MARK I inverted magnetron was used with a magnet of 1560 gauss field strength to obtain the data shown in Figure 9 for nitrogen. An extrapolation of the Hobson and Redhead data is also shown on this graph. The lower portion of this curve shows a change in slope of the pressure-current characteristics - a result which was apparently peculiar to this particular gauge. Later versions of the gauge did not give a change in slope. Two other things are noteworthy concerning these data. The sensitivity of the gauge was lower and the slope greater than reported by Hobson and Redhead[2]. Since the anode was not perfectly central within the magnetron cage, it was decided that the above results perhaps were not typical. Consequently, MARK II was built.

The MARK II variation of the gauge was used to study the anode voltage-cathode current characteristics at a number of nitrogen pressures between 1×10^{-8} torr and 2×10^{-11} torr. The results are shown in Figure 10.

The differences between anode characteristics of the normal magnetron gauge and the inverted magnetron gauge are worthy of note. See Figure 6. The inverted magnetron did not exhibit a decrease in cathode current as the anode voltage was increased above a certain value at low pressure as did the normal magnetron.

Figure 11 is also a plot of the inverted magnetron characteristics and shows the influence of anode voltage on the sensitivity of the gauge and the slope of its response characteristic. There was no apparent change in the slope between 6.0 KV and 3.0 KV. The sensitivity of the gauge (at constant pressure) did not increase substantially for anode potentials above 6.0KV. Ths slope of the response curves shown in Figure 11 are in good agreement with data shown in Figure 10. The curves shown in Figure 11 are not

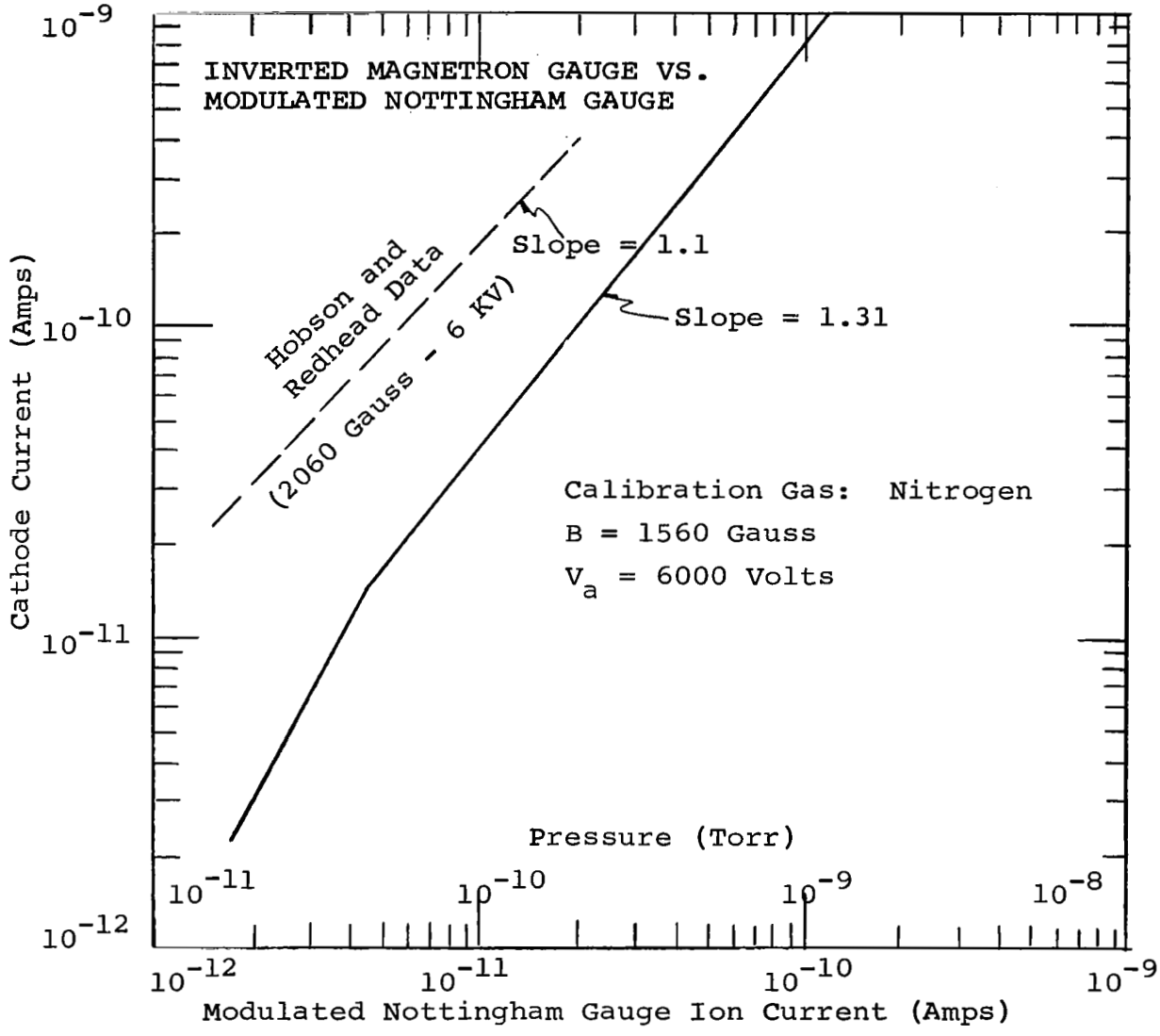
INVERTED MAGNETRON GAUGE VS.
MODULATED NOTTINGHAM GAUGE
Hobson and Redhead Data
(2060 Gauss - 6 KV)
Slope = 1.1
Slope = 1.31
Calibration Gas: Nitrogen
B = 1560 Gauss
V_a = 6000 Volts
Cathode Current (Amps)
10^{-9}
10^{-10}
10^{-11}
10^{-12}
Pressure (Torr)
10^{-11}
10^{-10}
10^{-9}
10^{-8}
10^{-12}
10^{-11}
10^{-10}
10^{-9}
Modulated Nottingham Gauge Ion Current (Amps)

FIGURE 9

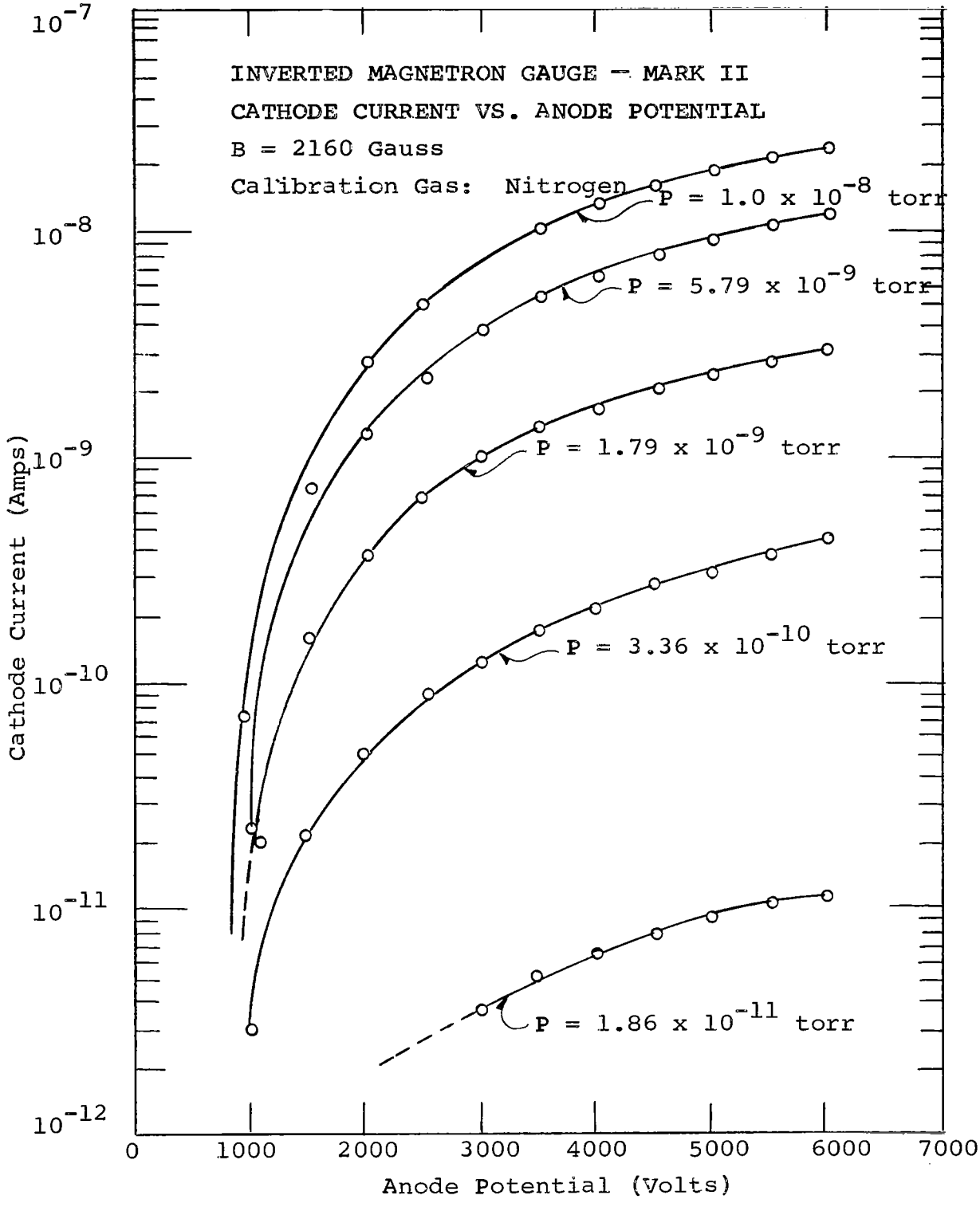
INVERTED MAGNETRON GAUGE — MARK II
CATHODE CURRENT VS. ANODE POTENTIAL
B = 2160 Gauss
Calibration Gas: Nitrogen
P = 1.0 x 10^-8 torr
P = 5.79 x 10^-9 torr
P = 1.79 x 10^-9 torr
P = 3.36 x 10^-10 torr
P = 1.86 x 10^-11 torr
Cathode Current (Amps)
10^-7
10^-8
10^-9
10^-10
10^-11
10^-12
0
1000
2000
3000
4000
5000
6000
7000
Anode Potential (Volts)

FIGURE 10

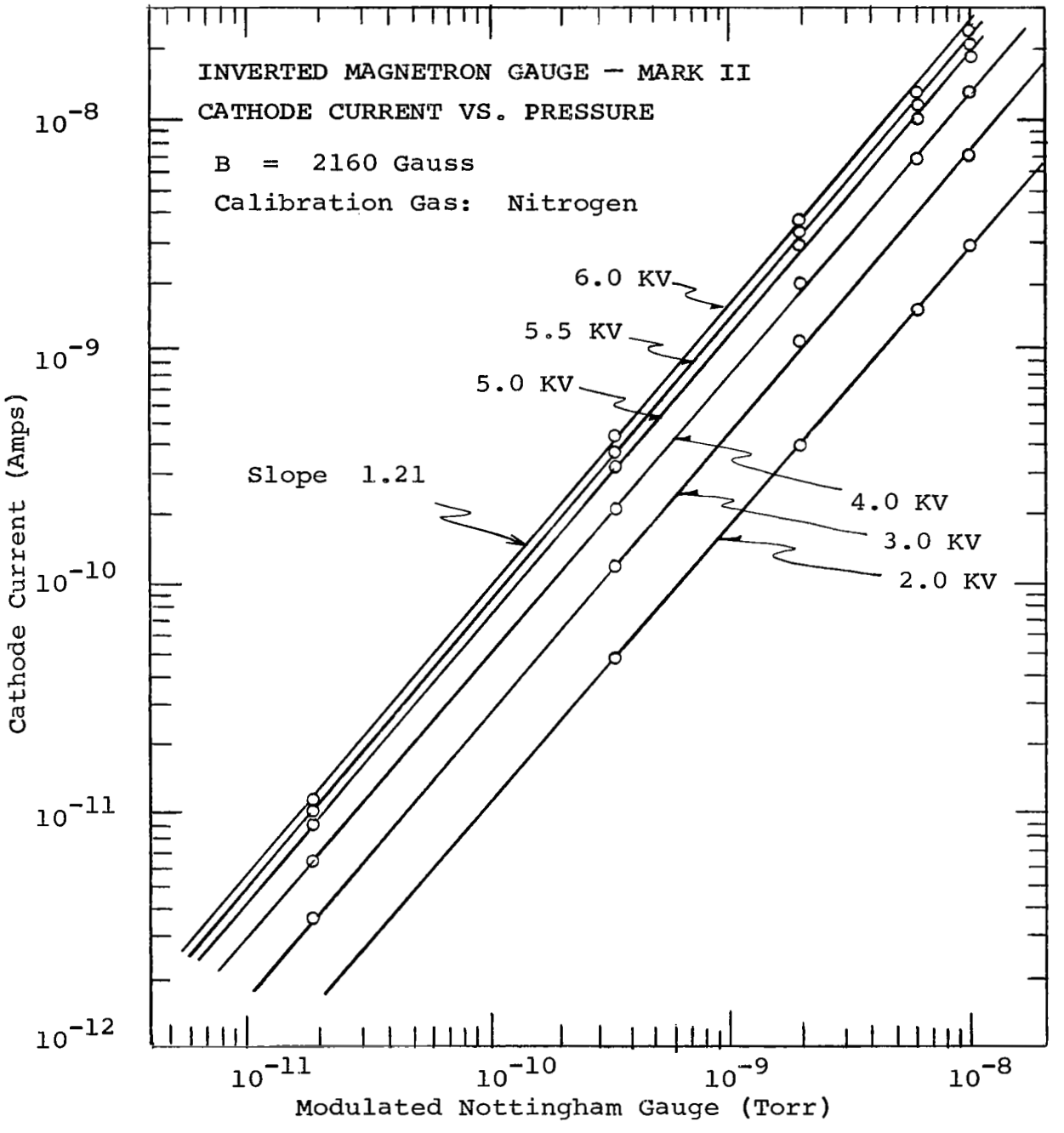
INVERTED MAGNETRON GAUGE — MARK II
CATHODE CURRENT VS. PRESSURE
B = 2160 Gauss
Calibration Gas: Nitrogen
6.0 KV
5.5 KV
5.0 KV
Slope 1.21
4.0 KV
3.0 KV
2.0 KV
Cathode Current (Amps)
10^-8
10^-9
10^-10
10^-11
10^-12
10^-11
10^-10
10^-9
10^-8
Modulated Nottingham Gauge (Torr)

FIGURE 11

in good agreement with published data by Hobson and Redhead[2] who showed a slope of 1.10 for the pressure current relationship at 6000 volts. The data of Figure 11 are more closely matched by a slope of 1.20. However, the sensitivity of this gauge was in good agreement at 10^{-8} torr with the Hobson and Redhead value of 2.5 amps/torr at 6 KV.

The response of the MARK II inverted magnetron gauge did not exhibit a constant ratio of helium-to-air sensitivity. This effect could be very important to the XHV experiments on the inverted gauge and therefore was examined during this investigation. Figure 12 shows the response curves for helium and nitrogen compared with the modulated Nottingham gauge. From the known nitrogen sensitivity and the helium to nitrogen ionization efficiency ratio, the sensitivity of the modulated Nottingham gauge for helium was computed to be 0.014 amps/torr. The measured sensitivity of the inverted magnetron for helium was then 0.12 amps/torr at 10^{-9} torr.

A second helium calibration performed approximately two months later yielded similar results as shown in Figure 12. Both the slope and sensitivity of the gauge had not changed substantially during this time although the magnet had been removed and the gauge baked repeatedly. It appeared that the characteristics of this gauge were repetitive.

The MARK III and MARK IV variations of the inverted magnetron gauge were used to obtain further data on the nitrogen sensitivity of this type of gauge. The data shown in Figure 13 however, do not agree with the previous nitrogen data shown in Figure 12. The anode voltage and magnetic field for the gauge were carefully set before the experiments and remained unchanged. However, the nature of the platinum coating on the inside of the glass envelope affected the results considerably because of field emission from the anode to the coating. The coating was originally applied to fix the envelope potential of the gauge and to electrostatically shield the gauge. However, during the initial start-up the

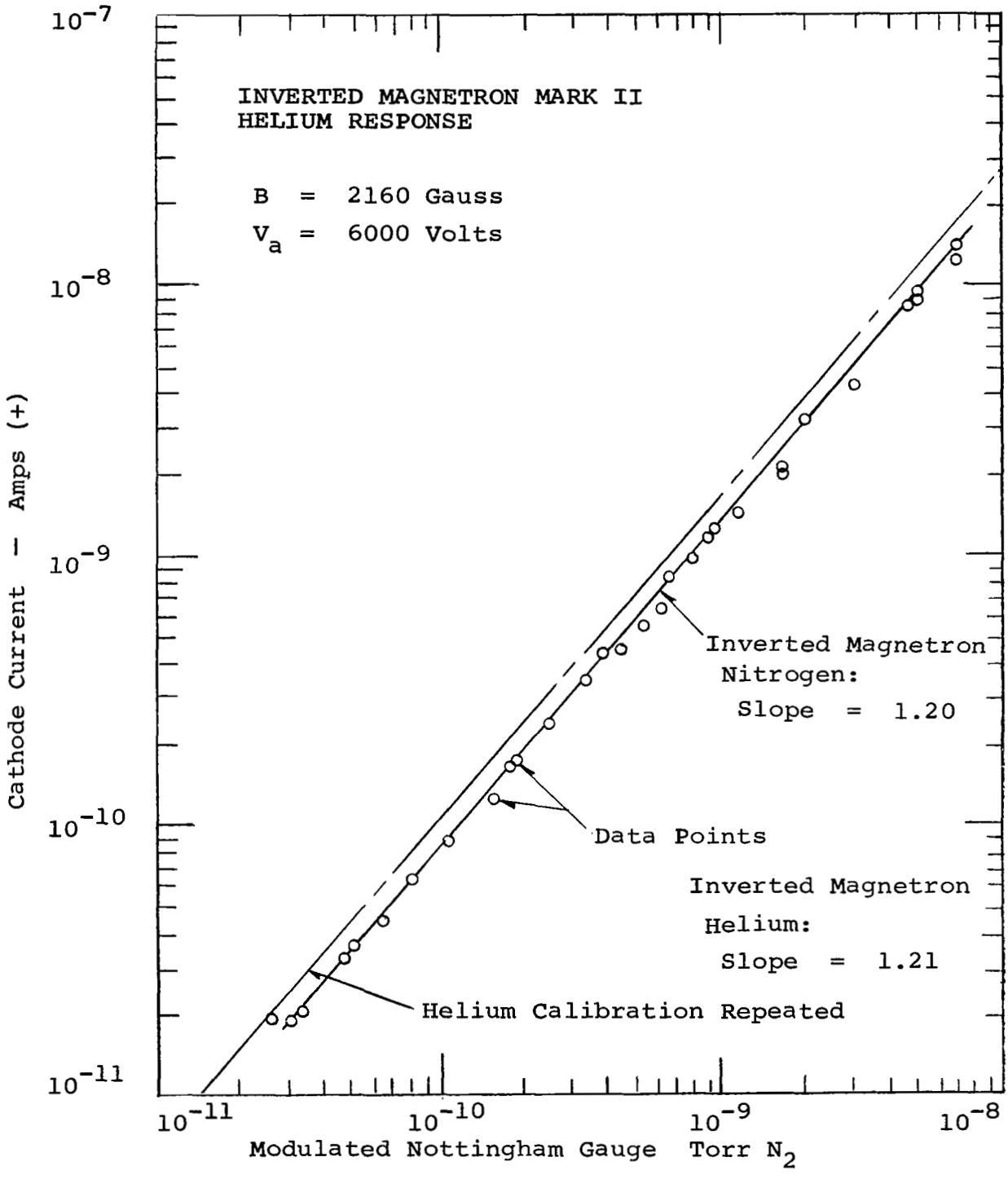
INVERTED MAGNETRON MARK II
HELIUM RESPONSE
B = 2160 Gauss
V_a = 6000 Volts
Inverted Magnetron
Nitrogen:
Slope = 1.20
Data Points
Inverted Magnetron
Helium:
Slope = 1.21
Helium Calibration Repeated
Cathode Current - Amps (+)
10^{-7}
10^{-8}
10^{-9}
10^{-10}
10^{-11}
10^{-11}
10^{-10}
10^{-9}
10^{-8}
Modulated Nottingham Gauge Torr N_2

FIGURE 12

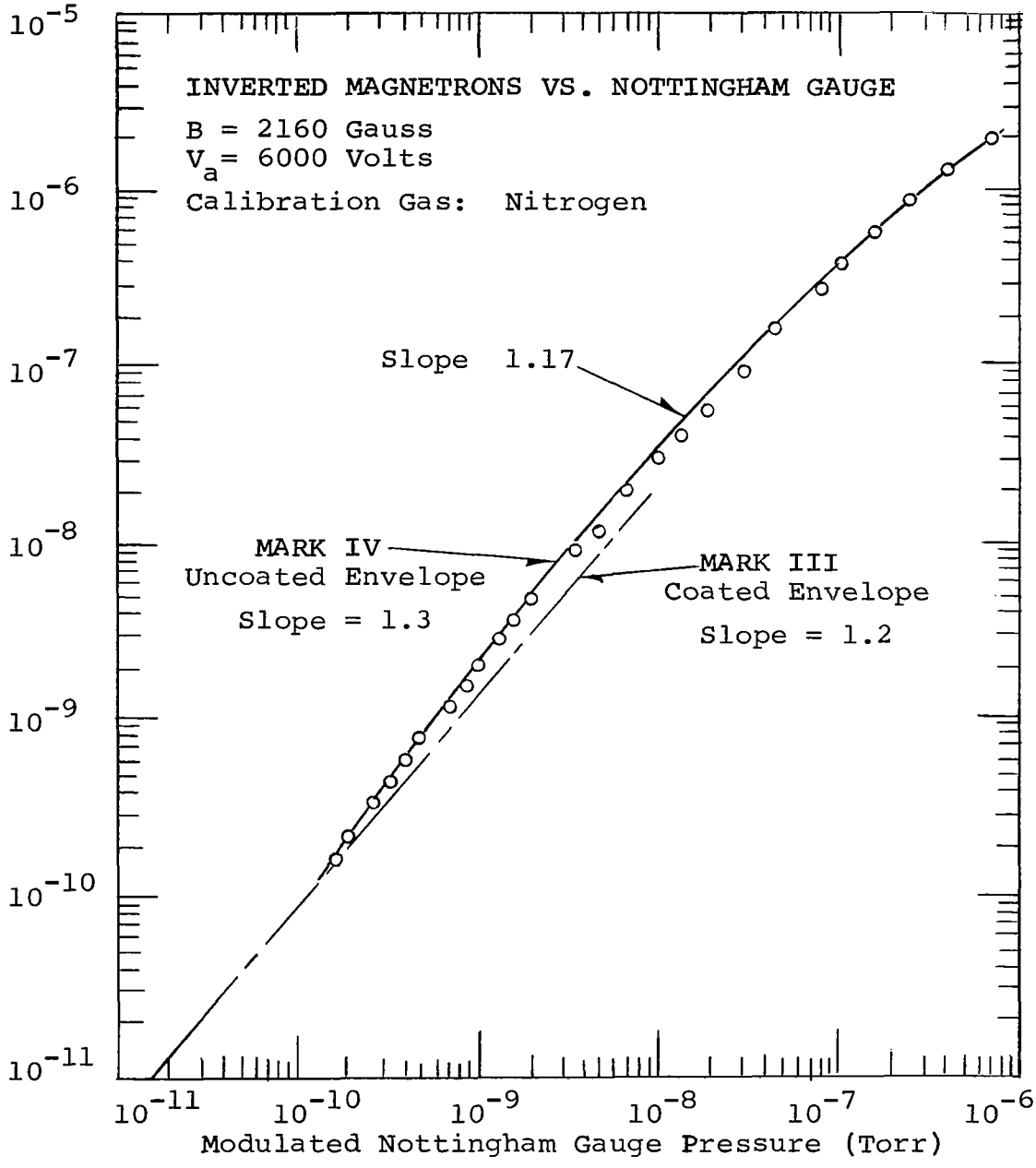
INVERTED MAGNETRONS VS. NOTTINGHAM GAUGE
B = 2160 Gauss
V_a = 6000 Volts
Calibration Gas: Nitrogen
Slope 1.17
MARK IV
Uncoated Envelope
Slope = 1.3
MARK III
Coated Envelope
Slope = 1.2
10^{-5}
10^{-6}
10^{-7}
10^{-8}
10^{-9}
10^{-10}
10^{-11}
10^{-11} 10^{-10} 10^{-9} 10^{-8} 10^{-7} 10^{-6}
Modulated Nottingham Gauge Pressure (Torr)

FIGURE 13

discharge refused to "strike" at potentials higher than 3800 volts and it would also extinguish itself if the anode potential was raised above this point once the gauge had started. As the anode potential was raised above 4500 volts, a pronounced field emission current was observed in the auxiliary cathodes after the discharge stopped. A Tesla spark coil was used to reduce the susceptibility of the gauge to field emission and the gauge then operated successfully up to 7000 volts.

The leakage and field emission currents in the inverted magnetron were studied without the magnetic field from 1000 volts to 6000 volts. A small negative current of the order of 10^{-13} amps was observed at low voltage which reduced and changed sign to a positive current of approximately 2×10^{-13} amperes as the anode voltage was increased to 6000 volts. This was interpreted to mean that a leakage current across the glass base of the tube predominated at low voltage and emission current predominated at higher voltages.

3.2.2.2 Results of Pressure Ratio Studies of Inverted Magnetron Gauge

The MARK IV variation of the inverted magnetron was installed in the XHV system. It was tubulated to the test chamber and operated at 6000 volts with a magnet of field strength 1925 gauss. The results were inconclusive. At cathode currents of less than 10^{-11} amps (the minimum shown in Figure 11 for the study of the UHV system) noise increased to a level which rendered electrometer current measurements quite dubious.

Since it is possible that an intermittent breakdown of the anode insulation was occurring in this gauge, its operation was not considered typical. The MARK V gauge was then fabricated for the remainder of the studies.

The major improvements incorporated in the new gauge were:—

1. No high voltage was applied to the base of the gauge. The general arrangement of the gauge is shown in Figure 14. It will be noted that the glass leakage distance between the anode and the cathode was increased to almost the whole length of the gauge.

2. Extreme care was used in fabricating the metal parts of the gauge. Special attention was given to polishing in order to reduce possible noise from field emission.

3. Special chemical cleaning methods were used to clean both the envelope and metal parts. This was followed by vacuum firing of the metal parts of the gauge using induction heating. The gauge elements were heated to approximately 900°C at 1×10^{-6} torr for several hours. Higher temperatures and lower pressures could not be used because of excessive evaporation rate of the metal parts.

Following construction and cleaning, the gauge was given a series of preliminary tests, both with and without magnetic fields. In the absence of a magnetic field, leakage currents were found to be very low and limited by the surface conductivity on the external regions of the gauge. With the magnetic field applied the gauge was operated down to 5×10^{-8} torr. The gauge sensitivity was close to that previously obtained with inverted magnetrons under similar conditions of voltage, magnetic field, and pressure.

This gauge was then installed in the XHV system. A magnet with a field strength of 2120 gauss at the center of the pole faces was used with the gauge. Data were obtained for three anode voltages; 4000 volts, 5000 volts, and 6000 volts. The data for 4000 volts and 5000 volts are shown in Figure 15. The data for 6000 volts are shown in Figure 16.

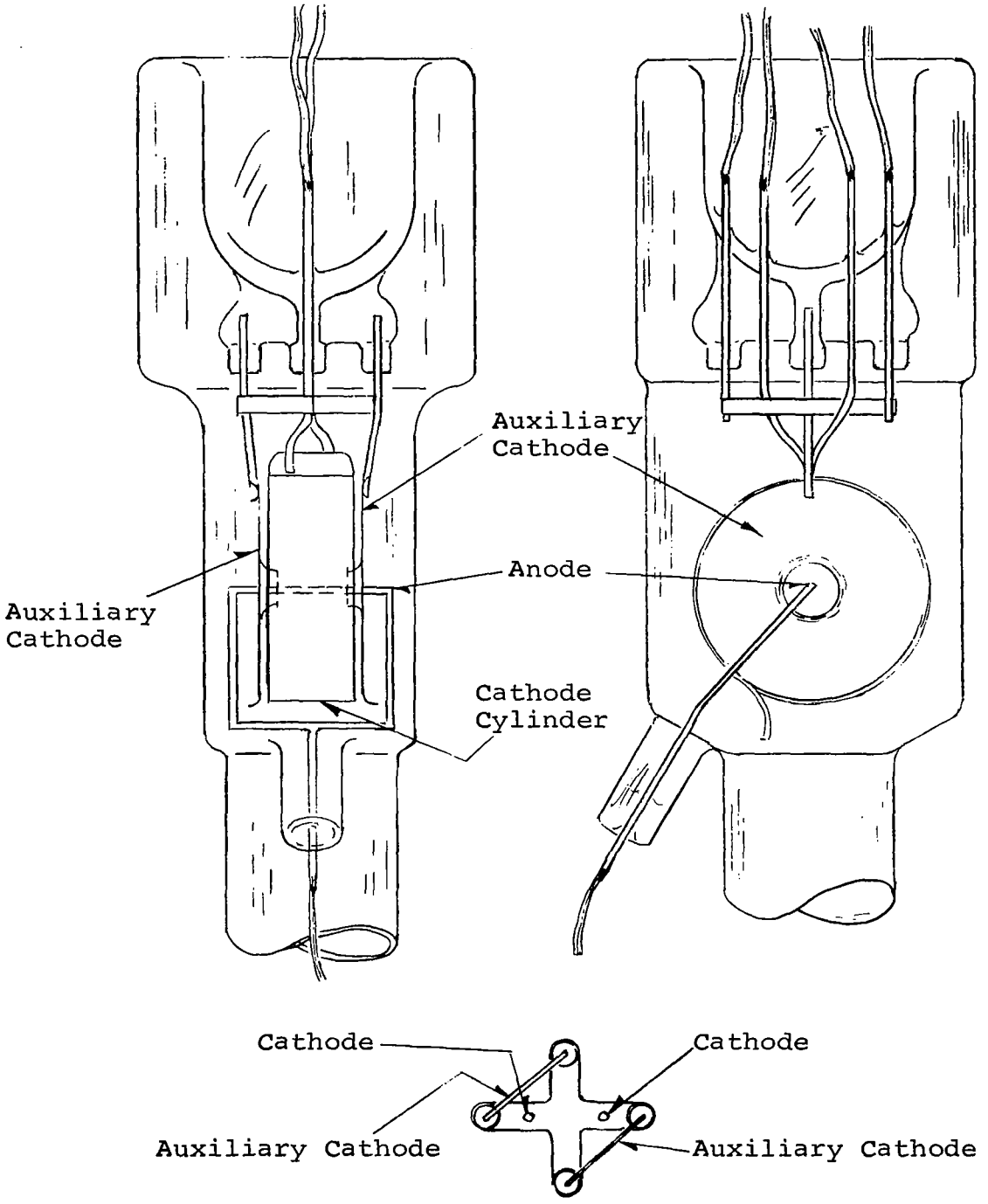

FIGURE 14 INVERTED MAGNETRON — NEW DESIGN (MARK V)

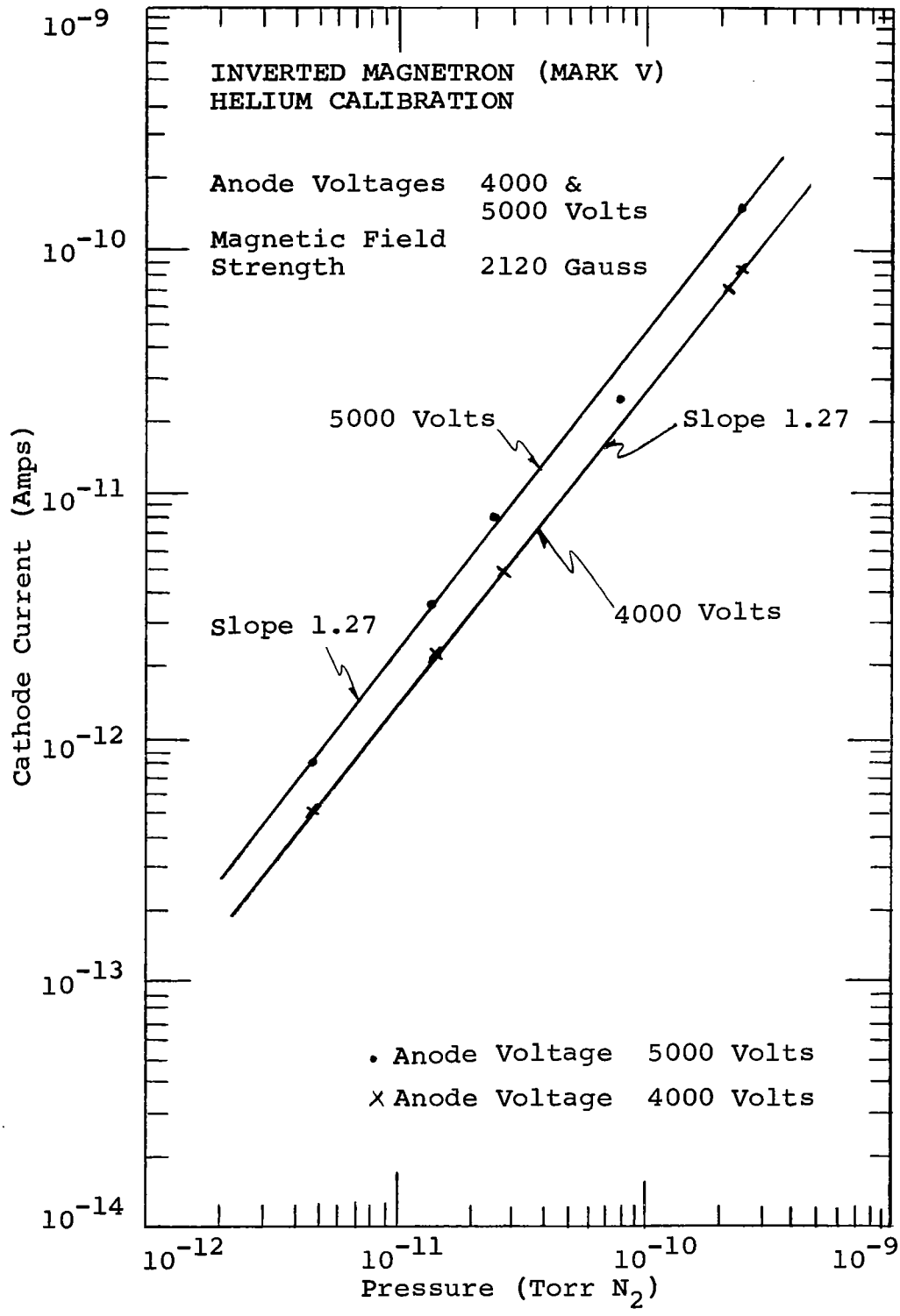
INVERTED MAGNETRON (MARK V)
HELIUM CALIBRATION
Anode Voltages 4000 & 5000 Volts
Magnetic Field Strength 2120 Gauss
5000 Volts
Slope 1.27
Slope 1.27
4000 Volts
• Anode Voltage 5000 Volts
X Anode Voltage 4000 Volts
Cathode Current (Amps)
Pressure (Torr N_2)
10^{-9}
10^{-10}
10^{-11}
10^{-12}
10^{-13}
10^{-14}
10^{-12}
10^{-11}
10^{-10}
10^{-9}

FIGURE 15

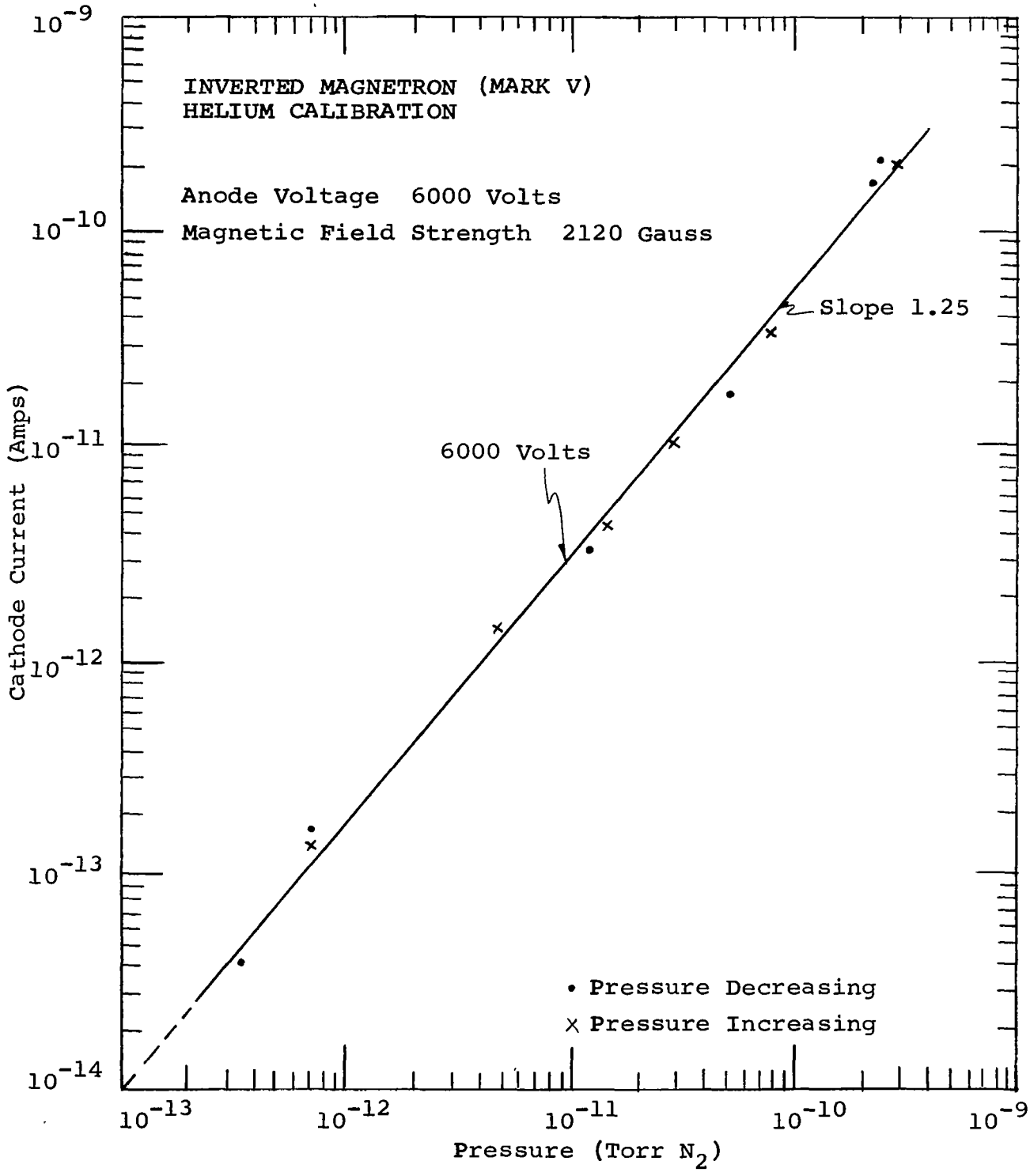
INVERTED MAGNETRON (MARK V)
HELIUM CALIBRATION
Anode Voltage 6000 Volts
Magnetic Field Strength 2120 Gauss
Slope 1.25
6000 Volts
• Pressure Decreasing
× Pressure Increasing
Cathode Current (Amps)
Pressure (Torr N_2)
10^{-9}
10^{-10}
10^{-11}
10^{-12}
10^{-13}
10^{-14}
10^{-13}
10^{-12}
10^{-11}
10^{-10}
10^{-9}

FIGURE 16

For this calibration the ratio of the upstream pressure to the pressure in the copper chamber was measured by means of the nude modulated gauge. The ratio of the pressures (torr N_2) was 7.3×10^4. The average temperature of the magnetron volume during the test was 218°K. The thermal transpiration corrections have been applied in Figures 15 and 16.

The Wayne-Kerr Dynamic Capacitor electrometer was used to measure the ion currents in this test.

However, during the test, a period of erratic and inconsistent performance was experienced. A low resistance leakage path occurred in the ion collector circuit. This was removed by using high voltage (Tesla) discharge to the collector. Consistent gauge performance again occurred after the high polarization charges had bled off. After the test, the collector circuit was thoroughly checked. The most likely cause of the trouble was traced to a slight deposit which was found to have formed on a ceramic passthrough. This passthrough is not heated to the maximum temperatures used during system bakeout. It is possible that contaminants collected on the passthrough and produced the intermittent "short".

Because the results were not conclusive a second XHV pressure ratio experiment was carried out.

Both the Wayne-Kerr and Keithley 410 electrometers were used for collector current measurement. Following the test, the gauge and magnet were removed from the XHV system. The magnet was found to have a field strength of 1960 gauss at the center of the pole faces. The results obtained for the run are shown in Figures 17 and 18.

In general, this model of the inverted magnetron had performance characteristics which were much superior to the gauges tested previously. It had good signal to background ratios in the 10^{-12} torr range; but like the normal magnetron, the signal to background ratio became approximately unity at 3×10^{-13} torr N_2. The gauge continued to operate at lower

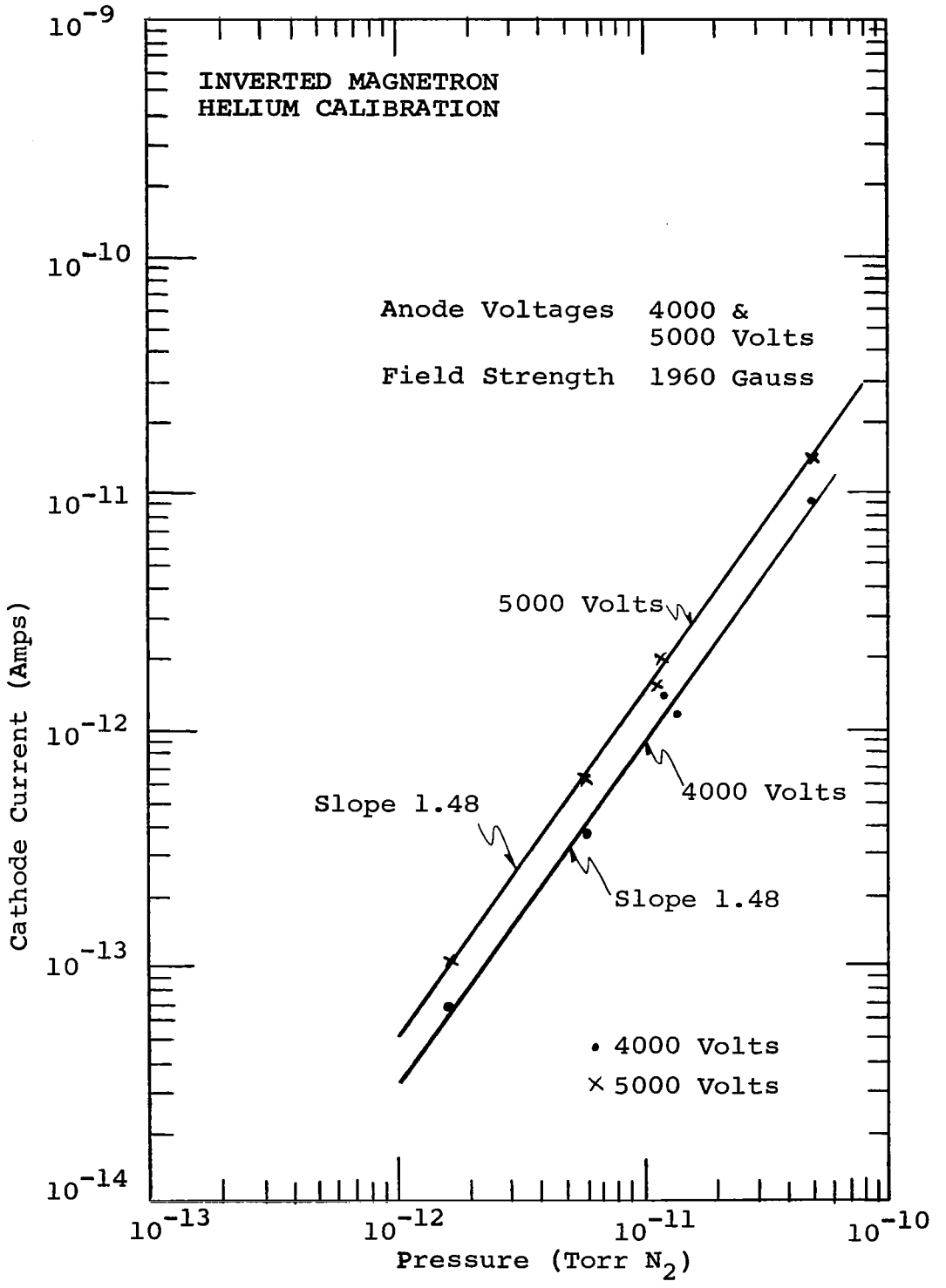
INVERTED MAGNETRON
HELIUM CALIBRATION
Anode Voltages 4000 &
5000 Volts
Field Strength 1960 Gauss
5000 Volts
4000 Volts
Slope 1.48
Slope 1.48
• 4000 Volts
× 5000 Volts
Cathode Current (Amps)
Pressure (Torr N_2)
10^{-9}
10^{-10}
10^{-11}
10^{-12}
10^{-13}
10^{-14}
10^{-13}
10^{-12}
10^{-11}
10^{-10}

FIGURE 17

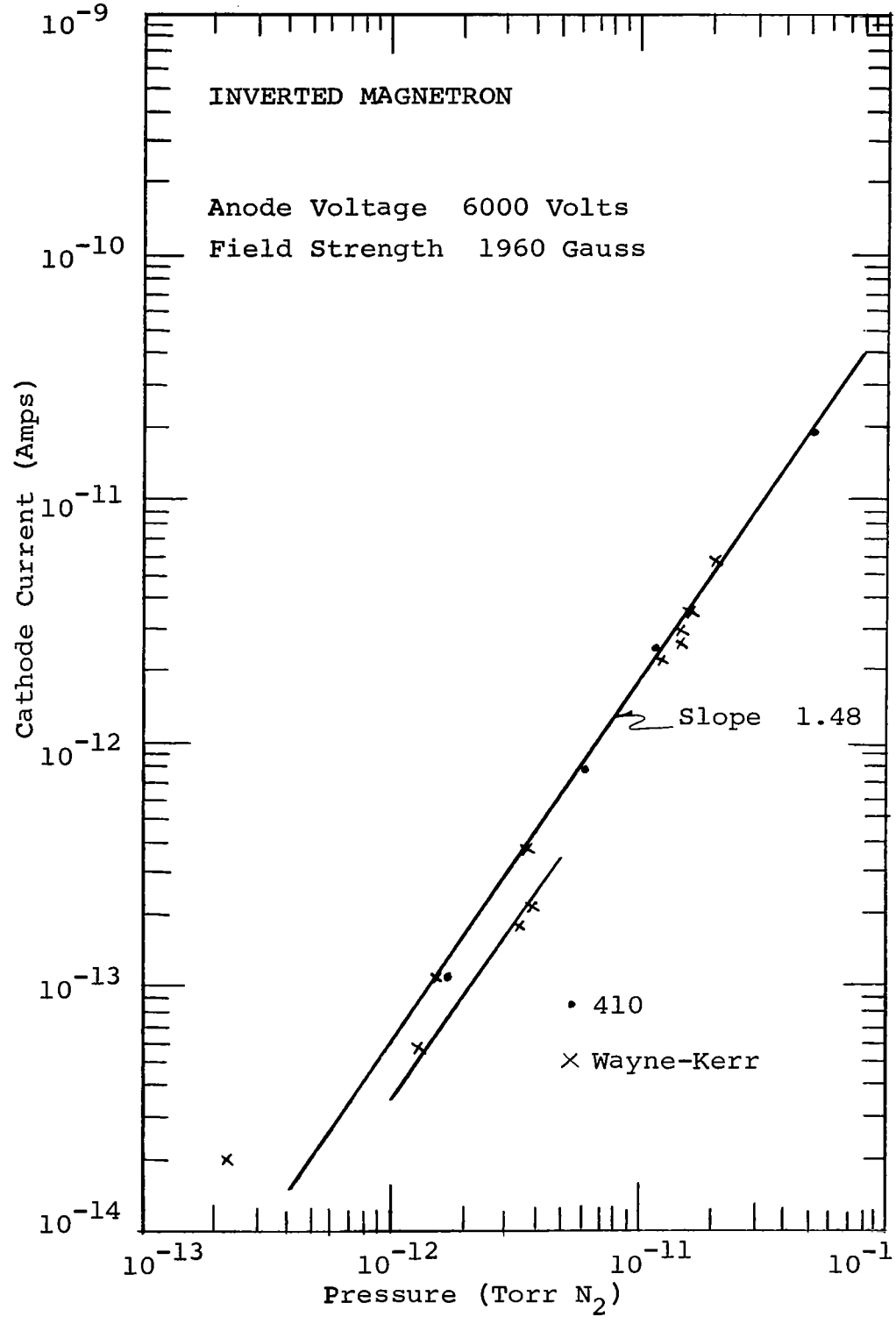
INVERTED MAGNETRON
Anode Voltage 6000 Volts
Field Strength 1960 Gauss
Slope 1.48
• 410
× Wayne-Kerr
Cathode Current (Amps)
Pressure (Torr N_2)
10^{-9}
10^{-10}
10^{-11}
10^{-12}
10^{-13}
10^{-14}
10^{-13}
10^{-12}
10^{-11}
10^{-10}

FIGURE 18

pressures but satisfactory calibration data could not be obtained because of noise and instabilities.

It will be noticed that the inverted magnetron was non-linear with a slope of 1.25 for the first calibration and 1.48 for the second. The slope was independent of the anode voltage but appeared to be a strong function of the magnetic field. The gauge sensitivity increased with anode voltage — the sensitivity being more than proportional to anode voltage. However, at the higher anode voltages the data points scatter more than at lower voltages. It appeared that the gauge stability decreased at conditions involving high anode voltages and lower magnetic fields. The investigation showed that the sensitivity of the inverted magnetron increased at higher anode voltages but anode voltage had little or no effect on the slope. The slope appeared to be a strong function of magnetic field. Gas composition had little or no effect when sensitivities are measured in terms of torr N_2.

During the course of this program some five different variations of the inverted magnetron design have been studied both by the gauge comparison method and the XHV pressure ratio technique. The main results of the various tests are shown in Table I. For comparison purposes data published by Hobson and Redhead[2] are also included in the table.

It will be noted that there is a wide variation in the gauge sensitivities. At comparable fields and voltages the data of Hobson and Redhead extrapolated to 10^{-10} torr suggest a sensitivity of 1.4 amps/torr. The gauge comparison method gave approximately 0.9 amps/torr at 10^{-10} torr N_2 while the pressure ratio technique gave 0.55 amp/torr. In addition, Hobson and Redhead quote a slope of 1.1 at 2060 gauss whereas the present work gave slopes between 1.2 and 1.3. Hobson and Redhead found that the slope decreased with increased magnetic field and also that gauge design considerably affected both the slope and sensitivity. It is known that

TABLE I

PERFORMANCE CHARACTERISTICS OF VARIOUS INVERTED MAGNETRON GAUGES

SUMMARY OF RESULTS

SOURCE OF DATA Gauge		SENSITIVITY Amps/torr*	Slope	VOLTAGE (volts)	MAGNETIC FIELD (gauss)	GAS
MARK I	Cross Calibration	0.39	1.88**	6000	1560	N_2
MARK II	Cross Calibration	0.9	1.21	6000	2160	N_2
MARK II	Cross Calibration	0.8	1.21	6000	2160	He
MARK III	Cross Calibration	0.9	1.20	6000	2160	N_2
MARK IV	Cross Calibration	0.9	1.30	6000	2160	N_2
MARK V	Pressure Ratio	0.55	1.25	6000	2120	He
MARK V	Pressure Ratio	0.38	1.27	5000	2120	He
MARK IV	Pressure Ratio	0.25	1.27	4000	2120	He
MARK V	Pressure Ratio	0.55	1.48	6000	1960	He
MARK V	Pressure Ratio	0.39	1.48	5000	1960	He
MARK V	Pressure Ratio	0.25	1.48	4000	1960	He
Hobson & Redhead [2]		1.4	1.10	6000	2060	N_2

* Amps/torr N_2 measured at or extrapolated to 10^{-10} torr N_2.

** Below 5×10^{-11} torr the slope was 1.88; above 5×10^{-11} it was 1.31 approx.

the permanent magnets used in this work gave considerable variation in the magnetic field strengths over the magnetron volumes. If the field used by Hobson and Redhead was more homogeneous it is not unlikely that the effective field strength of their 2060 gauss magnet would be considerably greater than the 2120 and 2160 magnets used here. This may explain the larger slopes and consequently the lower sensitivities observed in this study.

3.2.3 Suppressor Grid Gauge

3.2.3.1 Introduction

Before discussing the results of the suppressor grid gauge calibration in detail, a brief review will be given of the principle of operation[8] of the suppressor grid gauge. (See Figure 19 for a schematic illustration of the gauge and of the processes discussed below.)

Electrons from the cathode are accelerated toward the grid by the cathode-grid potential difference. A certain fraction of the electrons are immediately collected at the grid surface. However, a substantial fraction of the electron flux from the cathode passes through the grid into the ionization volume inside the grid cage. Ions are generated in this ionization volume by collisions between the electrons and neutral gas atoms or molecules in the volume. These ions are extracted from the ionization volume by the electric field in this volume established by the potential difference between the grid cage and the collector and collector shield electrodes. A substantial fraction of the ions generated are extracted and arrive at the collector. The ion arrival rate at the collector constitutes the measured ion current.

Although this is the principal mechanism of operation of the gauge, there are several secondary mechanisms which tend to render the interpretation of the measured collector current ambiguous. The auxiliary electrodes (suppressor grid

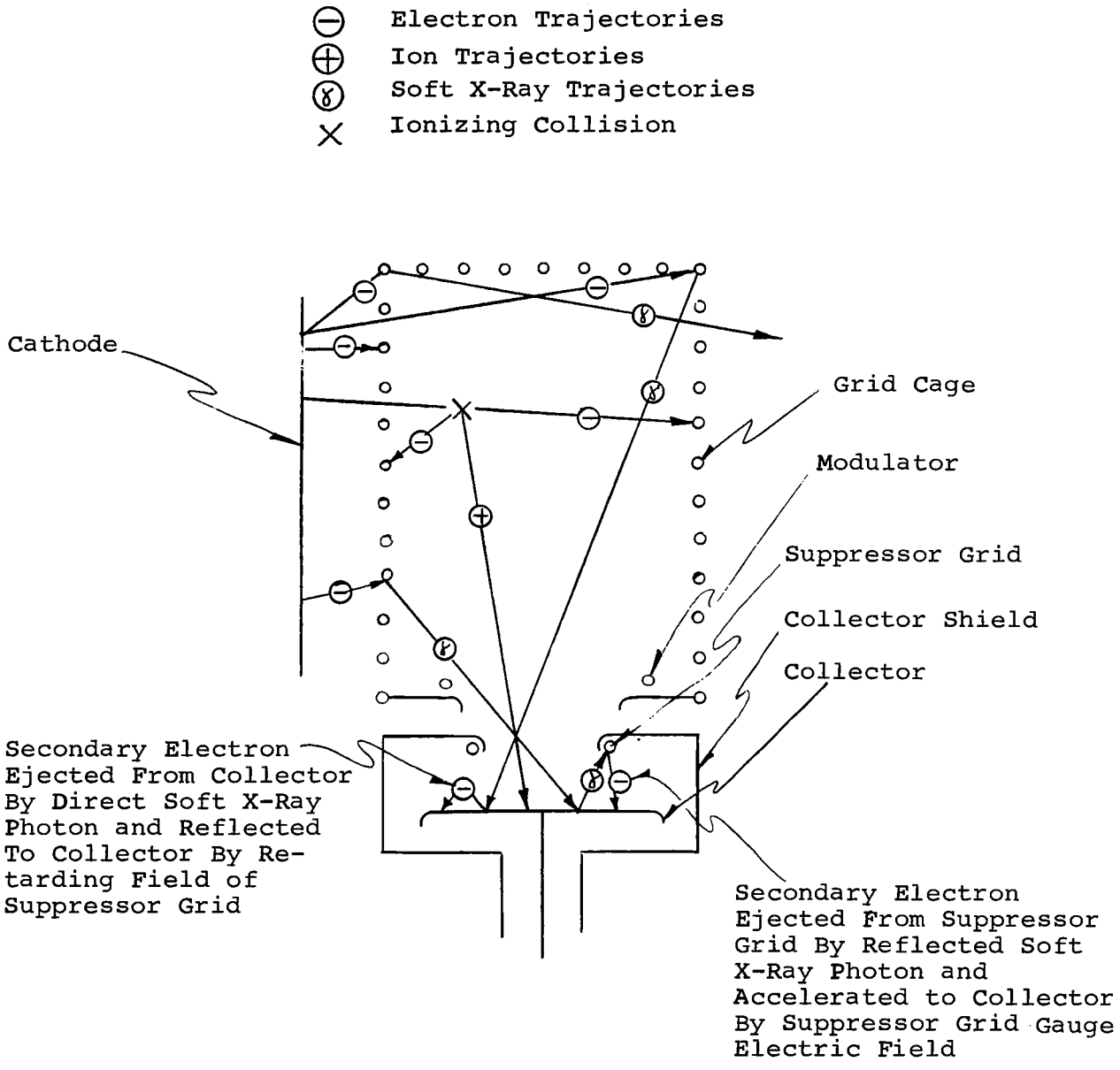

SCHEMATIC OF SUPPRESSOR GRID GAUGE
ILLUSTRATING TYPICAL PROCESSES AND TRAJECTORIES

FIGURE 19

and modulator) are introduced to remove this ambiguity. The suppressor grid gauge is specifically designed to eliminate or suppress the strongest or the most intense of these secondary mechanisms, that is, the soft X-ray-induced secondary electron emission from the ion collector. This secondary electron emission constitutes a negative current leaving the ion collector which is indistinguishable from a positive ion current arriving at the collector. Electrons leaving the cathode are accelerated to the grid to increase their probability of generating ions in collisions with neutral gas atoms or molecules in the grid cage. The accelerated electrons have sufficient energy as they strike the surface of the grid (where they are all collected eventually) that their probability of ejecting a soft X-ray photon is enhanced. The soft X-rays radiate from the surface of the grid and a fraction of them arrive at the surface of the ion collector. For the soft X-ray photons striking the collector surface there is a certain probability that they will eject secondary electrons from this surface. These secondary electrons are then accelerated to the grid constituting a negative current leaving the collector which is equivalent to a positive ion current arriving at the collector. This secondary emission current from the ion collector therefore renders the interpretation of the measured collector current ambiguous since an unknown fraction of the total measured collector current is not due to ions but is due to secondary electron emission. Thus, the measured collector current is not only related to the ion production rate and (therefore gas density) but is also related to the production rate of secondary electrons. As the gas density is decreased, the number of ions generated decreases and at very low pressures the ion arrival rate at the collector constitutes a current that is small compared to the soft X-ray-induced secondary electron emission current from the collector. The ion current, which

is proportional to pressure, is thus completely obscured by the secondary electron emission current as the pressure becomes sufficiently low. Thus, pressure measurement is no longer possible.

A description of how the suppressor grid acts to eliminate or suppress the secondary electron emission from the collector follows. The secondary electron emission current from the collector can be eliminated or suppressed by placing a suppressor grid above the surface of the collector and applying a sufficiently high negative voltage that a repulsive field for electrons is created at the surface of the collector. The soft X-ray-ejected secondary electrons are immediately returned to the surface of the collector under the action of the repulsive field generated by the suppressor grid. The time average of secondary electron emission and subsequent re-absorption is thus zero. The suppressor grid has therefore effectively suppressed the soft X-ray-induced secondary electron emission from the ion collector.

If the action described above were the only effect of the suppressor grid, the measured collector current would consist of ion current only and would be a function of pressure only. The suppressor grid gauge would then be capable of measuring very low pressures. However, while the action described above is the principal effect produced by the suppressor grid it is not the only effect. There is a secondary effect resulting from the action of the suppressor grid which induces a new kind of secondary electron current: A small fraction of the soft X-ray photons incident upon the collector surface are reflected and a small fraction of these reflected photons strike the suppressor grid and eject secondary electrons which are accelerated to, and collected by, the ion collector. These secondary electrons arriving at the collector constitute a negative current which subtracts from the ion current in any measurement

of the total collector current. This new kind of secondary emission current is not only very much smaller than the secondary emission current which the suppressor grid suppresses, but it it opposite in sign. The net result is that the suppressor grid gauge has a substantially lower limit of detectability for pressure than the conventional Bayard-Alpert or Nottingham ion gauges.

The ambiguity in interpretation of the measured collector current caused by the secondary electron emission current from the suppressor grid to the collector may be removed by introducing a modulation electrode. The function of the modulation electrode is as follows: A modulation grid is placed inside the grid cage at the ion exit aperture. The modulator is switched between grid potential and ground potential. It has a negligible effect on the ion trajectories between the grid cage and the collector, but with the modulator at ground potential, the ion collection efficiency is increased, and thus for the same pressure, the measured ion current is increased. The modulation grid has a negligible effect on the soft X-ray flux. The measurement of the collector current with the modulator at grid potential (I_1) and then at ground potential (I_2) provides sufficient data to separate the total collector current into two components: the true ion current (i), that part of the collector current related to pressure, and the secondary electron emission current (i_x), that part of the collector current related to the reflected soft X-ray-induced secondary electron emission current from the suppressor grid to the collector. The true ion current is then calculated from the equation[3].

$$i = \frac{I_2 - I_1}{(\alpha - 1)} ,$$

where (α) is the modulation coefficient determined experimentally, at pressures sufficiently high that the soft X-ray-induced

current may be neglected, according to the equation

$$\alpha = \frac{I_2}{I_1} .$$

The above modulation procedure yields a limit of detectability for pressure measurement that is lower than that attained with the suppressor grid only.

3.2.3.2 Results

The data reported here are the results of experiments conducted on the latest version of the suppressor grid gauge which has evolved from a series of modifications, improvements and developments. In fact, the latest version of the instrument is more accurately described as a modulated suppressor grid gauge. The construction of the final version of the modulated suppressor grid gauge is shown in Figures 20, 21, 22, and 23.

The suppressor grid gauge has been calibrated from approximately 10^{-5} torr to 10^{-13} torr N_2. The calibration gas was helium. The direct comparison method was used from 10^{-5} torr to 10^{-10} torr and the pressure ratio technique was used from 10^{-9} to 10^{-13} torr. Data were obtained for cathode emission currents of 1.0 and 10.0 Ma. In the lower pressure ranges data were obtained for several values of suppressor grid voltage. Some modulation data were also obtained at low pressures.

Figure 24 presents a plot of the suppressor grid gauge collector current as a function of pressure for an emission current of 10.0 Ma. It may be observed that even at a suppressor grid voltage of -485 volts, complete suppression of the soft X-ray-induced secondary electron emission current from the collector was not achieved. From these data it is also clear that the unsuppressed X-ray-induced residual current is approximately an order of magnitude higher than the

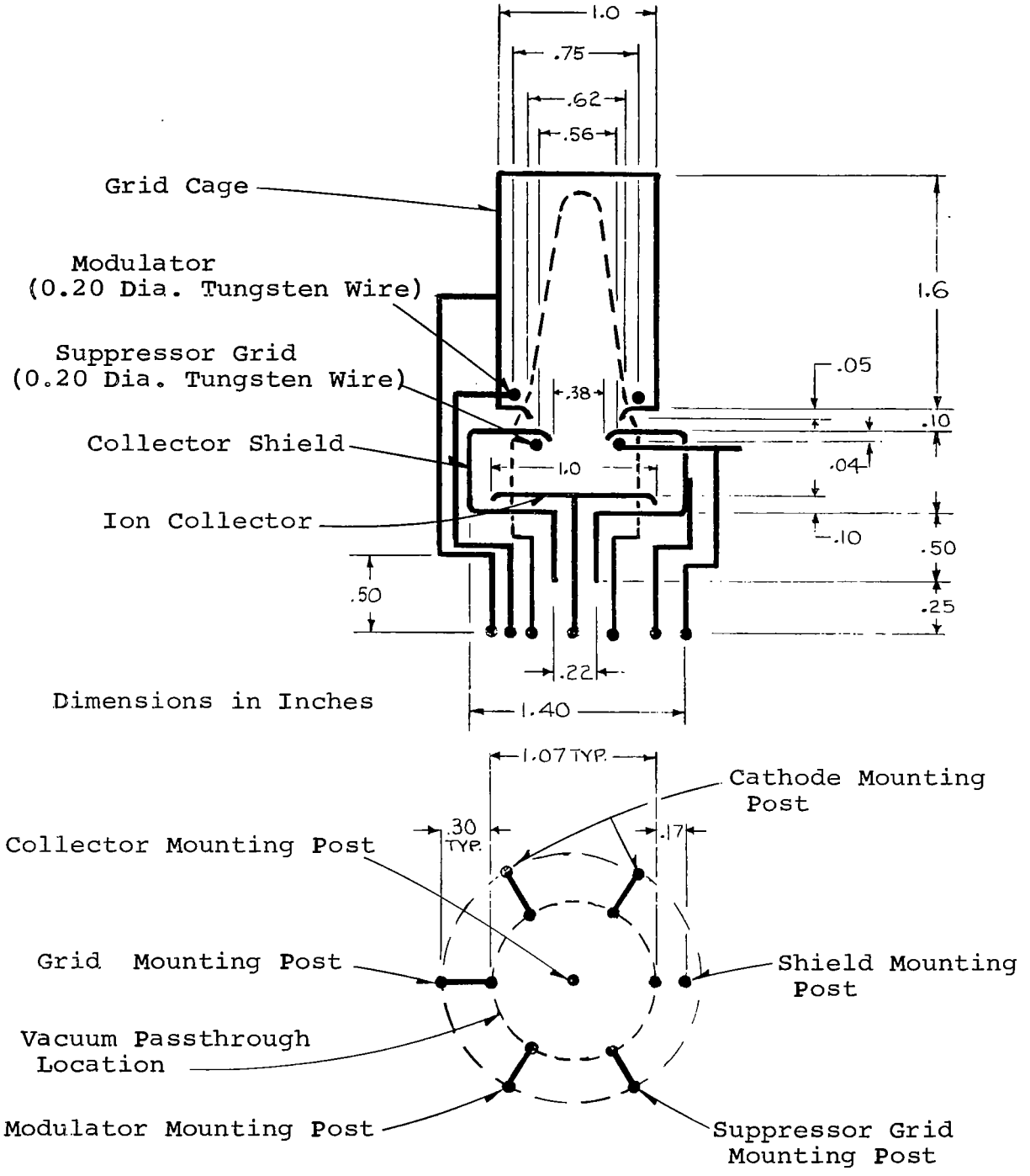

FIGURE 20 MODULATED SUPPRESSOR GRID GAUGE (FINAL VERSION)

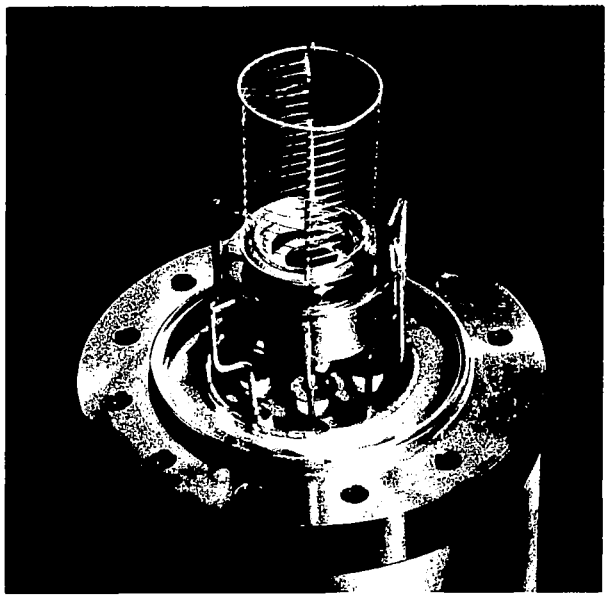

FIGURE 21

Suppressor Grid Gauge
Nude Configuration (Side View)

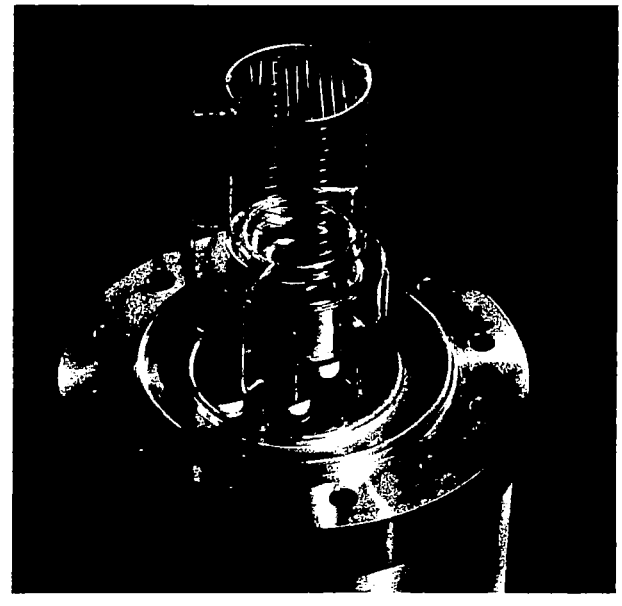

FIGURE 22

Suppressor Grid Gauge
(Rear View)

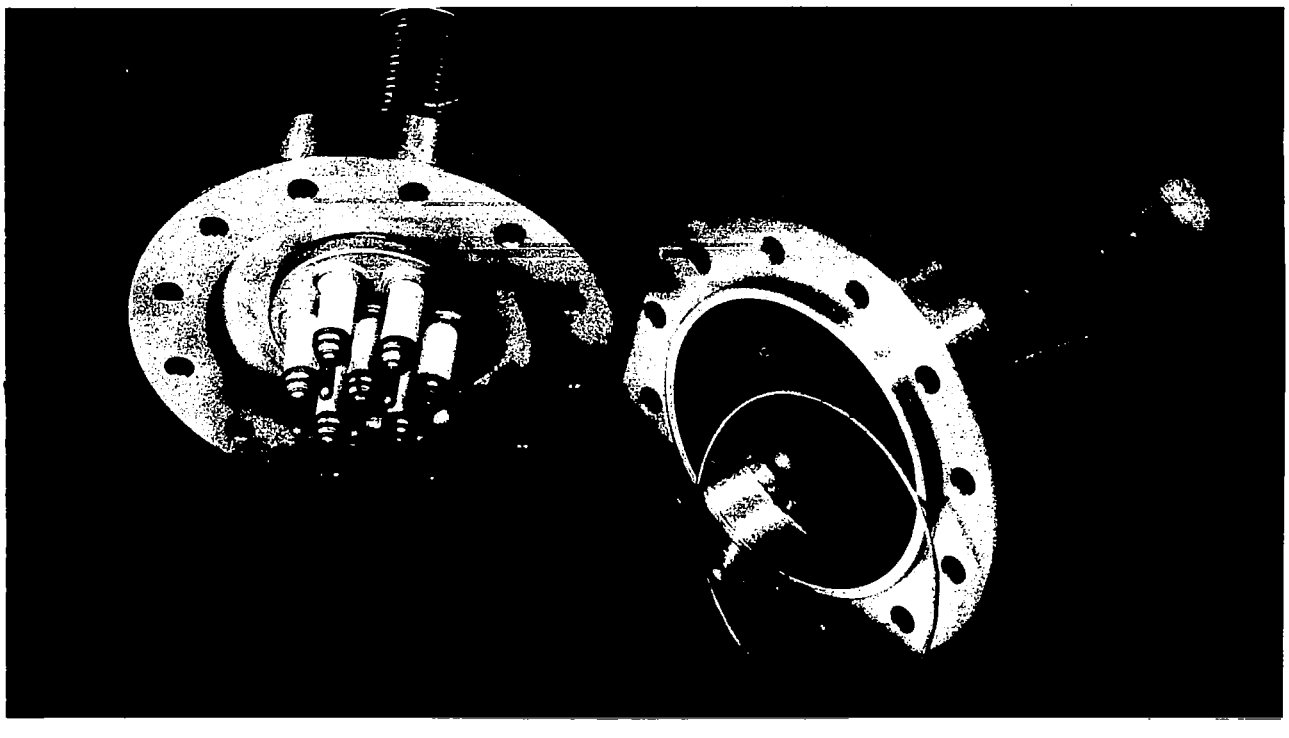

FIGURE 23

Suppressor Grid Gauge With Envelope and Gold Seal

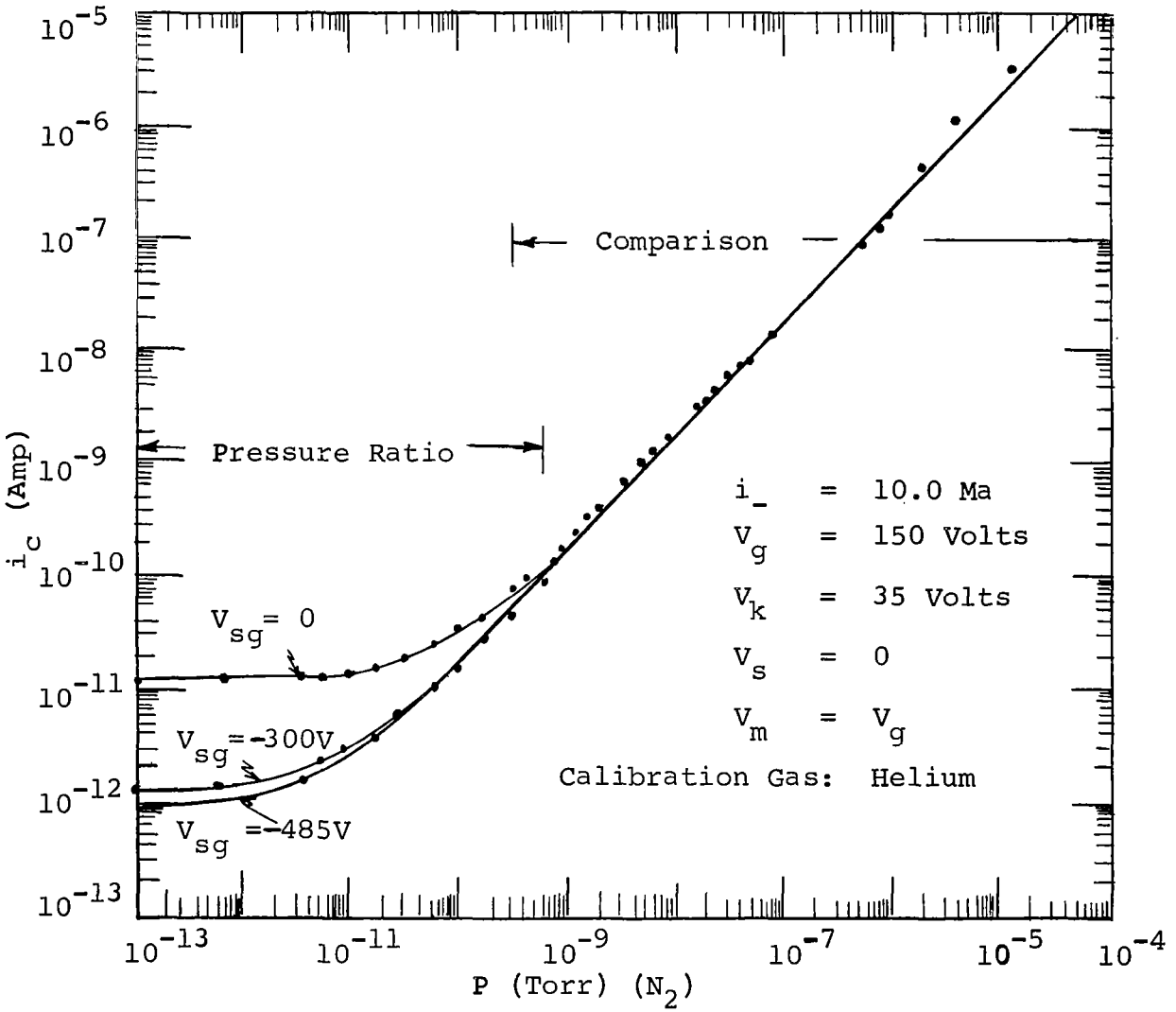

FIGURE 24 SUPPRESSOR GRID GAUGE CALIBRATION

residual current of a conventional Bayard-Alpert or Nottingham ion gauge. This result was anticipated and is consistent with the large area of the ion collector in the suppressor grid gauge. The fact that the suppressor grid gauge has a large unsuppressed residual current introduces no new problems since the gauge would normally be used in the suppressed mode of operation, that is, with this direct soft X-ray-induced secondary electron emission current from the ion collector completely suppressed.

Figure 25 presents a plot of the suppressor grid gauge collector current as a function of pressure for an emission current of 1.0 Ma. It is clear from the shape of the curves in Figure 25 that the secondary electron emission current from the ion collector is completely suppressed at the suppressor grid voltage of -665 volts. In fact, the measured residual current at this suppressor grid voltage was -5.4×10^{-14} amp. This negative value for the residual current not only indicates that the secondary electron emission current from the ion collector was completely suppressed but that the residual current now consists of a secondary electron emission current from the suppressor grid to the ion collector induced by soft X-rays reflected from the ion collector to the suppressor grid. The data of Figure 25 indicates that the total ion collector current passes through the value zero at a pressure of 2.7×10^{-12} torr N_2 for an emission current of 1.0 Ma. The total collector current is negative below this pressure since the true ion current, although positive, is smaller in magnitude than the negative secondary electron emission current from the suppressor grid to the ion collector. However, these data do not imply that the suppressor grid gauge cannot be used to measure pressures lower than 2.7×10^{-12} torr. In fact, the modulation technique may be used to sort out the various current components such that lower pressures may be measured.

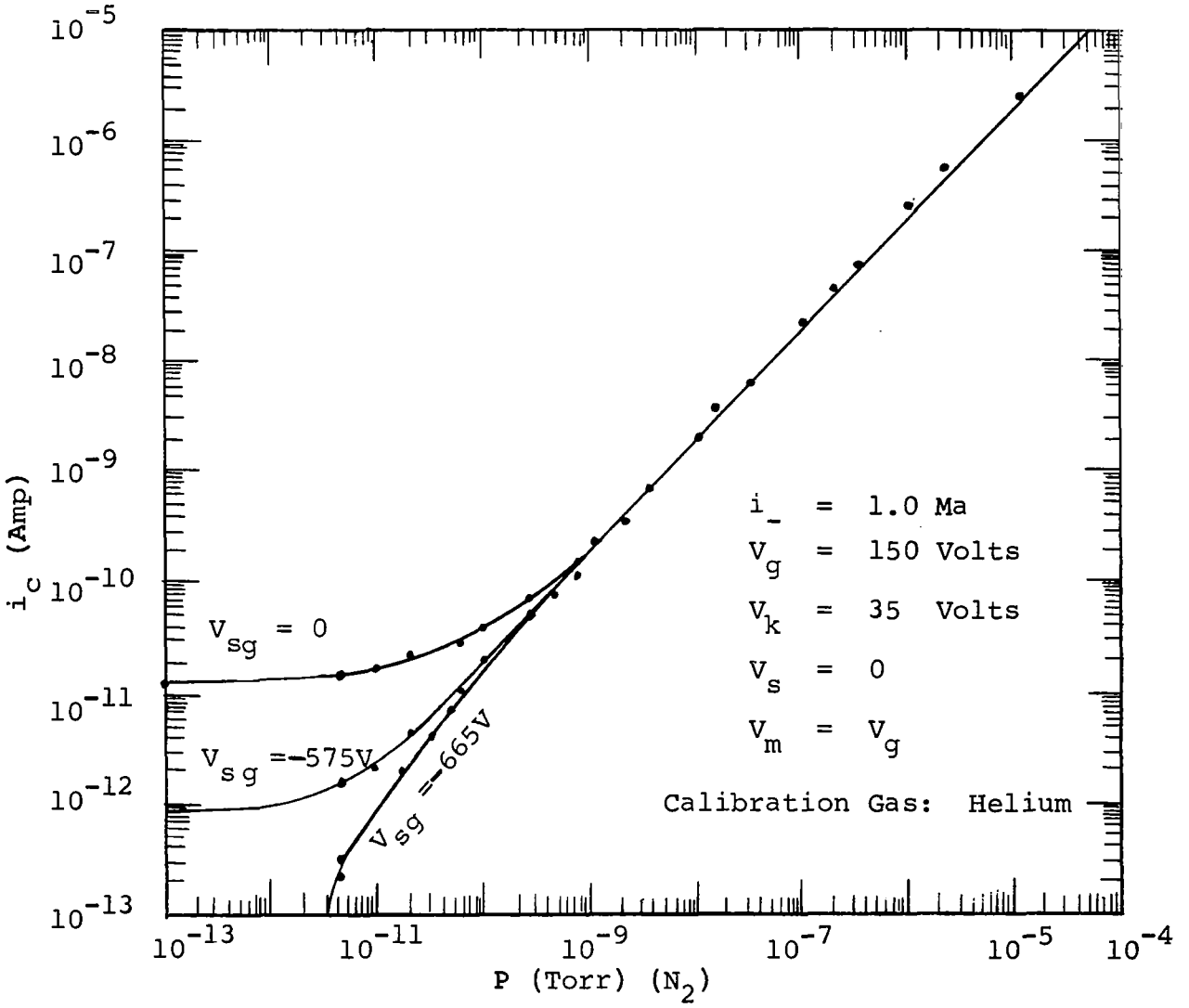

FIGURE 25 SUPPRESSOR GRID GAUGE CALIBRATION

Figure 26 gives the results of an experiment in which the modulation technique was used. The full curve gives the calculated true ion current as a function of pressure obtained from the modulation equations. The dashed curves give the total collector currents for the modulator at grid potential and at collector (ground) potential. It is apparent from Figure 26 that pressures lower than 10^{-12} torr N_2 may be measured with the modulated suppressor grid gauge.

The residual current of the suppressor grid gauge was measured for several grid voltages (V_g) and several suppressor grid voltages (V_{sg}). The ion collector current as a function of electron acceleration voltage is presented in Figure 27 for two suppressor grid voltages. From the shape of these curves it is clear that the residual current is of the form

$$i_{c_r} = k\ (V_g - V_k)^m$$

which indicates that the residual current is secondary electron emission from the ion collector induced by soft X-ray photons incident upon the collector which were ejected from the grid by electron bombardment. From the data presented in Figure 27 it may be observed that applying -300 volts to the suppressor grid reduces the residual current by approximately an order of magnitude.

Figure 28 presents data on the residual current as a function of suppressor grid potential. Although not shown on this curve, the residual current approaches zero somewhere between -575 volts and -665 volts. The data for an emission current of 1.0 Ma would yield a current similar in shape to that shown in Figure 28 but would be approximately one order of magnitude lower. For an emission current of 1.0 Ma the residual current is -5.4×10^{-14} amps at a suppressor grid potential of -665 volts. This latter residual current is different from the residual current shown in Figure 28 since it is a secondary electron emission current

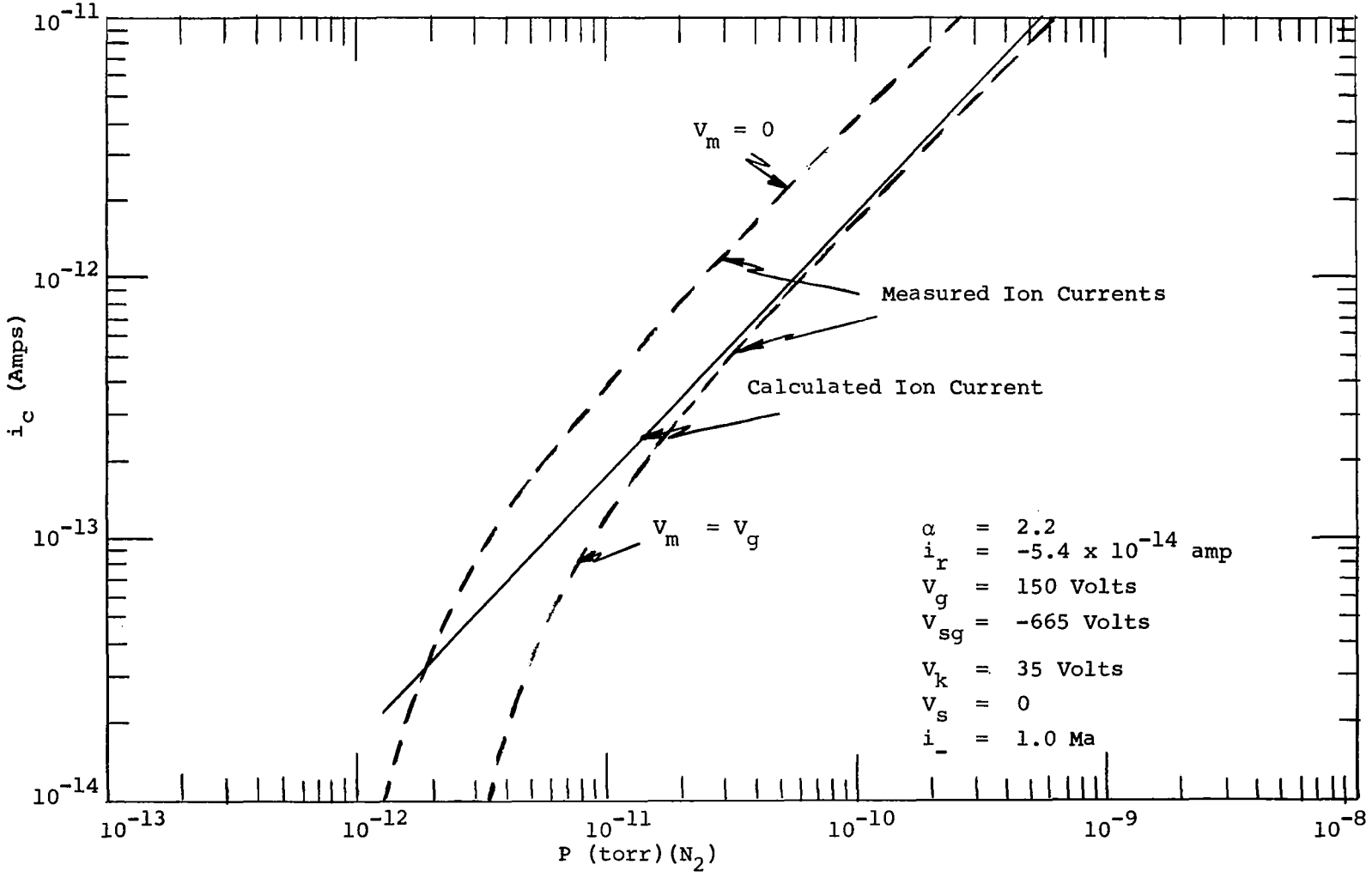

FIGURE 26 MODULATED SUPPRESSOR GRID GAUGE CALCULATED ION CURRENT AS A FUNCTION OF PRESSURE USING THE MODULATION TECHNIQUE

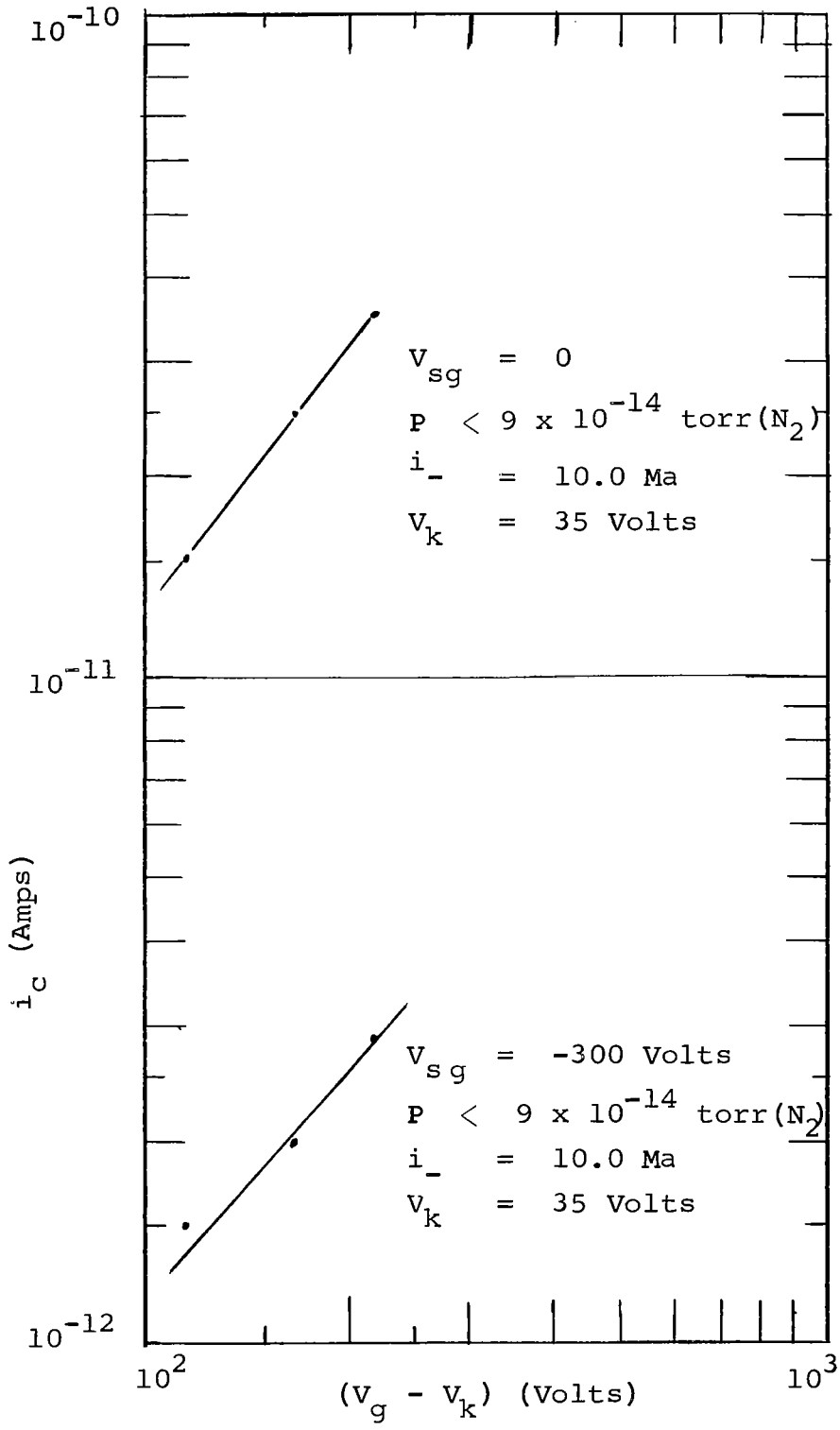

FIGURE 27 SUPPRESSOR GRID GAUGE RESIDUAL CURRENT AS A FUNCTION OF ELECTRON ACCELERATION VOLTAGE

from the suppressor grid to the collector whereas the current plotted in Figure 28 is a secondary electron emission current from the collector.

3.2.3.3 Discussion

In principle, the suppressor grid voltage could be adjusted to a value such that the secondary electron emission from the collector is not completely suppressed, but rather only reduced to a value which is equal in magnitude to the secondary electron emission from the suppressor grid to the ion collector. For this particular value of suppressor grid voltage the two secondary electron emission currents would be exactly equal but opposite in sign. Therefore, their total contribution to the collector current would be zero. That is, under this specific condition the suppressor grid gauge output current (collector current) would be only a function of pressure. While it is possible in principle to specify the exact value of suppressor grid voltage which reduces the total residual current to zero, it is not considered practical since very slight changes in the location of the suppressor grid would induce substantial changes in the repulsive electric field above the collector surface. This would in turn induce substantial changes in the fraction of the secondary electron emission from the collector that is reflected by the suppressor grid. Slight changes in the location of the suppressor grid are to be expected as a result of high temperature degassing required to clean the gauge. Under these conditions a new suppressor grid voltage must be determined which would again make the two secondary electron emission currents equal. This determination must be done experimentally at very low, known pressures. Thus, this mode of suppressor grid gauge operation is not considered practical.

It is considered much more practical to completely

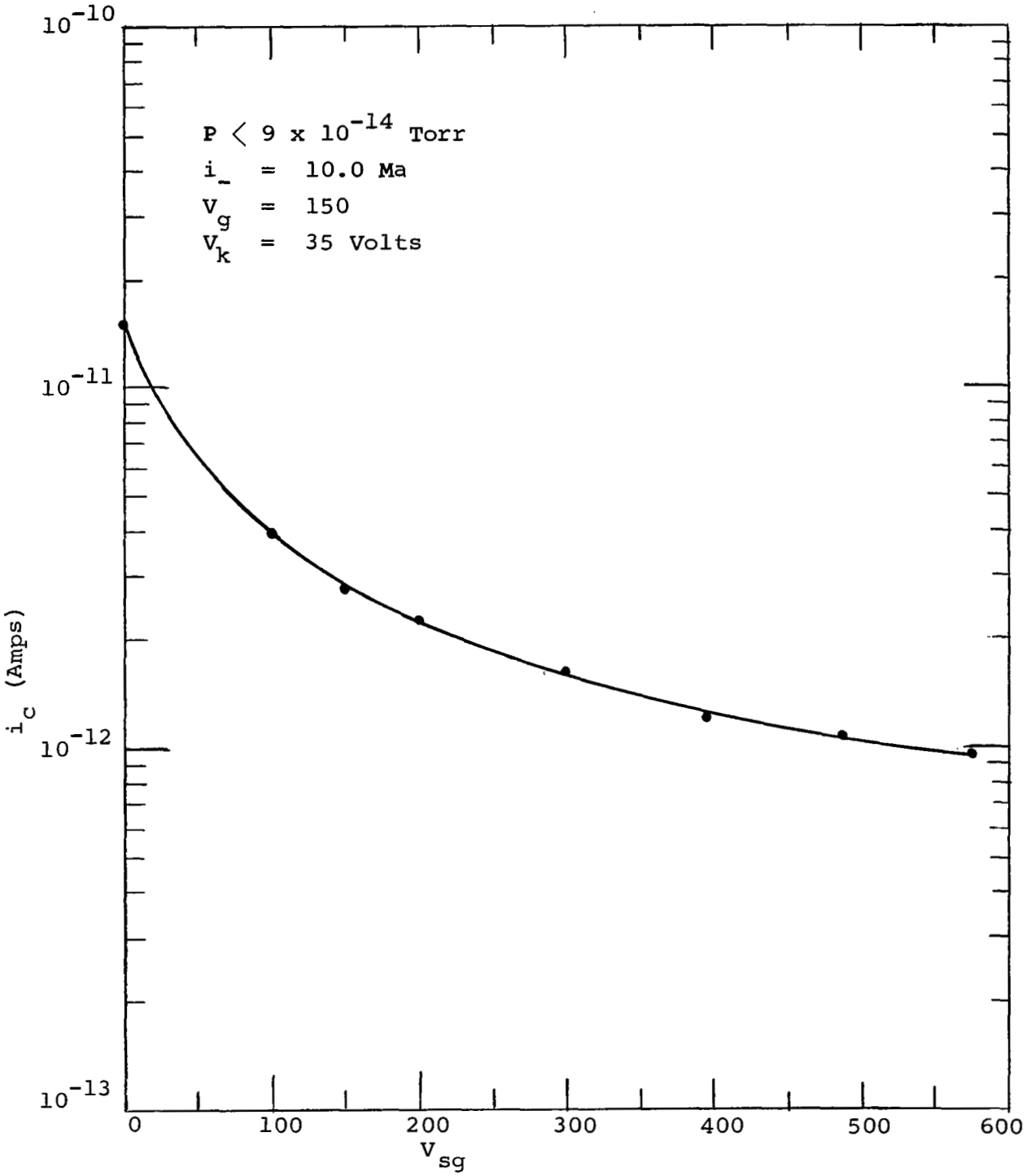

FIGURE 28 SUPPRESSOR GRID GAUGE RESIDUAL CURRENT AS A FUNCTION OF SUPPRESSOR GRID POTENTIAL

suppress the secondary emission current from the collector and apply the modulation technique to the secondary electron emission current from the suppressor grid to the ion collector.

The limit of detectability for pressure of the modulated suppressor grid gauge is not accurately known since the curves of Figure 26 are based on a small number of data points. However, if no new anomalies are encountered at lower pressures and a satisfactory signal to noise ratio can be achieved, it is estimated that the limit of detectability for pressure may approach 10^{-14} torr N_2, based on the present state-of-the-art in small current measurement techniques.

3.2.4 Nude Nottingham Gauge

During the course of the present program, a nude modulated ion gauge played an essential role in the pressure-ratio technique for gauge calibration in the XHV system. The gauge was mounted inside the experimental chamber of the XHV. It had the same gauge element structure (except for the modulating electrode) and the same operating parameters as the upstream gauge (See section 3.1.2). Consequently, by operating the two gauges at identical emission currents, the pressure ratio across the capillary, that is, the ratio between the upstream gauge and the nude gauge in the experimental chamber, was equal to the ratio ion currents of the two gauges. However, since the nude gauge operated in the range of 10^{-9} to 10^{-11} torr, it was essential that the residual current (X-ray) of the gauge be known accurately. The method used was essentially the same as that described by Redhead[3]. A modulating electrode was mounted within the grid structure of a nude Nottingham gauge which had the following characteristic dimensions:— grid, 27 mm diameter, 39 mm long (closed ends); outer grid or shield, 38 mm diameter, 46 mm long; modulator 0.51 mm diameter, located about 0.3 mm from grid; collector 0.13 mm diameter.

When the gauge was operated at 3.0 Ma emission, the sensitivity was 0.1 amp/torr N_2. A grid voltage of 148 volts was used; the filament bias was 36 volts.

When the modulator is at grid potential (V_g) the total collector current $(I)_{V_m=V_g}$ is given by

$$(I)_{V_m=V_g} = i_c + i_r$$

where i_c = positive ion current
i_r = residual current

When the modulator is at ground potential a fraction $(1 - \alpha)$ of the positive ions are collected at the modulator. The resulting collector current is:

$$(I)_{V_m=0} = \alpha\, i_c + i_r$$

These equations may be solved simultaneously to obtain both α and i_r and hence values of i_c. A convenient method of doing this is to subtract the above equation and solve for i_c so that

$$i_c = \frac{(I)_{V_m=V_g} - (I)_{V_m=0}}{1 - \alpha}$$

This value of i_c may then be substituted in the first equation, which on rearranging gives

$$(I)_{V_m=V_g} = \frac{1}{1 - \alpha}\left[(I)_{V_m=V_g} - (I)_{V_m=0}\right] + i_r$$

Consequently, a linear plot of $(I)_{V_m=V_g}$ versus $(I)_{V_m-V_g} - (I)_{V_m=0}$ should yield a straight line with a slope of $\frac{1}{1 - \alpha}$ and an intercept of i_r.

Typical plots of the above equation are shown in Figures 29 and 30. Reasonable linear results are obtained to support the general procedure. At 3.0 Ma emission where the gauge sensitivity is 0.10 amp/torr N_2 the residual current was found to be 1.4×10^{-12} amps or 1.4×10^{-11} torr N_2. At 6.0 Ma emission the residual current was found to be 3.2×10^{-12} amps. It will also be noted that the modulation factor varied from 0.57 at 3.0 Ma to 0.52 at 6.0 Ma. According to the theory presented by Redhead[3], α should remain constant with variations in the emission current and the value of i_r should be proportional to the emission current. The above data agree with these requirements within approximately 12%. However, recently Appelt[9] and Hobson[10] have examined the modulation procedure in more detail and in general the evidence suggests that a single modulating parameter as presented above is perhaps an oversimplification of the overall process. Nevertheless, the above procedure appears to yield consistent results at any one setting of the emission current down to ion currents equal to about 50% of the residual current. That is for 3.0 Ma emission the modulated nude gauge has given constant results down to approximately 7×10^{-12} torr.

In order to obtain accurate measurements of ion currents below 10^{-9} torr with such a gauge it is imperative that the residual current be small and accurately known. This requires not only a procedure for measuring the residual current, but also the requirement that the gauge be clean. Vigorous electron bombardment (250 Ma at 500 volts) at low pressures (10^{-9} torr and lower) for several hours was generally adequate to obtain low residual currents. Redhead[11] has also shown that the modulation method is useful in detecting the presence of anomalous residual ion currents. Redhead[11] and Alpert[12] have interpreted this effect as an oxygen ion desorption current from the grid. These adsorbed gases are also desorbed as neutrals which again

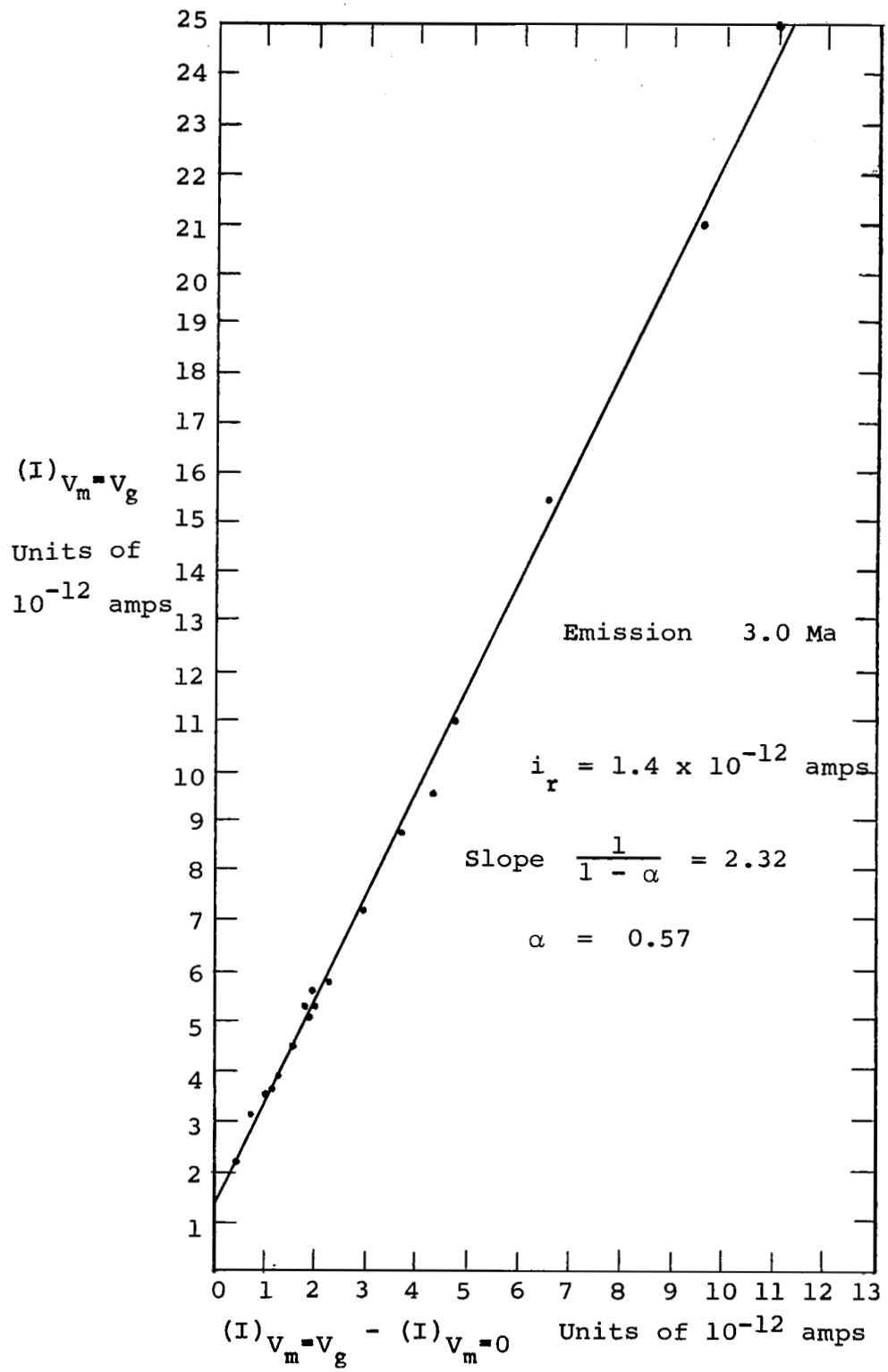

FIGURE 29 NUDE MODULATED NOTTINGHAM GAUGE DATA

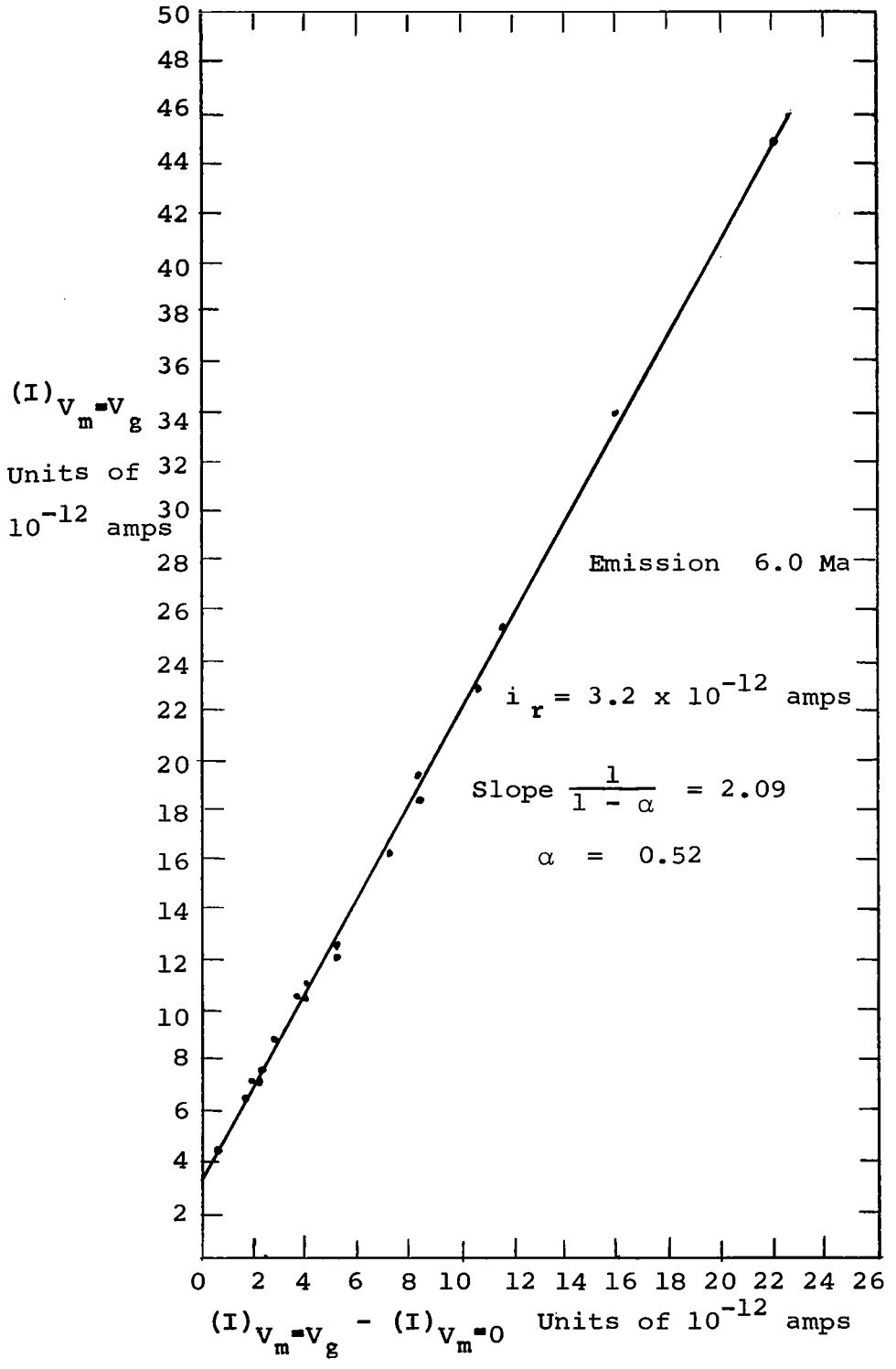

FIGURE 30 NUDE MODULATED NOTTINGHAM GAUGE DATA

indicated gauge pressures larger than true system pressures. The modulation technique then is useful, not only in evaluating the true X-ray-induced secondary electron emission from the collector, but also in detecting adsorbed gases, such as oxygen, which manifest themselves through anomalous residual currents. Thus, in order to use a hot filament gauge with confidence to measure pressures in the UHV range, it is required that the total residual current equal the X-ray residual current. However, these procedures are not without practical difficulties. An important requirement is that the gauge never be exposed to likely contaminants and that high pumping speeds be available during the outgassing procedures. A nude gauge inside a cryogenically pumped system is one method of exposing the gauge elements to high pumping speeds to facilitate degassing. In practical systems where possibilities of contamination may not always be eliminated, it may not always be possible to guarantee low residual currents. Hence, the measurement of pressure in the 10^{-12} torr range by the modulation procedure may not always be feasible.

3.2.5 Feasibility of Nitrogen Calibrations Using Pressure Ratio Technique in XHV

In previous work on gauge calibration in the XHV system by the pressure ratio method, helium gas has been used exclusively. It has been established that at 10°K and the pressures involved, the amount of helium adsorbed is so small that pressure changes will not introduce pressure ratio errors by causing significant amounts of helium to be adsorbed or desorbed from the walls of the experimental chamber. However, it would be attractive if the XHV system could be used for calibration of gauges using gases other than helium. Nitrogen and/or argon calibrations would be useful. In order to use the pressure ratio technique for nitrogen for instance, it would be necessary to develop background pressures in the

system several orders of magnitude below the desired minimum calibration temperature. In addition it would be necessary to establish these pressures at temperature levels where significant adsorption of nitrogen would not interfere with the pressure-ratio method. Operation of the system at 10°K under these circumstances is not feasible because nitrogen would be cryopumped with high efficiency. The temperature must be in excess of 77°K, probably of the order of 85°K.

An experiment was conducted to determine the practicability of using nitrogen as a calibration gas in the XHV range. The XHV system was operated with the experimental chamber at a number of temperatures in the region of 80°K. The background pressures established are shown in Figure 31. The inverted magnetron which had been previously calibrated in the XHV system was used for pressure measurement. The data showed that at the temperatures required for nitrogen calibration (85°K), background pressures were approximately 1×10^{-10} torr N_2. Consequently, the pressure ratio technique would only be practical down to values of approximately 1×10^{-8} torr for nitrogen.

Much lower calibration pressures would be feasible for neon and hydrogen. However, the interest in these gases is not as high as for nitrogen and helium and no experimental measurements were made with them.

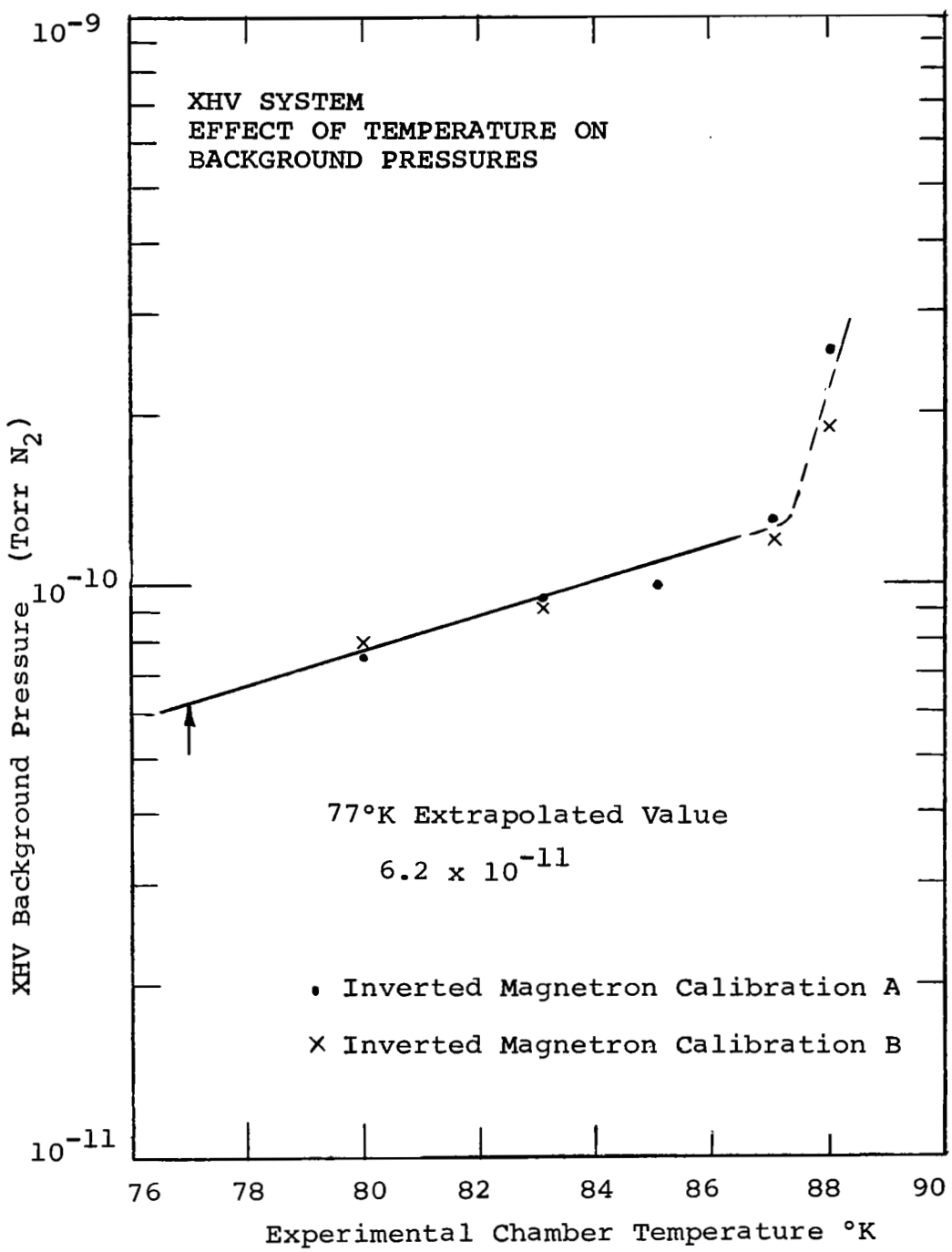
XHV SYSTEM
EFFECT OF TEMPERATURE ON
BACKGROUND PRESSURES
77°K Extrapolated Value
6.2 x 10-11
• Inverted Magnetron Calibration A
× Inverted Magnetron Calibration B
XHV Background Pressure (Torr N2)
10-9
10-10
10-11
76
78
80
82
84
86
88
90
Experimental Chamber Temperature °K

FIGURE 31

4.0 DIRECTIONALITY STUDIES

The main objective of this section of the program was to determine the sensitivity dependence of a gauge on the flux incidence angle. For this work a nude modulated Nottingham ion gauge was mounted in a beam of argon atoms in such a way that the gauge could be rotated through 90 degrees while maintaining the center of the gauge in the center of the beam. A schematic diagram of the experimental arrangement is shown in Figure 32.

Argon gas was allowed to flow from the "upstream" system at a pressure of approximately 10^{-4} torr through a capillary into the experimental chamber. The chamber was maintained at 9 $\pm$1°K. At this temperature, the walls of the experimental chamber cryopumped the argon with a high capture probability. The nude modulated ion gauge was mounted directly on the axis of the beam opposite the outlet of the capillary at a known distance from it. A capillary was used because, according to beam theory[13], the intensity of the molecular beam on the axis of the capillary is not less than the intensity which would be obtained with an orifice having the same diameter as the capillary. The intensity may be calculated from beam theory for a sensor located both on the normal to plane of the orifice and at various angles to it. However, for a capillary, the intensity at an angle to the axis is less than that for an orifice and, in general, the value is not easily predicted by theory. Clausing[14], however, has calculated the intensity distribution for a length to diameter ratio of one. The advantage of using a capillary is that the total amount of gas which must be cryopumped is reduced over that for an orifice. For the present work, two capillary sizes were used. In the preliminary beam studies the capillary was 4.0 cm long by 0.25 cm diameter. In the directionality measurements the capillary was 0.25 cm long and 0.25 cm

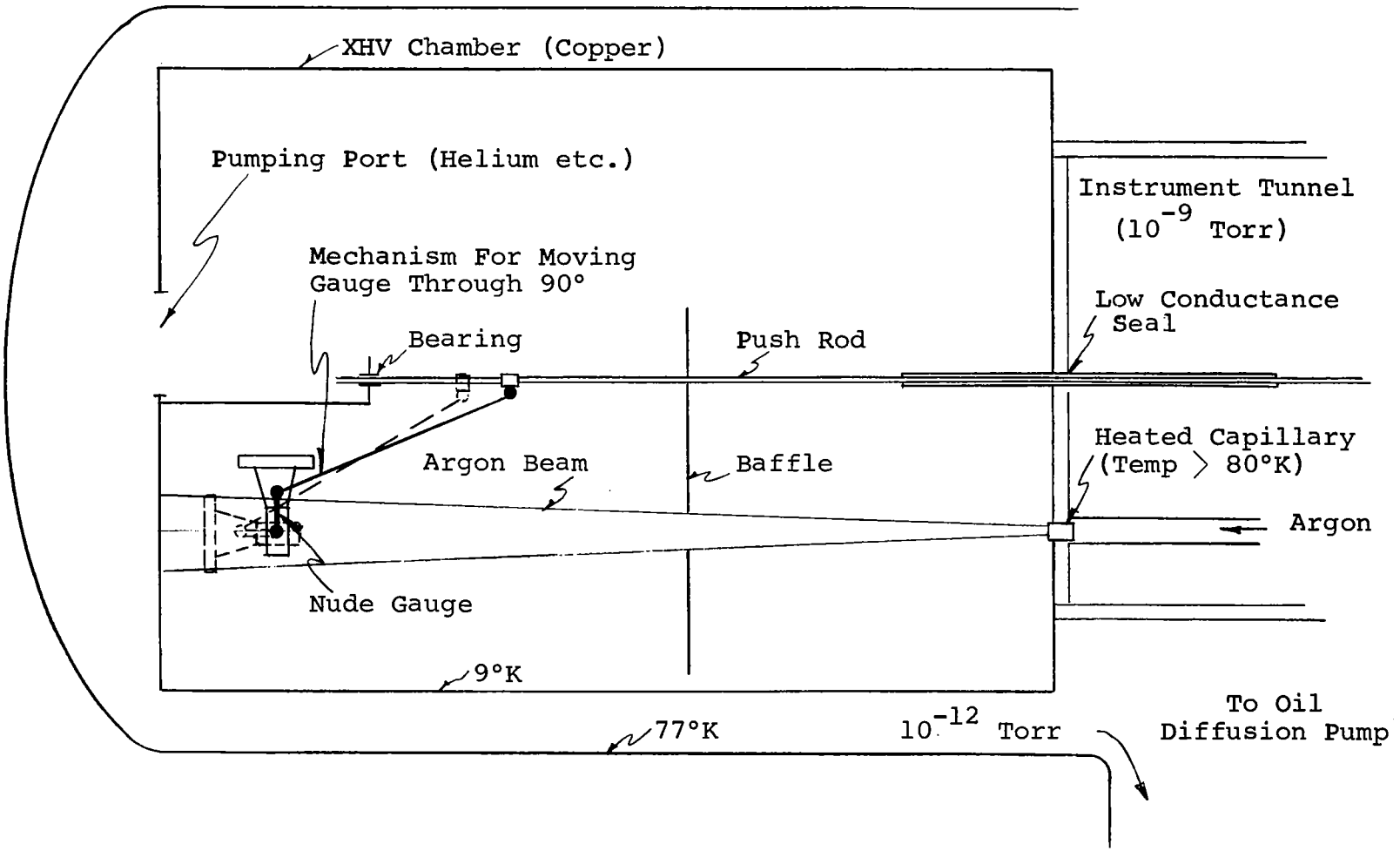

FIGURE 32 APPARATUS FOR MEASURING THE EFFECT OF FLUX ANGLE ON OUTPUT OF NUDE ION GAUGE — SCHEMATIC

diameter. Hence, for the latter work, Clausing's calculations could be used to determine the variation of beam intensity over the gauge structure. For the gauge and beam dimensions used, Clausing's data indicates that the intensity would be 4% lower at the top and bottom of the gauge than at the center. Over the area of the gauge the decrease would be approximately 2%.

Both the nude modulated gauge in the beam and the upstream gauge were operated with emission currents of 3 Ma. At these currents the gauge sensitivities are 100 Ma/torr N_2. For this reason the argon pressures are most easily expressed in terms of torr nitrogen. The ratio of the argon to nitrogen sensitivity for this type of gauge is approximately 1.2. The temperature of the argon beam was between 110 and 120°K. At these temperatures, the RMS velocity of the argon is approximately 260 m/sec.

4.1 RESULTS

The results of the effect of changing the angle at which the gauge was mounted in the atomic beam are shown in Tables IIand III. It will be noted that gauge output signal increased as the angle between the beam and the axis of the gauge decreased. The amount of the increase was greatest between 30 and 15 degrees (See Figure 33). The magnitude of the increase was approximately 24% over that when the beam passed through the gauge at right angles to the grid axis.

The cause of the increased signal was back scattering of atoms from the structure used to hold the nude gauge. This structure was a flange, 3 3/4 inches in diameter and located at right angles to the grid axis, 2 inches from the center of the grid. The geometry involved indicates that as the gauge was rotated some back scattering would occur even at 75 degrees. It would gradually increase at high

TABLE II

EFFECT OF BEAM ANGLE ON SENSITIVITY OF NUDE ION GAUGE (INLET PRESSURE GAUGE READING 8.9×10^{-5} TORR)

BEAM ANGLE* (°)	NUDE GAUGE SIGNAL** (amps)
90	2.46×10^{-11}
75	2.49
60	2.52
45	2.61
30	2.66
15	2.94
0	3.05

* Angle between beam and axis of grid cylinder of gauge.

** Sensitivity of Nude Gauge 0.1 amp/torr N_2. The residual current of 1.3×10^{-12} amps as determined by the modulation technique have been subtracted to give the above results.

TABLE III

EFFECT OF BEAM ANGLE ON SENSITIVITY OF NUDE ION GAUGE
(INLET PRESSURE GAUGE READING 7.5×10^{-4} TORR)

BEAM ANGLE* (°)	NUDE GAUGE SIGNAL (amps)		
	Test 1	Test 2	Test 3
90	2.78×10^{-10}	2.63×10^{-10}	2.69×10^{-10}
75	2.84	2.77	
60	2.90	2.78	
45	2.92	2.83	
30	2.94	2.90	
15	3.25	3.22	
0	3.37	3.34	3.30×10^{-10}

* Angle between beam and axis of grid cylinder of gauge. Sensitivity of Nude Gauge 0.1 amp/torr N_2.

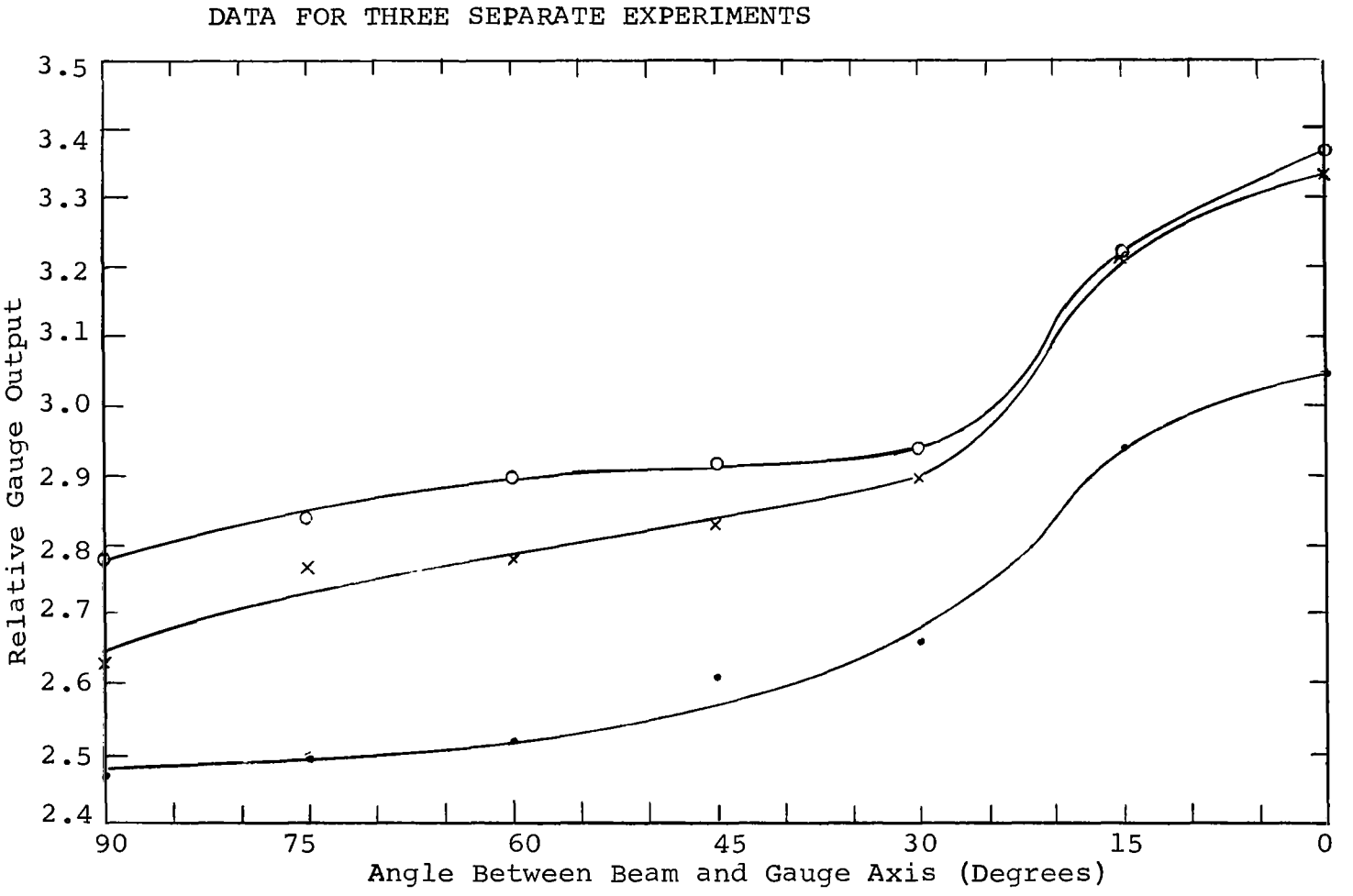

FIGURE 33 EFFECT OF FLUX ANGLE ON GAUGE SENSITIVITY

angles but between 30 and 15 degrees increase rapidly to almost the maximum value of back scattering. Assuming that back scattering from the gauge mounting structure follows a cosine law distribution, it has been estimated that the maximum increase in signal should be 21%. This agrees well with the value of 24% found experimentally. These results suggest that the output from a gauge is only dependent on the number density within the grid volume. If the gauge were supported so as to eliminate back scattering, it would appear then that the gauge output would be independent of orientation within a beam.

In the course of the above studies, direct measurements of the beam intensities in the absence of back scattering were made (normal incidence). These may be compared with the intensities expected on the basis of beam theory. Typical results are presented in Table IV. In general, the beam intensities measured in Tests 1 through 4 were closer to theoretical than in Tests 5 through 8 in which the measured sensitivities averaged approximately 20% lower than the theoretical values. In analyzing the data, several pertinent facts should be considered. First, the argon gas was fed to the beam capillary by means of a 1/2 inch in diameter stainless steel tube approximately 4 feet long. This tube was not isothermal. Consequently, it was necessary to estimate the number density at the beam capillary by applying a thermal transpiration correction to the measured number density (pressure) at the inlet end of the 1/2 inch tubing. This correction has been applied to data in Table IV.

Secondly, in order to accurately calculate the theoretical beam intensity, the temperature of the enclosure (furnace) in which the beam originates should be known accurately. Since the 1/2 inch tubing was not isothermal, the beam temperature is not defined. For the purpose of the calculation required in Table IV, the beam temperature was assumed to be the temperature at the inlet capillary.

TABLE IV

COMPARISON OF THEORETICAL AND EXPERIMENTAL VALUES OF ARGON BEAM INTENSITIES

TEST No.	UPSTREAM GAUGE READING torr N_2	TEMPERATURE AT BEAM INLET °K	BEAM "PRESSURE" MEASURED torr N_2	BEAM "PRESSURE" THEORETICAL torr N_2
1	1.3×10^{-4}	112	3.9×10^{-10}	3.7×10^{-10}
2	1.05×10^{-4}	112	3.3×10^{-10}	3.0×10^{-10}
3	7.4×10^{-4}	112	2.6×10^{-9}	2.1×10^{-9}
4	7.3×10^{-4}	112	2.7×10^{-9}	2.1×10^{-9}
5	8.9×10^{-5}	115	2.46×10^{-10}	3.8×10^{-10}
6	7.5×10^{-4}	115	2.78×10^{-9}	3.2×10^{-9}
7	7.5×10^{-4}	115	2.63×10^{-9}	3.2×10^{-9}
8	7.5×10^{-4}	115	2.69×10^{-9}	3.2×10^{-9}

Tests 1 through 4 with capillary 40 cm long x 0.25 cm diameter.

Tests 5 through 8 with capillary 0.25 cm long x 0.25 cm diameter.

In fact, the beam temperature would have been somewhat greater than this.

Thirdly, an ion gauge was used to measure the "upstream" pressure. The gauge was not calibrated for argon and in addition, it is known that the type of gauge used becomes non-linear at a gauge reading of about 10^{-4}. Consequently, at the higher pressure levels the quoted values are probably low. The non-linear characteristics of the "upstream" gauge probably account for the lack of direct proportionality between the beam and the furnace "pressure" as indicated by the upstream gauge.

It is also possible that at the higher pressures, departures from theoretical performance were caused by adsorption effects and the use of pressures in excess of those required for true molecular flow relationship.

Nevertheless, despite the above uncertainties, the measured beam intensities were close to theoretical.

4.2 MEASUREMENT OF BACKGROUND INTENSITIES DURING ARGON BEAM STUDIES

Three main sets of experiments were carried out with argon beaming but in each case experimental difficulties prevented the making of direct measurements of the signal to background ratio.

In the first set of experiments, the gauge for measuring the beam intensity operated satisfactorily but the background gauge was incorrectly located. In the second series of tests, a calibrated gauge was used to measure background intensities during beaming but the nude gauge in the beam failed during outgassing immediately prior to making intensity measurements. In the third test the nude beam gauge operated well but a new background gauge failed to measure low pressures satisfactorily. However, despite these difficulties good estimates of the signal to background ratios should be provided by comparison of the three sets of

results because in each series the capillary diameter was not changed and the upstream pressure gauge readings were maintained at comparable levels. And, in general, the beam intensities were shown to be reproducible and roughly proportional to the reading of the inlet pressure gauge. With a beam intensity (calculated from the upstream pressure) of 1.9×10^{-9} torr N_2, the background pressure was less than 2×10^{-13} torr N_2. Under these conditions the signal to background ratio was greater than 9.5×10^3. These results were obtained with the nude gauge operating at 3.0 Ma emission.

However, care had to be exercised in not operating the hot filament nude gauge for excessive periods of time along with high beam intensities. It appeared that significant thermal desorption of argon occurred when those areas which had previously adsorbed argon were exposed to the thermal load from the nude gauge. But these effects were not critical. For instance, in the above quoted signal to background ratio of 9.5×10^3 the gauge had been operating for six minutes.

In order to maintain low background values the following precautions were adopted:

1. The hot filament gauge in the beam was operated intermittently.

2. The surface used to cryopump the beam was in good thermal contact with the refrigerating medium and was not unduly exposed to the heat load of the gauge.

3. The beam was collimated and baffled so that significant amounts of gas outside the useful beam were not cryopumped by regions exposed to thermal radiation from the gauge.

4. The beam was operated only as required in order to decrease the total amount of gas cryopumped.

5.0 DYNAMIC RESPONSE OF ION GAUGE

5.1 INTRODUCTION

The question has been frequently raised: What are the dynamic response characteristics of an ion gauge? In conventional frequency response terminology this question may be thought of as follows: Over what frequency range of sinusoidal pressure variation is the output of an ion gauge flat or independent of frequency? The measurement of the dynamic response characteristics of an ion gauge involves several specialized problems requiring rather specialized experimental methods which depart from the conventional frequency response techniques. It is only possible to conduct a conventional frequency response test on an ion gauge if sinusoidal density variations can be introduced directly into the grid cage of the ion gauge. This requires that a diffuse gas source be placed inside the grid cage and the gauge be surrounded with a pump having unlimited speed. The apparatus required would alter the potential distribution inside the grid cage in a complex manner. This method was therefore rejected. Another method considered was to place the ion gauge in a sinusoidally-chopped atomic beam and to surround the gauge with a pump having an unlimited speed. The chopping frequency would then be varied and the amplitude of the gauge response measured as a function of chopping frequency. Although the pumping requirements can be reasonably well satisfied for certain gases by cryopumping at very low temperatures, there are several serious problems encountered in this technique. A rough estimate of the speed of response of an ion gauge indicates that no attenuation in response will be observed until the chopping frequency approaches 10^6c/s. Thus, a critical test of the ion gauge dynamic response requires a very high rotational velocity of the chopper. The shaft support bearings and

drive motor of a high-speed chopper are somewhat incompatible with ultrahigh vacuum conditions. The most serious problem concerns the intrinsic properties of the chopped beam. The chopped beam gas source is a Maxwellian gas, thus, in each packet of atoms in the chopped beam there is a wide distribution of velocities. At high chopping frequencies this velocity distribution tends to smear the atomic packet and adjacent atomic packets in the chopped beam soon overlap unless the total length of the beam is very short. This requires that the beam detector (ion gauge) be very near the chopper. This problem can be resolved with multiple chopping or velocity selection but the apparatus is complicated and not well suited to this application.

Rather than consider the dynamic response characteristics of an ion gauge in terms of conventional frequency response techniques, it is probably more meaningful in the usual ion gauge application to measure the time constant of the instrument. The time constant is the time the gauge requires to respond to the gauge. Accurate dynamic measurements may be made if the time interval over which the pressure variation occurs is large compared with the gauge time constant. An experiment was conceived which would at least put an upper limit on the ion gauge time constant. That is, from the results of the experiment it should be possible to conclude that the ion gauge time constant is less than a certain value.

The experiment is a dynamic desorption experiment in which a short, steep rise, gas pulse is obtained by flash desorption of a gas from a pulse heated, cold filament onto which has been previously adsorbed a specific gas. If the cryogenic temperature of the filament is not far from the normal boiling temperature of the gas to be used, the gas may be almost completely desorbed from the filament in a few microseconds. The desorption requires a very small amount of energy.

A convenient choice of cryogenic temperature for the filament during adsorption is 77°K. At this temperature argon is a natural choice of gas since it is easily adsorbed at relatively high coverage on a 77°K filament. Argon is also a particularly suitable gas for study of gauges, being inert and having an ionization probability rather like nitrogen. Negligible adsorption of argon occurs at room temperature so that the experimental apparatus may be maintained quite gas-free except for the cold, flash desorption filament.

5.2 APPARATUS

The experimental apparatus for the ion gauge dynamic response experiment consisted of a Nottingham ion gauge and a flash desorption filament in a metal envelope. The desorption filament was welded to heavy mounting posts which passed through the bottom of a liquid nitrogen dewar. The dewar was mounted on the gauge envelope with metal sealed flanges. The length of the desorption filament support posts was such that the filament position was 1.5 cm from the grid cage and parallel to the grid cage axis. The filament was 10 microns diameter and 2 cm long. A 95% transparent, grounded, tungsten grid was placed between the desorption filament and the grid cage to shield the gauge from the desorption filament electrical firing pulse and to prevent electrons from the gauge filament from reaching the desorption filament during firing. The support posts passed up through the liquid nitrogen and out of the dewar to the filament pulsing circuit secured to the outside of the dewar. An all-metal, UHV, controlled leak valve was welded into the metal gauge envelope to provide for back-filling the envelope with argon. The complete assembly was secured to an ultrahigh vacuum system through an all-metal valve such that the experimental apparatus could be isolated from the vacuum system during back-filling with argon

(See Figure 34). The pulsing circuit for the flash desorption filament consisted of a capacitor connected in series with the filament leads by a relay which was energized by a manually operated auxiliary circuit. The heating pulse time interval and the total energy in the heating pulse may be varied independently by varying the capacitance and the charging voltage. The time interval of the heating pulse is determined by the instantaneous decay rate of the RC circuit which even though non-linear, is a function of the product of the instantaneous filament resistance and the capacitance. The total energy in the heating pulse is a function of the product of the squared charging voltage and the capacitance. The capacitor was charged by momentarily switching it into an auxiliary circuit containing a battery of known voltage immediately prior to pulsing the flash desorption filament. One of the relay contacts which closed the desorption filament-capacitor circuit was used in another auxiliary circuit to provide a trigger pulse to start the scope sweep circuit. The scope input could be connected either across the desorption filament to measure the time history of the voltage appearing across the filament or directly to the ion gauge collector to measure the time history of the gauge output ion current resulting from flashing the adsorbed argon off the desorption filament. The DC scope had an input impedance of 1 meg and a bandwidth of 2.0 Mc/s. See Figure 35 for the circuit schematic.

5.3 PROCEDURE

The argon leak system was evacuated and purged several times and the leak valve then closed. The apparatus was pumped down and degassed. The Nottingham gauge was degassed by electron bombardment at 1200°C. The flash desorption filament was heated by direct current to 2200°C for degassing. The envelope was induction heated to 550°C. After

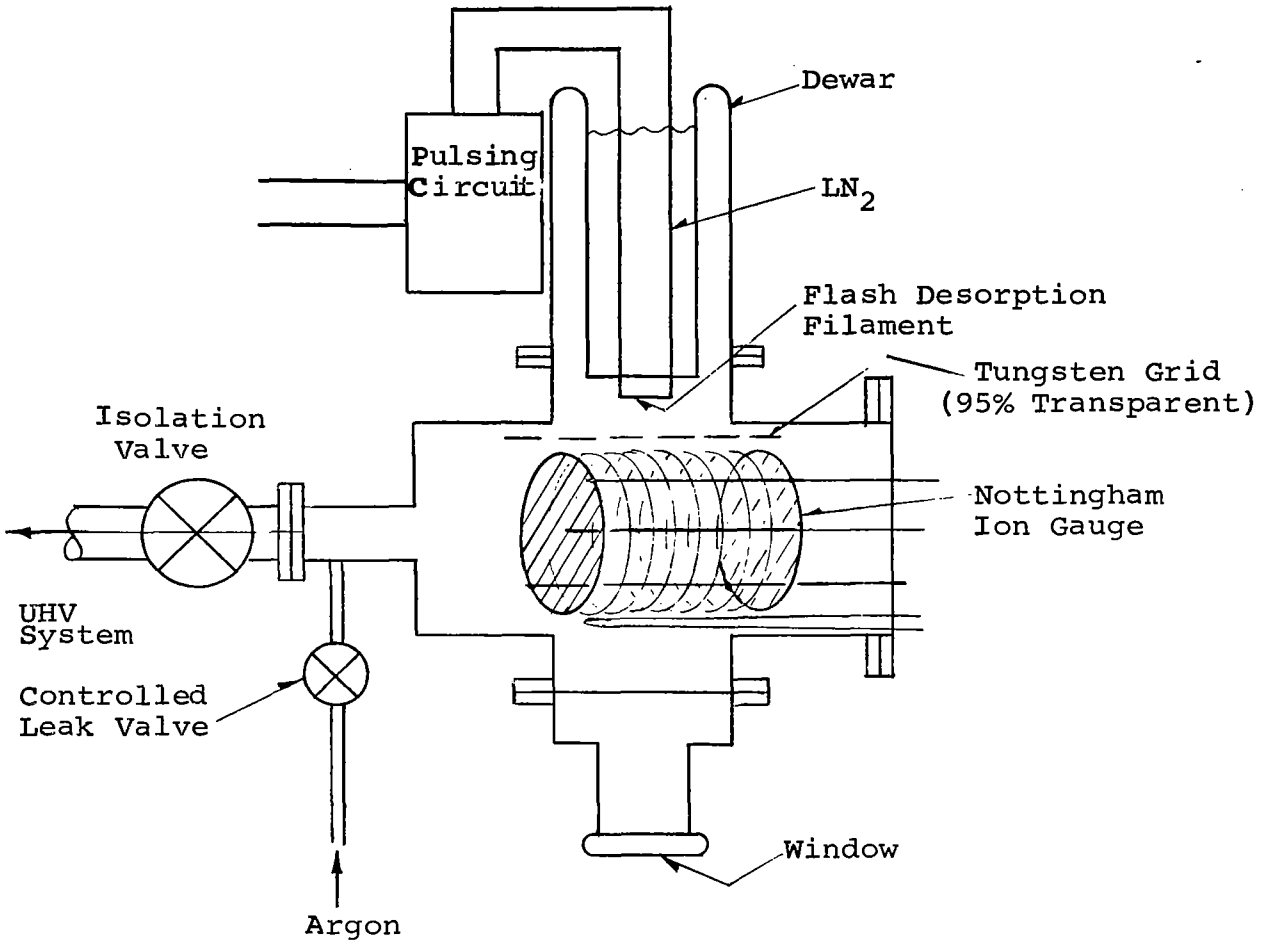

FIGURE 34 DYNAMIC RESPONSE APPARATUS (SCHEMATIC)

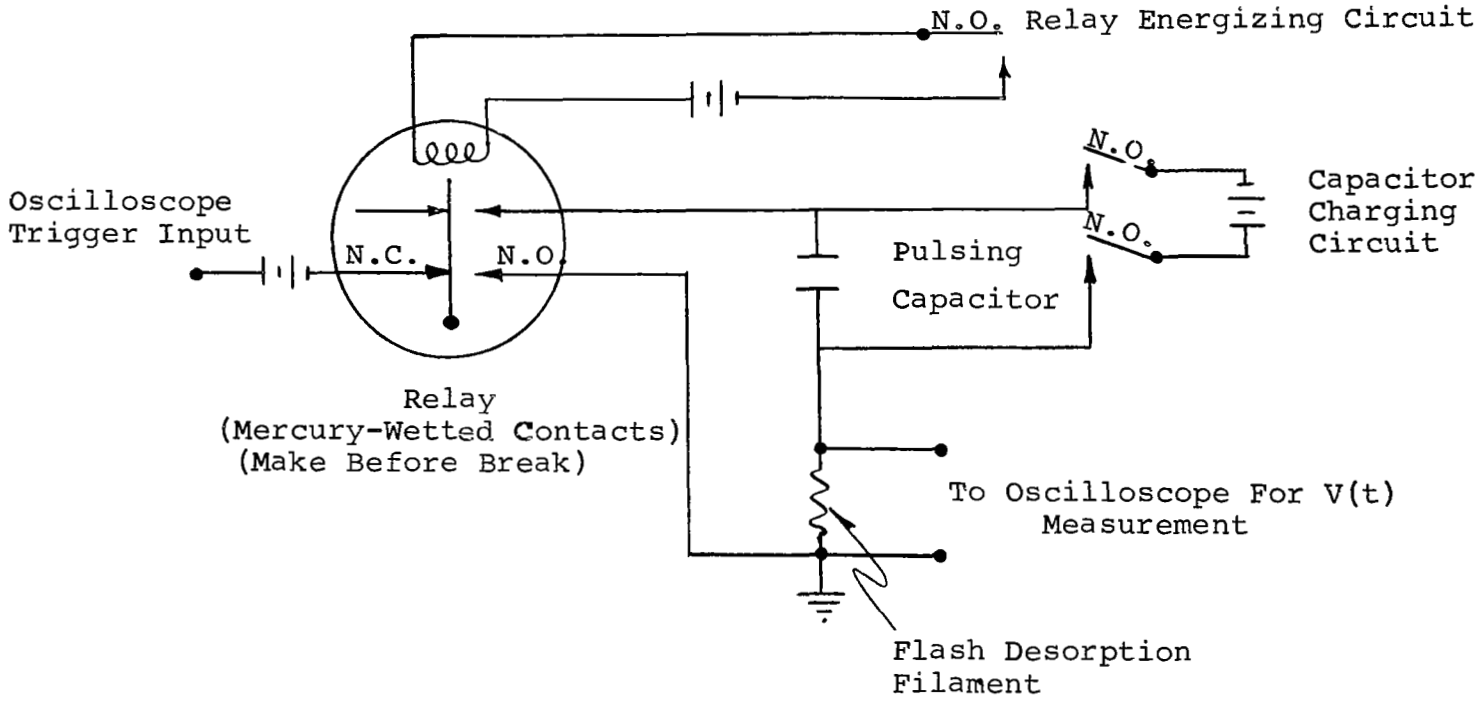

FIGURE 3.5 FLASH DESORPTION FILAMENT PULSING CIRCUIT

degassing the pressure dropped to 6×10^{-10} torr N_2 as determined by the Nottingham gauge operating at standard voltages and emission current.

The integral liquid nitrogen dewar was filled and sufficient time allowed for the desorption filament to cool to 77°K. The temperature of the filament was determined by measuring its resistance. After the filament had cooled to 77°K with the remainder of the apparatus at 300°K and the ion gauge operating, the valve between the UHV system and the apparatus was closed and the gauge envelope back-filled to 10^{-5} torr N_2 with argon. The leak valve was then closed and the gauge envelope evacuated by opening the valve to the UHV system. As soon as the system had pumped the argon from the gauge enclosure, the capacitor was charged and the desorption filament pulsed.

The time history of the voltage appearing across the desorption filament during application of the current pulse was displayed on the scope and the trace photographed. The above procedure was repeated several times to assure that there were no variations in the measured parameters. After the filament voltage time history and the capacitor discharge period were measured, the above procedure was repeated with the ion gauge collector current displayed directly on the scope and the trace was photographed. This was repeated several times for each of several scope sweep speeds so as to define accurately the leading edge of the collector current pulse and also to obtain data on the maximum amplitude and the total duration of the collector current pulse.

The entire experiment was repeated for different values of energy stored in the capacitor and for different capacitor decay periods.

5.4 RESULTS

The measured results for various pulsing capacitors and charging voltages used in this series of experiments are very similar, showing no degradation in response of the ion gauge as shorter pulsing periods were applied to the desorption filament. However, the shortest pulsing period provided the most critical test of the dynamic response of the gauge. Since even the shortest pulse used did not exceed the flat response range of the gauge, only these results will be presented in detail and later discussed in detail.

The measured duration of the current pulse through the desorption filament was 7 microseconds. From the measured voltage time history across the desorption filament during the heating current pulse and from the known heat capacity and resistivity of tungsten, the final temperature of the desorption filament was calculated to be 194°K occurring, of course, at 7 microseconds. From isotherm data on adsorbed argon it is known that little of the adsorbed argon on the filament will be desorbed before the temperature reaches approximately 90°K. The filament reached this temperature in approximately 0.5 microsecond.

The time at which the trace of the ion current first began to show a positive slope was 60 microseconds after the beginning of the current pulse. That is the first indication at the gauge output, of the transient gas pulse desorbed from the filament, appeared 53 microseconds after the filament had reached its final temperature. The maximum gauge output current appeared at 500 microseconds after the beginning of the heating pulse and the collector current had returned to its initial value (before desorption) at 9.5 msec after the beginning of the heating current pulse. The maximum value of the collector current (at 500 microseconds) corresponded to a pressure of 2×10^{-8} torr N_2. See Figure 36 for reproductions of the ion current time history at three different sweep speeds.

a) Initial Rise of Desorption Pulse
Ordinate: 5 x 10^{-9} Amp/cm
Abscissa: 10 μsec/cm

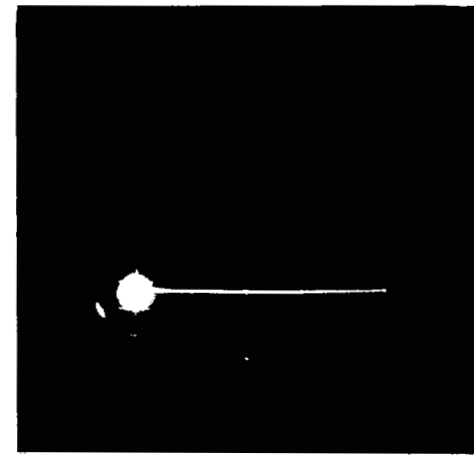

b) Peak of Desorption Pulse
Ordinate: 5 x 10^{-9} Amp/cm
Abscissa: 100 μsec/cm

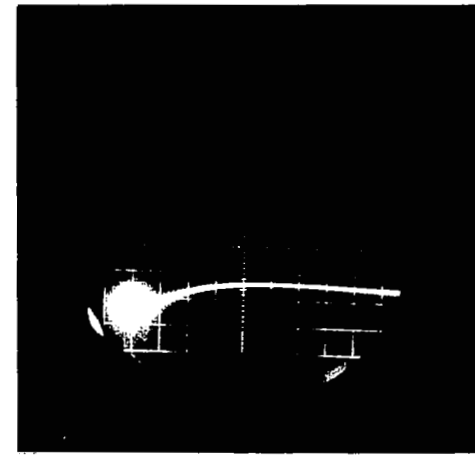

c) Complete Desorption Pulse
Ordinate: 1 x 10^{-9} Amp/cm
Abscissa: 1 msec/cm

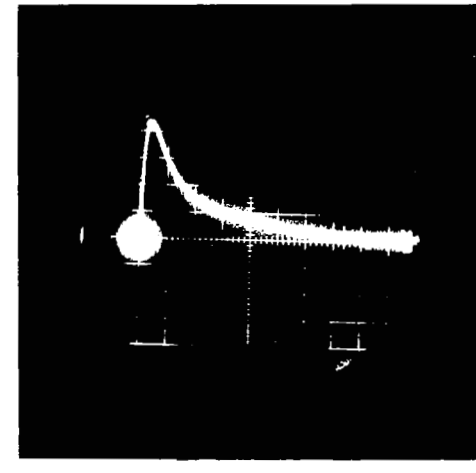

FIGURE 36 ION COLLECTOR CURRENT-TIME HISTORIES

5.5 DISCUSSION

In the following discussion the above measured data will be interpreted and compared with calculated data. The first, and perhaps the most significant, question to be answered is what is the minimum period of time between the entrance of a gas atom into the grid cage and the appearance of an ion at the collector. It should be remembered that gas atoms at ordinary temperatures travel very much slower on the average than ions in only modest electric fields. Thus, the shortest transit time between grid and collector will occur if the slow moving atom is ionized immediately as it passes through the grid and is subsequently accelerated by the electric field to the ion collector. It is here assumed that the ion is created with nearly zero initial velocity. Under these conditions the ion trajectory is defined by

$$r \frac{d^2r}{dt^2} + \frac{e}{m} \frac{V_g}{\ln \frac{r_g}{r_c}} = 0$$

where r = radial distance from the center of the collector to the ion,

$\frac{e}{m}$ = ion charge to mass ratio,

V_g = grid voltage (taking the collector voltage at zero)

$\frac{r_g}{r_c}$ = ratio of grid radius to collector radius.

This equation may be solved for the time an ion requires to travel from a point near the grid to the collector. The exact result is rather cumbersome but is closely approximated by

$$\tau_{g,c} = \left(\frac{\pi \, m \ln \frac{r_g}{r_c}}{2e \, V_g} \right)^{1/2} r_g .$$

Using this equation the minimum time of response has been

calculated for the gauge and gas used in these experiments. The calculated result is

$$\tau_{f,g} = \frac{X_{f,g}}{\left(\frac{8}{\pi}\frac{kT}{m}\right)^{1/2}}$$

where $X_{f,g}$ = distance between desorption filament and the grid,

T = mean temperature of the gas atoms leaving the filament (taken to be the same as the filament temperature),

k = Boltzmann constant,

m = mass of the argon atom.

This gives the shortest transit time (on the average) for argon atoms to traverse the distance from the desorption filament to the grid. It may be observed that even though some argon atoms left the filament about 6.5 microseconds before the filament reached a temperature of 194°K, they arrive later than the atoms leaving at maximum temperature, requiring about 66 microseconds to make the trip. Remembering that the time to reach maximum filament temperature, the heating period (τ_h) was

$$\tau_h = 7\ \mu\text{sec},$$

is now possible to calculate the time at which a signal should have appeared at the ion collector if no other delay periods are involved in the gauge itself. This minimum period (τ_{min}) is simply the sum of all the above periods.

$$\tau_{min} = \tau_h + \tau_{f,g} + \tau_{g,c}.$$

From the above calculated data

$$\tau_{min} = 7 + 50 + 2.6 = 59.6\ \mu\text{sec},$$

which is to be compared with the measured value of 60 μsec.

While the agreement is closer than the experimental accuracy would support, it does imply that there are no substantial, unknown, delay periods involved in the ion gauge. Further it is clear that the response time of the gauge depends mostly on the location and temperature of the gas source. In fact, the gauge "sees" the gas within a very few microseconds after the gas arrives in the vicinity of the gauge.

The total ionization probability for a gas atom passing through the grid is in general, substantially less than unity. Thus, much of the initial direct beam of the gas pulse from the desorption filament passes through the grid and diffuses throughout the system. Consequently, the mean gas density in the gauge rises steadily until an equilibrium pressure is reached throughout the experimental volume. The time constant to reach equilibrium after releasing a short gas pulse in the system is given approximately by

$$\tau_{eq} \simeq \frac{L}{\bar{v}} ,$$

where L = mean significant dimension of the system,

$\bar{v}$ = the mean temperature of the gas (taken to be the temperature of the filament at which most of the gas is desorbed, in this experiment probably about 90°K)

For the apparatus of this experiment

$$\tau_{eq} \simeq 465 \ \mu\text{sec.}$$

Although this calculation is rather coarse, it indicates that the time of maximum measured gauge response (500 μsec) is of the proper order of magnitude. Thus, this long delay should not be interpreted as a slow rise in output of the gauge (as for an over-damped system) but rather as an almost instantaneous response to a relatively slow rise in the actual density in the gauge.

The calculated time required for the UHV system to pump the apparatus back to its initial value (before flash

desorption) is about 22 msec which does not agree with the measured value of 9.5 msec. However, since the bottom of the liquid nitrogen dewar was actually in the vacuum space of the apparatus, this surface could cryopump argon and may well account for the above discrepancy.

From the data of this experiment and the interpretative analysis presented, it is concluded that the response time of an ion gauge is actually of the order of a few microseconds but that very much larger delays in response may be experienced. These delays depend only on the location and temperature of the gas source.

6.0 APPRAISAL OF GAUGE PERFORMANCE IN XHV RANGE

The purpose of this section of the report is to summarize the most important operating characteristics of the gauges studied, particularly with reference to the potential of each gauge for development and future application at extremely low pressures.

One method which may be used as a basis for gauge comparison is to examine the variation of gauge sensitivity with pressure. The results of the present study are summarized in Figure 37 which is a plot of the ion current as determined from the gauge measurements versus the number density expressed as pressure in torr nitrogen. It should be emphasized that the ordinate (gauge current) in Figure 37 has different meanings for several of the gauges considered. For the magnetron gauges the ordinate represents the actual cathode current as measured. However, for both the nude modulated gauge and the modulated suppressor grid gauge the ordinate is the value of the ion current obtained after performing the experimental and calculational procedures associated with the modulating and the suppression techniques. Figure 37 includes the lower limit for which consistent pressure measurements were obtained in the present study for each of the gauges. Also indicated are estimates of probable and possible extensions of the gauge performances to lower pressure levels.

The lowest pressures measured were 3×10^{-13} torr by means of both the magnetron gauges. The sensitivity of the normal magnetron at 3×10^{-13} torr was nearly twice that of the inverted magnetron. However, the non-linear slope of the normal magnetron was greater than the inverted magnetron. Extrapolation of the data suggested that at the various voltages and field strengths used to obtain the data in Figure 37, the sensitivity of the inverted magnetron would equal that of the normal magnetron at 2×10^{-14} torr. Below this pressure the sensitivity of the inverted magnetron

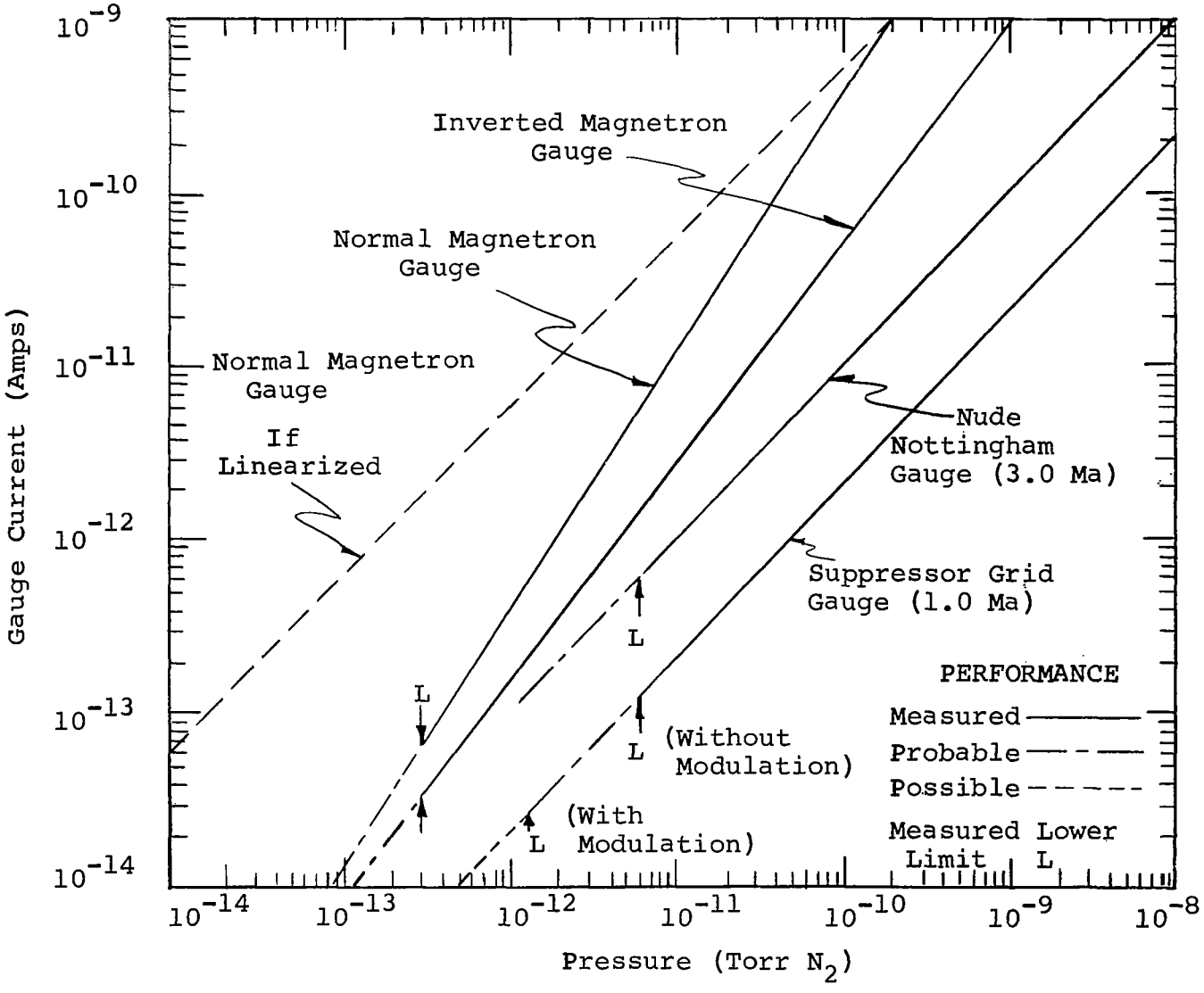

FIGURE 37 COMPARISON OF GAUGES IN XHV RANGE

should be higher.

The sensitivities of both the nude Nottingham gauge and the suppressor grid gauge are lower than the magnetron gauges. However, these gauges are fundamentally linear sensors and would eventually have higher sensitivities than non-linear magnetrons if they could be designed to operate at pressures below approximately 1×10^{-13} torr. The difference in the sensitivities of the nude gauge and the suppressor grid gauge is mainly dependent on the emission currents used. However, as shown in the detailed discussion of the suppressor grid gauge (Section 3.2.3) there appears to be an upper limit to the emission which may be used with the suppressor grid gauge. More information is required to determine the nature of the oscillations found at high emissions in the suppressor grid gauge and developing methods of eliminating these oscillations[15].

From the data obtained it is obvious that the greatest advantages would be obtained if the non-linearity of the normal magnetron could be eliminated. Theoretically there does not appear to be any reason why the linear region should be restricted to pressures above 2×10^{-10} torr.

Other important aspects to be considered in the use of these gauges in XHV are summarized below.

Normal Magnetron Gauge

The normal magnetron has the highest sensitivity among the gauges studied. It is linear down to 2×10^{-10} torr and non-linear below this pressure. It is easily cleaned and because it dissipates negligible power, it operates at normal temperature with normal degassing rates. Since it operates at normal temperature, chemical reactions occur at relatively low rates and contamination is therefore a less serious problem than in hot gauges. Its construction is relatively simple and relatively rugged. It is the most reliable of the gauges studied at very low pressures. It

does, however, tend to be noisy at very low pressures. It requires a relatively high voltage and a magnet which is sometimes an inconvenience. There is also a substantial delay in starting at very low pressures.

Inverted Magnetron Gauge

The inverted magnetron gauge is non-linear over its entire pressure range and has an intermediate sensitivity. Its construction, operation, and performance are otherwise similar to the normal magnetron. However, for optimum performance it requires a higher anode voltage and magnetic field strength than the normal magnetron.

Modulated Nottingham Gauge (Nude)

The modulated Nottingham gauge is linear to pressures slightly lower than 10^{-11} torr. It requires no magnets or high voltage. Its sensitivity is rather low and construction is complicated and rather fragile. Vigorous, prolonged, and repeated degassing is required for proper operation in the UHV range and the gauge is very easily contaminated. The gauge dissipates 15 to 20 watts and therefore operates with some parts rather hot which leads to high degassing rates if contaminated. The hot filament produces chemical reactions which lead to spurious results. Physical reactions occur at the electron bombarded grid which lead to anomalous indicated pressures. The modulation technique requires additional operations and eventually (below 10^{-12} torr) becomes non-linear, requiring the introduction of a second modulation coefficient which must be measured experimentally at very low pressures (of the order of 10^{-15} torr).

Modulated Suppressor Grid Gauge

The modulated suppressor grid gauge is similar to the modulated Nottingham gauge in its characteristics and performance but its construction is more complex and requires a higher degree of precision in the location of the elements.

The power supply is more complicated since moderately high voltages may be required for complete suppression. While its limit of detectability for pressure is lower than other hot cathode gauges, the output current is very small at very low pressures and must be processed with extreme care. The residual current is negative which introduces recording difficulties with some commercial electrometers.

7.0 PROBLEMS ASSOCIATED WITH PRESSURE MEASUREMENT IN THE EXTREME HIGH VACUUM RANGE

In the experimental work under the present program it has become very clear that one of the major problems encountered in reliable pressure measurements in the XHV range is associated with making reliable very small current measurements. Even though the National Research Corporation Applied Physics Laboratory is equipped to measure currents of the order of 10^{-17} amp, the actual measurement, under practical conditions, of currents much below 10^{-13} amp is extremely difficult if reasonable reliability is desired.

Materials ordinarily used for gauge lead passthroughs and circuit insulators may have leakage currents of the order of 10^{-10} amp. After careful cleaning, leakage currents may be of the order of 10^{-14} to 10^{-15} amp. If the insulator is electrically guarded, that is, if its low potential end is driven at a potential nearly equal to the high potential end, leakage currents may drop to 10^{-16} to 10^{-17} amp.

However, if the potential is changed on either end of an insulator a dielectric polarization or depolarization current may arise which may be many orders of magnitude higher than the above current. Thus, if guarding is to be effective the potentials must be controlled with precision.

Many materials which have high resistivity are very susceptible to surface contamination and consequent surface leakage currents. Also some materials which have high resistivity and are not overly sensitive to surface contamination have high polarizabilities. Thus, it is sometimes necessary to use a combination of materials to achieve adequately low leakage currents in very small current measurements.

In the present program a helium gas refrigerator has been used to reduce the temperature of the experimental chamber to 10°K. The expansion engines on the refrigerator produce considerable amounts of vibration -- generally at about 5 c/s. These vibrations are transmitted to gauge elements and conductors and induce microphonics. Efforts have been made to reduce the amount of vibration transmitted by use of flexible joints and anti-vibration pads. However, these were only partially successful. Mechanical foreline pumps may also contribute to serious microphonic effects.

The power supplies which apply the operating voltages to the gauge electrodes are usually not ultrastable and noise-free. The variations in these supply voltages are coupled to the ion collector through interelectrode capacitance, which even though small, can induce dynamic currents in the collector circuit of substantial magnitude. These dynamic variations in the ion current measuring circuit induce polarization currents between ground and the collector circuit resulting from polarization of the circuit insulators. If the noise pulse in the power supply is large or long, the induced polarization currents in the dielectric materials supporting the circuit may be large and require a considerable period to decay to a negligible level. Line voltage variations produce transients in the electrometer which momentarily upset the potential drop across the electrometer input and thus on the collector circuit. These also induce dielectric polarization currents, which again may be relatively large and require a considerable time to decay to a negligible level. These problems can be solved by using a separate ultrastable power supply for each circuit in the gauge and isolating each supply from the line separately such that line noise is completely filtered.

Noise in the gauge itself is frequently a serious problem at very low pressures. If the noise spikes are large they induce large changes in potential across the input to the electrometer which, because of the relatively long time constant of the electrometer, requires a relatively large period to decay to a negligible level. The intrinsic noise also induces dielectric polarization currents in the collector circuit. It is thus highly desirable to shield the ion collector from the gauge noise. In some cases this requires the introduction of additional auxiliary electrodes.

Each of these sources of noise or spurious signal may be eliminated under very special laboratory conditions with highly specialized apparatus. However, it is usually necessary to make very low pressure measurements under less ideal conditions. In order to develop practical methods of measuring very low pressures, advances are required in two basic areas. Firstly, gauges with increased sensitivity (amps/torr) and larger signal to noise ratios are required. Fundamental changes in gauge design may be necessary in order to achieve the sensitivity required for measuring very low pressures. The techniques used in a gauge designed to operate at 10^{-5} torr may indeed be completely inadequate for measurements of 10^{-15} torr, and yet the tendency has been to try and push the usefulness of high pressure gauges to lower and lower values without fundamental changes in design. Secondly, advances are required in the techniques of measuring exceedingly small currents. Major difficulties presently result from such effects as dielectric polarization, instabilities and noise in power supplies, capacitance effects between gauge elements, microphonics, and leakage currents caused by inadequate insulating materials.

At the present time there appear to be very good prospects for eliminating many of these difficulties. Vastly superior systems incorporating both the gauge, its power supplies, leads and current measuring apparatus should then be possible.

REFERENCES

1. P. A. Redhead, Private Communication, June 1964.

2. J. P. Hobson and P. A. Redhead, Canad. J. Phys. 36, 271, (1958).

3. P. A. Redhead, Rev. Sci. Instr., 31, 343, (1960).

4. F. Feakes and F. L. Torney, Jr., Trans. 10th Natl. Vac. Symp., 257, (1963) The Macmillan Company, New York.

5. J. R. Roehrig and J. C. Simons, Jr., Trans. 8th Natl. Vac. Symp., 511 (1961) Pergamon Press, New York.

6. P. A. Redhead, Canad. J. Phys. 37, 1260 (1959).

7. F. L. Torney, Jr. and F. Feakes, Rev. Sci. Instr., 34, 1041, (1963).

8. W. C. Schuemann, Trans. 9th Natl. Vac. Symp., 1, (1961) Pergamon Press, New York.

9. G. Appelt, Vakuum-Technik, 11, 174 (1962).

10. J. P. Hobson, 24th Ann. Conf. on Physical Electronics, 274, (1964) Massachusetts Institute of Technology, Cambridge, Massachusetts.

11. P. A. Redhead, Vacuum, 13, 253, (1963).

12. D. Alpert, Coordinated Science Laboratory, University of Illinois Report R-167, April 15, 1963.

13. N. F. Ramsey, MOLECULAR BEAMS, p. 16, Clarendon Press, Oxford England (1956).

14. P. Clausing, Physica, 9, 65, (1929) also Zeits. f. Physik, 66, 471, (1931).

15. F. Feakes and F. J. Brock, Consultation Report, NASA Langley, In Preparation.